Environment CANADA Environnement
10209261 VOL ISS 78 861000
EXC # 001
TD 171.5.C3 R46
REPORT EE

OOFF

MODELLING THE SPREADING, INFILTRATION AND EVAPORATION OF CHEMICAL SPILLS ON GRASS AND IMPERMEABLE SURFACES

EE-78

MODELLING THE SPREADING, INFILTRATION AND EVAPORATION OF CHEMICAL SPILLS ON GRASS AND IMPERMEABLE SURFACES

by

R. Belore
S.L. Ross Environmental Research Limited
Ottawa, Ontario

and

E. McBean
Edward A. McBean and Associates
Waterloo, Ontario

This report has not undergone detailed technical review by Conservation and Protection and the content does not necessarily reflect the views and policies of Environment Canada. Mention of trade names or commercial products does not constitute endorsement for use.

This unedited version is undergoing a limited distribution to transfer the information to people working in related studies. This distribution is not intended to signify publication and, if the report is referenced, the author should cite it as an unpublished report of the Branch indicated below.

Any comments concerning its content should be directed to:

Environment Canada
Environmental Protection Directorate
River Road Environmental Technology Centre
Ottawa K1A 0E7

EE-78

October 1986

SUMMARY

During the development of the EnviroTIPS manuals by the Environmental Emergencies Technology Division (E.E.T.D.) of Environment Canada, it was found that existing spreading models were not suitable for application to chemical spills on land. This study was then commissioned to develop and validate a more accurate model.

To achieve this objective relatively large scale laboratory experiments were conducted to provide the necessary data to test the new models being developed. Water was used as the test chemical for obvious reasons of economy and safety. Various viscosities were simulated by doping the water with Carboxy - Methyl - Cellulose to increase its viscosity. Two extreme test surfaces were used in the testing; sod placed over loosely packed top soil to provide a highly permeable terrain, and painted plywood to simulate an impermeable hard-packed soil surface. Tests were conducted on both level and sloped surfaces (10^{o} from horizontal). The spreading rate, chemical depth and infiltration rate (where applicable) were measured for a range of chemical flow rates in both the two- and three-dimensional tests.

A detailed 2-dimensional mathematical model was then developed which includes the following main elements: a surface affinity depth which controls the liquid depth at the leading edge of the spill, frictional resistance due to the passage of fluid over the ground's surface, and the preservation of continuity which also permits the inclusion of evaporation and infiltration terms. In the three-dimensional model the frictional flow resistance term was omitted to reduce the computational effort required in executing the model. This results in a slight over-estimate of spill spreading rate and ultimate pool size. The results of both models were in good agreement with the laboratory data thus providing some validation for the model's algorithms. A comparison of the new model's estimates of chemical pool size to those used in the present EnviroTIPS manuals indicates that the estimates of pool size in the TIPS manuals can be an order of magnitude or more too high.

In order to extend the use of these models to a wide range of chemical and terrain types two key model input parameters must be evaluated. The contact angle of the chemical on the terrain on which it is spilled and the Manning's roughness coefficient of the terrain (to the specific chemical) are needed for the proper implementation of the models. Further study should concentrate on evaluating these parameters as well as applying the models to full-scale chemical spill occurrences (either experimental or spills of opportunity).

RÉSUMÉ

À la préparation des ENVIROGUIDES de la Division des techniques d'intervention d'urgence, d'Environnement Canada, il a été constaté que les modèles d'étalement étaient inapplicables aux déversements de matières chimiques sur le sol. La présente étude a donc été commandée pour élaborer et vérifier un modèle plus fidèle.

À cette fin, des essais en laboratoire ont été menés à une échelle relativement grande pour obtenir les données nécessaires à la vérification des nouveaux modèles. Pour des raisons évidentes d'économie et de sécurité, c'est l'eau qui a servi aux manipulations. Pour accroître sa viscosité, on lui a ajouté de la carboxy-méthyl-cellulose. Deux surfaces aux caractéristiques extrêmes ont servi aux essais: du gazon reposant sur de l'humus faiblement compacté, pour simuler un terrain très perméable; du contre-plaqué peint, pour simuler un sol imperméable, fortement compacté. Les essais ont eu lieu sur des surfaces horizontales et inclinées (10°). La vitesse d'étalement, la profondeur et la vitesse d'infiltration (s'il y avait lieu) ont été mesurées pour toute une gamme de vitesses d'écoulement, tant à deux qu'à trois dimensions.

Un modèle mathématique détaillé bidimensionnel a alors été construit. Il comprend les principaux éléments suivants: la profondeur d'affinité surfacique, qui commande la profondeur du liquide sur le sol; et le maintien de la continuité, qui permet l'inclusion des termes de l'évaporation et de l'infiltration. Dans le modèle tridimensionnel, la résistance à l'écoulement due à la friction est omise, pour alléger le calcul exigé dans l'exécution du modèle. Il s'ensuit une légère surestimation de la vitesse d'étalement et de la dimension finale de la mare. Les résultats des deux modèles concordaient bien avec les résultats obtenus en laboratoire, confirmant en quelque sorte les algorithmes du modèle. La comparaison des estimations des dimensions modélisées de la mare et des dimensions données dans les ENVIROGUIDES montre que ces dernières peuvent être au moins dix fois trop grandes.

Afin d'élargir l'application de ces modèles à une variété de matières chimiques et de types de terrains, deux paramètres déterminants d'entrée doivent être évalués pour que les modèles soient opérants: l'angle de contact de la matière sur le terrain et le coefficient de rugosité de Manning du terrain (à l'égard de la matière chimique). Les études ultérieures devraient porter sur l'evaluation de ces paramètres ainsi que sur l'application des modèles à des déversements chimiques de grandeur réelle (tant expérimentaux qu'accidentels).

TABLE OF CONTENTS

		Page
1.0	INTRODUCTION	1
1.1	General	1
1.2	Basics of the Spill Process	1
1.3	Focus of This Study	3
2.0	MATHEMATICAL MODELLING	6
2.1	Review of Spill Models in the Technical Literature	6
2.1.1	Complex Models	6
2.1.2	Simple Models	6
2.2	Infiltration, Evaporation and Flow Resistance Models	7
2.2.1	Infiltration	7
2.2.2	Evaporation	8
2.2.3	Flow Resistance	9
2.3	Mathematical Basis for the Spill Model Developed in This Study	9
2.3.1	Overview of the Methodology	9
2.3.2	Mathematical Formulation	12
2.3.3	Complicating Aspects of the Mathematical Formulation	16
3.0	PHYSICAL MODELLING	19
3.1	General	19
3.2	Experimental Set-Up	19
3.3	Tested Conditions	21
3.4	Summary of the Test Methods	27

TABLE OF CONTENTS (Cont.)

		Page
4.0	COMPARISON OF COMPUTED AND PHYSICAL MODELLING PROFILES	29
	4.1 Introduction	29
	4.2 Two-Dimensional Analyses	30
	4.2.1 Modelling Results Using Water	30
	4.2.2 Impact of Different Surface Slopes	30
	4.2.3 Impact of Alternative Viscosities	36
	4.2.4 Characterization of Infiltration and Evaporation Rates	40
	4.3 Three-Dimensional Analysis	44
	4.3.1 Modelling Results Using Water	44
	4.3.2 Impact of Alternative Viscosities	45
	4.4 Sensitivity Analysis Using the Spill Model	45
	4.5 Comparison of Model Outputs to Existing Methods of Chemical Pool Size Prediction	57
5.0	CONCLUSIONS AND RECOMMENDATIONS	59
	5.1 Conclusions	59
	5.1.1 Two Dimensional Model	59
	5.1.2 Three-Dimensional Model	60
	5.1.3 General Comments	60
	5.2 Recommendations	61
	REFERENCES	62
	APPENDIX	

LIST OF FIGURES

Figure No.		Page
1.1	Elements of the Spill Process	2
2.1	Schematic Depiction of Leading Edge of Spill	11
2.2	Standard Profile Types	17
2.3	Extrapolation Procedure when Surface Affinity Depth < Critical Depth	18
3.1	Schematics of Test Beds Used in Testing	20
3.2	Two Dimensional Test Bed with Plywood Surface	22
3.3	Constant Head Discharge Tank	22
3.4	Two Dimensional Sloped Bed with Plywood	23
3.5	Three Dimensional Test Bed with Plywood	23
3.6	Two Dimensional Test Bed with Soil and Sod Surface	24
3.7	Three Dimensional Test Bed with Soil and Sod Surface	24
4.1	Example of Physical and Mathematical Results for Plywood Surface	32
4.2	Example of Physical and Mathematical Results for Sod Surface	33

LIST OF FIGURES (Cont.)

Figure No.		Page
4.3	Standard Profile Types	34
4.4	Example of Physical and Mathematical Results for Steep Slope Conditions ($Y_c > Y_n$)	37
4.5	Example Prediction by Three Dimensional Model: Plywood	46
4.6	Example Prediction by Three Dimensional Model: Sod	47
4.7	Sensitivity of Two Dimensional Modelling Results to Alternative Infiltration Rates	51
4.8	Sensitivity of Two Dimensional Modelling Results to Alternative Evaporation Rates	52
4.9	Sensitivity of Three Dimensional Modelling Results to Alternative Infiltration Rates	54
4.10	Sensitivity of Three Dimensional Modelling Results to Alternative Evaporation Rates	56

LIST OF TABLES

Table No.		Page
3.1	Summary of Run Experiments	26
4.1	Modelling Results of Water - Two Dimensional Analyses	31
4.2	Impact of Alternative Viscosities - Two Dimensional Analyses	38
4.3	Estimates of Exponent for Predicting Manning's Coefficient for Variations in Viscosity	41
4.4	Comparison of Mathematical and Physical Modelling Results for Infiltration Prediction	43
4.5	Modelling Results of Water: Three Dimensional Analyses	48
4.6	Impact of Alternative Viscosities: Three Dimensional Analyses	49

1.0 INTRODUCTION

1.1 GENERAL

During the development of the EnviroTIPS manuals by EETD it was found that existing spreading models were not suitable for application to chemical spills on land. This modelling is important since the spreading of the chemical greatly affects both the evaporative flux and the infiltration rate of the chemical into the soil. A poor prediction of the chemical's pool size (by an inappropriate spreading model) also results in errors in the modelling of the dispersion of the chemical in air and soil. Inaccurate estimates of potential health hazard zones surrounding the spill site can then result. This could lead to inappropriate, or even dangerous action, by response personnel.

The development and validation of a more accurate model of the spread of chemicals on land is the subject of this report. The mathematical model development is a continuation of work by Farquhar and McBean (1984) and Allan et al (1985). To test the validity of the models being developed, relatively large-scale laboratory tests have been conducted. The results of the experimental program have been used to calibrate and validate the simulation models.

1.2 BASICS OF THE SPILL PROCESS

In schematic form, the elements of the spill process are as indicated in Figure 1.1. Presuming a vertical spill, there is a region of supercritical flow emanating away from the point of impingement. If the surface is not sloped to a large extent (which will be defined more carefully in Chapter 2), the region of supercritical flow is followed by a hydraulic jump, a transition to more quiescent, or lower velocity flow. The sloped surface of the spill profile provides the forcing function to move the leading edge or "bore" away from the source of the spill. The depth at the bore, referred to as the surface affinity depth is a result of surface tension between the liquid being spilled, and the underlying surface.

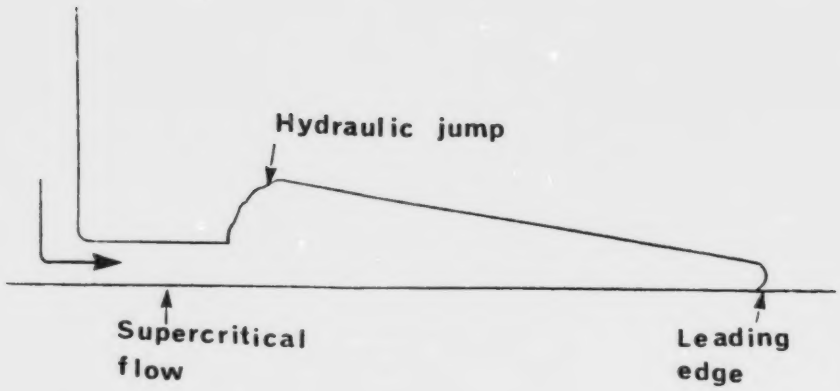

Figure 1.1 Elements of the Spill Process

Eventually, the hydraulic jump will be driven back to a position just slightly downstream from the jet, thereby reducing the extent of the supercritical flow field. At the same time, the depth increases and the velocity decreases throughout the subcritical flow field. The end result of these two processes is that the source loses its ability to influence liquid motion throughout the pool, and therefore, does not affect the overall areal extent of the spill. Under these conditions the increase in the pool's surface area will be controlled solely by the unbalanced hydrostatic head that exists within the pool, since the energy that is introduced by the velocity of the inflowing liquid is dissipated within the bulk of the pool.

A complete study of the spill problem must therefore include an analysis of each of the following components:

i) overland flow, described in terms of a supercritical flow field, a hydraulic jump, a subcritical flow field, and a moving bore;
ii) infiltration into the soil; and,
iii) evaporation into the atmosphere.

It is, of course, the degree to which these factors are included within existing mathematical models which differentiates between them. The differences between the models arise because of the alternative levels of mathematical sophistication employed.

1.3 FOCUS OF THIS STUDY

The following factors must be taken into account when simulating the overland spill process in the laboratory or when mathematically modelling the process:

i) source parameters which describe the spilled chemicals, the jet's radius, initial inflow and the rate of decay of the spill towards zero; and

ii) environmental parameters which describe the soil and atmospheric conditions, determine the resistance to flow, and the rates of infiltration and evaporation.

The wide range of possible chemical types and flow rates, soil types, atmospheric conditions etc. during a spill has made it necessary to narrow the scope of this study to achieve maximum benefit from the work.

A major concern in this study was the development of a spill model, with the following desirable characteristic. It should be:

i) reasonably simple, to allow usage by a variety of individuals;
ii) be general in form, which indicates the model cannot be strictly regression-based; and,
iii) be able to be used on a micro-computer.

To respond to these concerns, within time and budget constraints, we have concentrated our efforts on the spill of viscous liquids. For the purposes of this study, spilled liquids may be classified as cryogenic, highly viscous and viscous. Cryogenic liquids present a special case because of overwhelming evaporative losses and negligible infiltration once spilled. Infiltration is limited due to both the extensive loss of liquid through vaporization and the freezing of the soil layer under the liquid due to evaporative cooling. Highly viscous and viscous liquids are both removed from the soil surface by infiltration into the underlying soil profile, and to a lesser extent, by vaporization. Highly viscous liquids, such as crude oils, are generally found at oil fields, refineries and in pipelines and are not as routinely shipped by train or truck. The EETD priority list of hazardous chemicals is made up primarily of viscous liquids (liquids with viscosities similar to that of water) that are routinely shipped by truck or train and, therefore, susceptible to land spills. This class of liquid is therefore the most appropriate for the purpose of this study.

Flow rates used in the study were based on logistical considerations. Flows were kept high enough to produce easily measurable spreading rates and flow depths but not so high that special pumping equipment or excessive quantities of chemicals were needed in the testing.

Two soil types were used to bracket the wide range of possible conditions. A highly permeable condition (grass over a loosely compacted top soil) and an impermeable surface (plywood) were used during the experimental portion of the study. This provided a range of, and a high degree of control over, infiltration rates and surface roughness. A horizontal spill surface and a sloped surface (10^{o} from horizontal) were also modelled in the experimental program to provide data to check the mathematical model's validity when applied to sloped surfaces.

2.0 MATHEMATICAL MODELLING

2.1 REVIEW OF SPILL MODELS IN THE TECHNICAL LITERATURE

Few mathematical models exist in the technical literature which address the problem of chemical spills on land. The models which do exist will be discussed under the categories of complex and simple models.

2.1.1 Complex Models

A highly complex, numerical model was developed by Wall (1984). A rigorous characterization of the momentum equation and frictional resistance along the liquid/solid interface provided the opportunity for an excellent prediction of the location of the hydraulic jump. However, the model formulation does not include the surface tension aspects that occur at the leading edge of the spill. As a consequence, the radius of the moving bore was consistently over-estimated by the model. As well, the lengthy execution time of the model, because of the complex numerical analysis, detracts from the usefulness of Wall's model. This latter aspect is consistent with many numerical integration models, of which this is one. There are also difficulties with respect to both convergence and numerical dispersion.

2.1.2 Simple Models

The simple models are derived assuming simplification in the momentum aspects of the spill process. The models include:

- Abbott (1961), Fay (1969), Hoult and Suchon (1970) and Fannelop and Waldman (1971) who all developed theories and analytical models to quantify the spreading of oil over calm water. Raj and Kalelkar (1974) adapted the Fannelop and Waldman (1971) solution to the spreading of viscous liquids over solids. They applied this model to the spill of liquids (e.g. gasoline) over water by assuming that the relative differences between the two viscosities were sufficiently high so that the

water could be considered as a solid surface. These models assume: (i) an instantaneous spill; (ii) the sudden liquid release no longer influences the motion of the pool; and (iii) there is no evaporation from the pool.

- Tanner (1979) developed some analytical models for drop formation on horizontal surfaces, with particular attention to the conditions near the edge and the surface tension forces acting there.

- Raisbeck and Mohtadi (1974) developed a model to simulate the spread of petroleum products over both permeable and impermeable Arctic soils, assuming that the slick reaches and maintains its equilibrium height. However, in the case of the spill of a viscous liquid onto a natural soil: 1) the inflow driving mechanisms will not be quickly dissipated; and 2) the pool depth will be controlled by the soil roughness. Therefore, for viscous liquids, the assumption of a constant pool thickness may not be justified. Significant merits of this model relevant to this study include its simplicity, and the characterization of the leading edge of a spill.

2.2 INFILTRATION, EVAPORATION AND FLOW RESISTANCE MODELS

2.2.1 Infiltration

Infiltration is defined as the vertical flow of liquid into a soil system. Numerous mathematical models of infiltration have been described in the technical literature (e.g. Huggins and Monke (1966), Horton (1935), Holtan (1975)). A good overview of the available models is in Viessman et al (1977). Although many models of infiltration have been developed, very few have examined fluids other than water. A noteworthy exception is Anderson and Jones (1984) who considered gasoline.

Because of the very limited research conducted on infiltration of fluids other than water, it is not feasible at this time to utilize models beyond those developed for water. In this regard, a general model that has been widely accepted is

$$f = f_c + (f_o - f_c)\bar{e}^{kt} \qquad (2.1)$$

where f = infiltration rate (m/hr), f_o = initial infiltration rate, f_c = steady-state, or long-term infiltration rate, k = decay constant and t = time. The characteristics of (2.1) are an initial rapid infiltration rate followed by an exponential die off over time. The model describes the pattern of infiltration rate by decreasing the rate as the surface soil becomes saturated. However, the parameters used in the model in the technical literature all relate to water.

2.2.2 Evaporation

Evaporative flux models involve the estimation of the net rate of vapor transfer. The liquid mass flux evaporated has been characterized by

$$e = k_m \left[\frac{M}{\rho_1 60^2}\right] \frac{P_v}{R_g T_g} \qquad (2.2)$$

where M = gram-molecular mass, ρ_1 = liquid density at T_p (g/m^3) and $k_m = 0.0292\, S_c^{0.67} v_w^{0.676} (2R_p)^{-0.11}$. This equation has been verified by Mackay and Matsugu (1973) against experimentally-measured evaporation rates.

2.2.3 Flow Resistance

Resistance to shallow, liquid flow over natural soils or through vegetation, is a complex phenomena. It is necessary to use a flow resistance component which, while representing in a realistic manner the flow resistance, retains an appropriate degree of computational and data collection effort. The most frequently used flow resistance model is Manning's equation.

$$v = C_m \frac{R^{2/3} S_f^{1/2}}{n} \qquad (2.3)$$

where v = velocity, C_M = factor assigned because of the units employed, R = the hydraulic radius and S_F = the friction coefficient.

The understanding of the process of resistance to the shallow flow of a liquid has not been developed to the point where a general resistance model is available; therefore, the estimation of various flow resistance equation parameters, especially for a liquid other than water, is difficult. In fact, applications of this model to liquids other than water, were not identified in a search of the technical literature.

2.3 MATHEMATICAL BASIS FOR THE SPILL MODEL DEVELOPED IN THIS STUDY

2.3.1 Overview of the Methodology

The following elements are included in the Spill Model:

(i) the surface affinity depth which controls the liquid depth at the bore, leading edge, or wetting front;

(ii) frictional resistance arising from the fluid passing over the surface is characterized by Manning's equation. (Little work has been done for liquids other than water and will be the focus of analysis in Section 4.2.3.)

(iii) subsets (i) and (ii) refer to momentum aspects of the spill process. The additional stipulation is the preservation of continuity -- the quantity spilled must have evaporated, infiltrated, or still be within the spill profile.

Considerations of (i) through (iii), while retaining a relatively simple model, are developed in the following manner for each time increment of calculation:

- The extent of the spill excursion is estimated. The calculations proceed by computing back from the surface affinity depth toward the origin of the spill, reflecting the increased depth necessary to overcome surface frictional resistance. Simultaneously, evaporative and infiltrated fluxes are removed from the spill as losses of fluid, as depicted in Figure 2.1.

The profile calcualtion proceeds until the law of conservation of mass is satisfied, wherein:

volume of fluid released to the spill	=	volume of fluid within the spill profile	+	volume lost to evaporation	+	volume lost to infiltration	(2.4)

An important complicating feature to the above procedure is that the surface profile calculations must be initiated at the leading edge, but the volume of fluid lost to evaporation and infiltation is not known until the length of the profile has been estimated. The implication is that the flow at the leading edge is not known (because of the intervening losses) and must be estimated. The result is that the calculations must be undertaken in an iterative manner as per:

(i) estimate distance to leading edge from the spill origin;
(ii) calculate losses to evaporation and infiltration, and thus the new flow rates for locations between the origin of the spill and the leading edge;

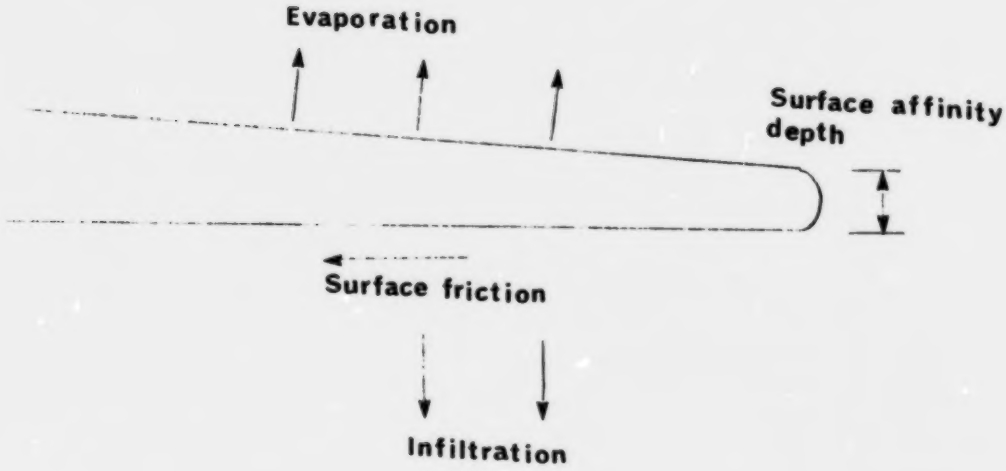

Figure 2.1 Schematic Depiction of Leading Edge of Spill

(iii) proceed with the calculation of the backwater profile until Eqn. 2.4 is satisfied, which then establishes the distance to the leading edge from the spill origin;

(iv) check the distances implied in (i) and (iii) -- if they are within acceptable bounds, the calculations for this time increment are satisfied and proceed to (v). If not, use the estimate from (i) in (iii) and re-execute the calculations;

(v) proceed to calculations for the next increment of time within the spill period.

2.3.2 Mathematical Formulation

The fluid surface profile computation method is based on the integration of an ordinary differential equation,

$$\frac{dy}{dx} = \frac{S_o - S_f}{1 - \frac{Q^2 B}{gA^3}} \qquad (2.5)$$

where y = depth of flow, x = location, S_o = slope of the bottom surface, S_f = frictional slope of the fluid, Q = flow, B = top-width, g = acceleration due to gravity and A = cross-sectional flow-through area. This equation has been extensively used in mathematical modelling.

A closed-form integration of Equation (2.5) is not possible in this instance making it necessary to resort to numerical integration procedures. Position-computing methods are particularly appropriate for this problem (McBean and Perkins 1970).

To demonstrate the form of solution, the gradually-varied flow equation, Equation (2.5) is written in terms of the specific energy, E, defined as

$$E = y + \frac{q^2}{2gA^2} \tag{2.6}$$

where q = flow per unit width.
Noting that

$$\frac{dE}{dy} = 1 - \frac{q^2}{gA^3}\frac{dA}{dy} \tag{2.7}$$

or, using (2.5)

$$\frac{dE}{dx} = S_o - S_f \tag{2.8}$$

Inverting (2.8) gives

$$\frac{dx}{dE} = (S_o - S_f)^{-1} \tag{2.9}$$

which, upon Taylor's series expansion, becomes

$$x_{n+1} = x_n + \frac{\Delta E}{2}(1 - 1/2\,\nabla)x'_{n+1} \tag{2.10}$$

or

$$x_{n+1} = x_n + \frac{\Delta E}{2}(x'_{n+1} + x'_n) \qquad (2.11)$$

substituting (2.8) into (2.11) gives

$$x_{n+1} = x_n + \frac{\Delta E}{2}[(S_{o_{n+1}} - S_{f_{n+1}})^{-1} + (S_{o_n} - S_{f_n})^{-1}] \qquad (2.12)$$

Recalling the potential losses of fluid to evaporation and infiltration, a general mathematical structure requires definition of flows and depths for calculation of each end of a finite increment, Δx, over which the calculation is being made. Specifically, consider the following definitions:

q_1, y_1 - the flow and depth at downstream location, and,
q_2, y_2 - the flow and depth at upstream location.

where potentially, $q_1 = q_2$ (if evaporation and infiltration fluxes are small).

Employing Manning's equation to represent the friction, and substituting (2.3) into (2.12), obtains:

$$x_{n+1} = x_n + 1/2[(y_2 + \frac{q_2^2}{2gy_2^2}) - (y_1 + \frac{q_1^2}{2gy_1^2})] \cdot$$

$$[(S_o - \frac{q_2^2 n^2}{C_m^2 y_2^{10/3}})^{-1} + (S_o - \frac{q_1^2 n^2}{C_m^2 y_1^{10/3}})^{-1}] \qquad (2.13)$$

Rewriting (2.13) for more clarity of analysis, obtains

$$x_{n+1} = x_n + \left[\frac{y_2 - y_1}{2} + \frac{1}{4g}\left(\frac{q_2^2}{y_2^2} - \frac{q_1^2}{y_1^2}\right)\right] \cdot$$

$$\left[\left(S_o - \frac{q_2^2 n^2}{C_m^2 y_2^{10/3}}\right)^{-1} + \left(S_o - \frac{q_1^2 n^2}{C_m^2 y_1^{10/3}}\right)^{-1}\right] \qquad (2.14)$$

The computer model has been structured to solve Equation (2.14). Obviously, when there is no infiltration/evaporation, the model could be simplified, but in the form of (2.14), it retains a generalized, mechanistic character.

The initiation of the calculations is commenced at the location of the leading edge or bore (i.e., at $x_1 = 0$, depth y_a = the surface affinity depth). The surface affinity depth is calculated from

$$y_a = \sqrt{\frac{2\gamma(1-\cos\theta)}{\rho_g}} \qquad (2.15)$$

where ρ_g = fluid density, γ = surface tension at the fluid-air interface, and θ = the contact angle between the fluid and the solid surface. The temperature dependency of these coefficients is to be noted.

It is to be noted that Thibodeau (1977) employed Equation (2.15) and related phenomena in examining spills in a flowing aqueous environemnt.

2.3.3 Complicating Aspects of the Mathematical Formulation

As with all models, there are situations where difficulties arise and this spill process is certainly no exception. A number of difficulties were encountered during the model development:

i) The numerical model can converge to the wrong surface profile. This situation can arise when the surface affinity depth is less than the critical flow depth, a condition which does not match any of the alternatives for surface calculations as depicted in Figure 2.2. To avoid this problem a simple extrapolation procedure is used in the model as schematically depicted in Figure 2.3.

ii) No information was identified in the technical literature dealing with frictional resistance for fluids other than water. Consequently, the development of an adjustment procedure for other fluids is required (see Section 4.2.3).

iii) To increase the model's computational speed, accuracy was sacrificed. This can lead to a calculated profile which is "lumpy" and must be manually smoothed. A smoother profile can also be obtained by re-defining the convergence criteria (typically $y = y_2 - y_1$, is the most critical) but at the expense of a longer execution time.

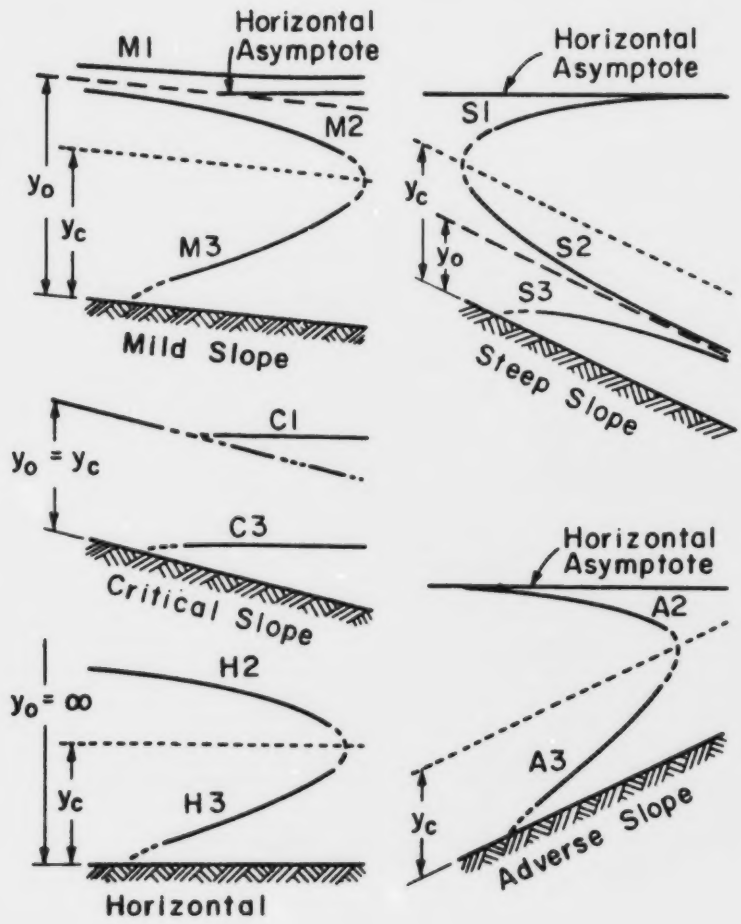

Figure 2.2 Standard Profile Types

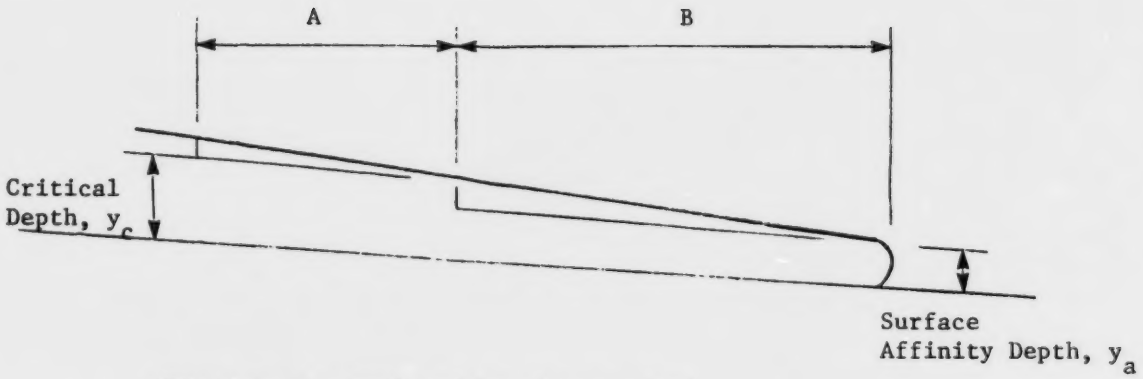

-Distance A calculated by the standard equation, Equation 2.12

-Distance B calculated by similarity of triangles and assuming a straight-line surface profile over the regions A and B

Figure 2.3 Extrapolation Procedure when Surface Affinity Depth < Critical Depth

3.0 PHYSICAL MODELLING

3.1 GENERAL

A review of the technical literature failed to identify any measurements of chemical spreading on solid surfaces, either from experimental or actual spills, which could be used to validate a comprehensive surface-spreading model. Therefore, a major component of this study was an experimental program to gather such data.

3.2 EXPERIMENTAL SET-UP

The experimental work was conducted in the relatively large-scale test beds illustrated in Figure 3.1. The basins were constructed with perforated bottoms to prevent flooding of the soil layer and to allow the measurement of chemical infiltration during the sod-over-soil tests.

Both two-and three-dimensional tests were conducted within the study. The 2-dimensional tests included the addition of chemical to both horizontal and sloped surfaces (See Figure 3.1). For the horizontal tests, the chemical source was applied to the centre of the surface with measurements then taken at both sides of the source for duplication of results. In the sloped tests, the chemical was applied to the elevated end of the platform with measurements made downstream from the source.

A smaller number of tests were conducted in the 3-dimensional test facility illustrated in Figure 3.1. Infiltration, chemical depth and spreading rate were measured radially from a central chemical source in these experiments.

The series of photos labelled as Figures 3.2 to 3.7 further illustrate the experimental set-up. Figure 3.2 is an overall view of the 2-d test arrangement with the liquid discharge point positioned in the centre of the horizontal test bed. Figure 3.3 is a close-up of the constant-head arrangement used for the

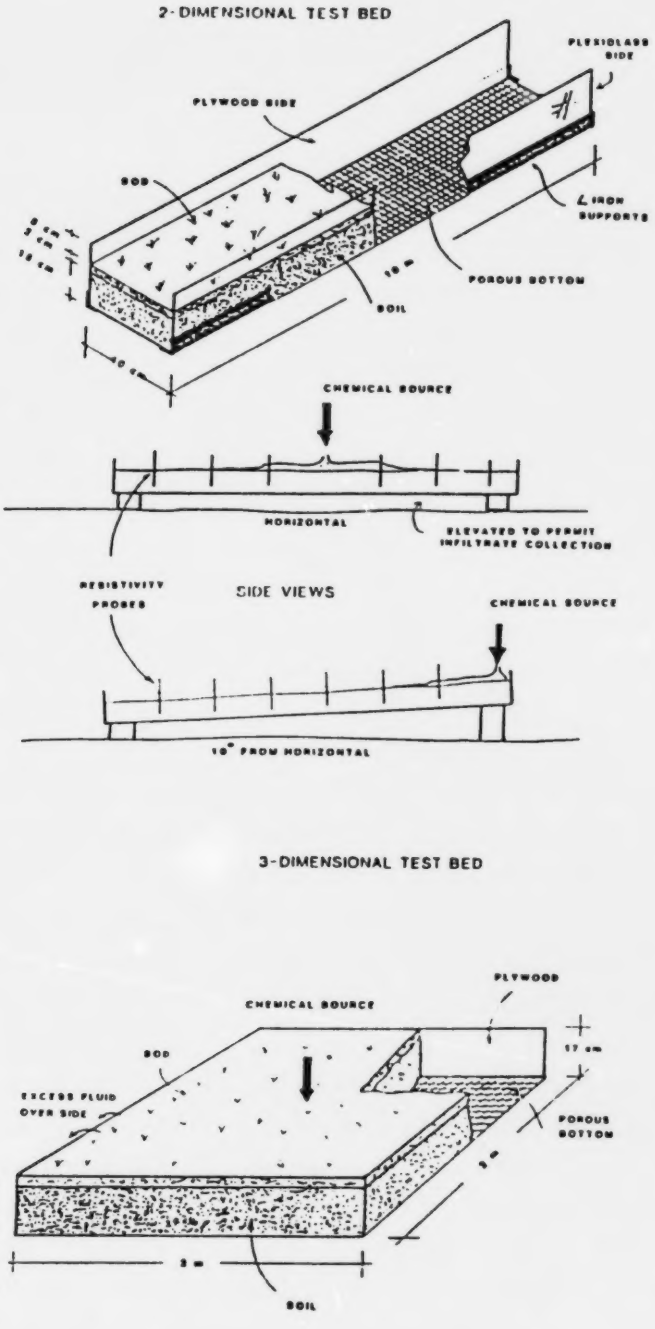

Figure 3.1 Schematics of Test Beds Used in Testing

discharge of chemical. The bottom of the column was fitted with an adjustable slot for the 2-d tests which created a uniform flow across the width of the basin. In the 3-d tests a point source (round hole) was used for the discharge. Flow rates were controlled by varying the slot width or hole diameters. Figures 3.4 and 3.5 illustrate the set-ups for the sloped 2-d tests and 3-dimensional tests respectively. The vertical resistivity probes seen in the 3-d test were used to monitor the radial spreading rate of the chemical.

Figures 3.6 and 3.7 show the two test beds with sod in place. The sensitivity probes and data acquisition system used to measure spreading and infiltration rates can be seen in Figure 3.6.

3.3 TESTED CONDITIONS

The following conditions were varied during the testing.

1) surface type
2) chemical flow rate
3) chemical type
4) test bed slope

Two surface types were studied during the testing. Plywood was utilized to simulate an impermeable surface because of its logistical advantages and the consistent roughness which it provided. The second surface studied was natural sod placed over a loosely packed top-soil. This media provided a highly permeable situation and a realistic roughness parameter.

Chemical flow rates were generally maintained in the 20 to 80 l/min range. These flows provided measurable spreading rates and chemical depths while not requiring large quantities of liquid or special pumping systems.

Water was the primary "chemical" used in this test for obvious reasons. In order to evaluate the effects of viscosity on the speading process Carboxy-Methyl-Cellulose (CMC) was added to water to increase its viscosity.

Figure 3.2
Two Dimensional Test Bed With Plywood Surface

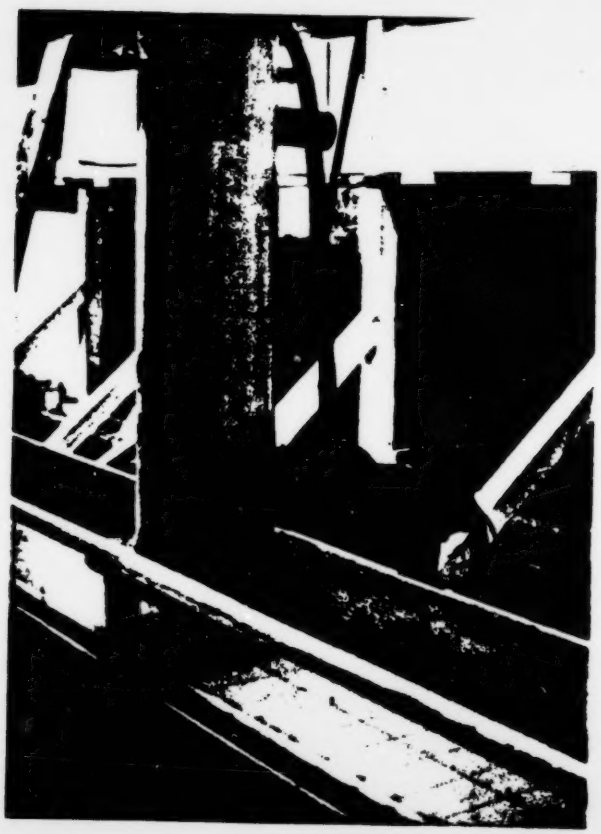

Figure 3.3
Constant Head
Discharge Tank

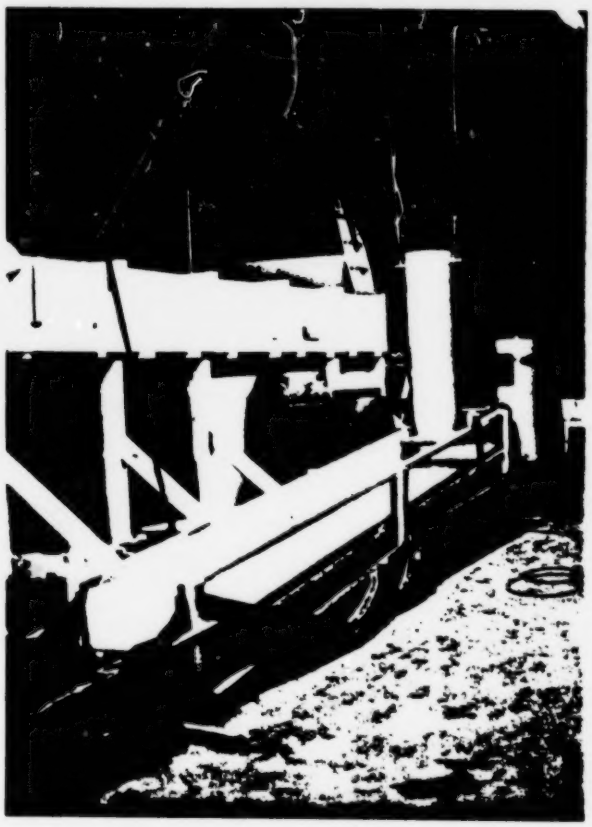

Figure 3.4
Two Dimensional
Sloped Bed With
Plywood

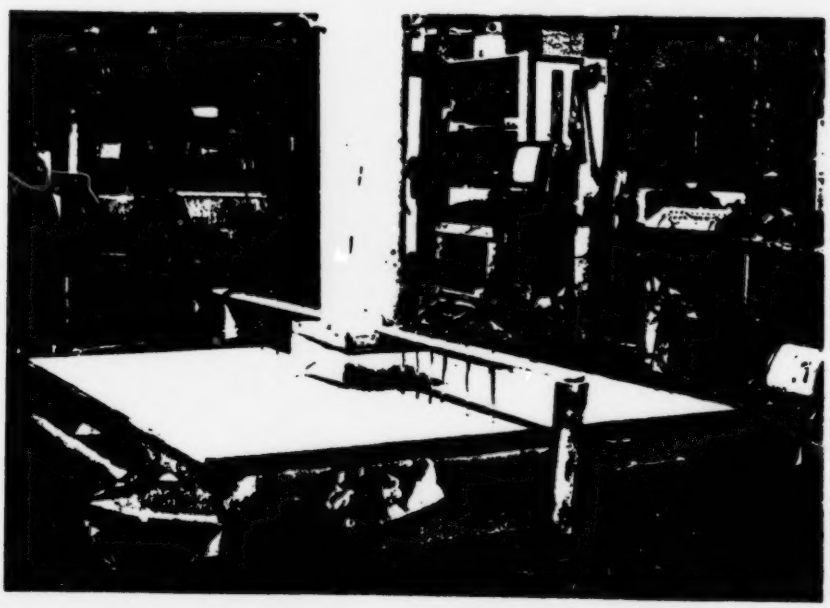

Figure 3.5 Three Dimensional Test Bed With Plywood
(Resistivity probes used for timing spreading rate)

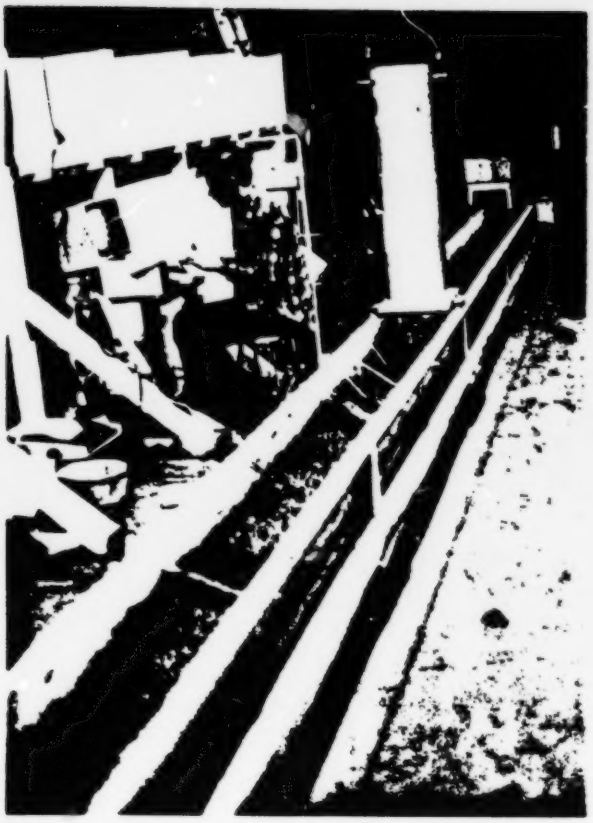

Figure 3.6

Two Dimensional Test Bed With Soil and Sod Surface (Note Resistivity Probes and Data Acquisition System)

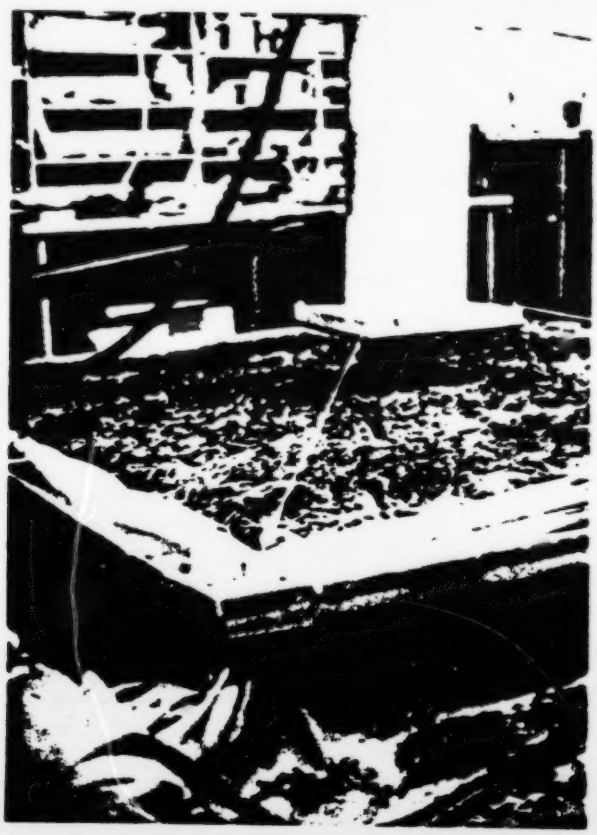

Figure 3.7

Three Dimensional Test Bed With Soil and Sod Surface

This worked well in the plywood tests but problems were encountered in the sod experiments. It appears that soil particles can absorb or "strip" the CMC from the doped-water thus reducing its viscosity. The viscosity values reported in this document for the sod experiments are therefore best-estimates of the liquid viscosity during each test.

Tests were conducted for both horizontal and sloped (10^{o} from horizontal) surfaces.

A summary of the test conditions and an associated run number for each experimental run is shown in Table 3.1. Subsequent reference to the individual experiments will use these designated run numbers.

Table 3.1 Summary of Run Experiments

Run No.	Fluid Viscosity	Slope	Surface	Flow Rate ($m^3/s.m$)
2-Dimensional				
1	water	flat	plywood	.00046
2	water	flat	plywood	.0012
3	water	flat	plywood	.0017
4	water	10°	plywood	.00140
5	water	10°	plywood	.00306
6	water	10°	plywood	.00386
7	water	flat	sod	.00048
8	water	flat	sod	.0012
9	water	flat	sod	.0017
10	water	10°	sod	.00096
11	water	10°	sod	.0024
12	water	10°	sod	.0034
13	c = 15	flat	plywood	.00038
14	c = 15	flat	plywood	.00187
15	c = 15	flat	plywood	.0020
16	c = 46	flat	plywood	.00032
17	c = 46	flat	plywood	.0015
18	c = 46	flat	plywood	.0018
19	c = 65	10°	plywood	.00061
20	c = 65	10°	plywood	.0030
21	c = 65	10°	plywood	.00368
22	c = 5	flat	sod	.00038
23	c = 5	flat	sod	.00118
24	c = 5	flat	sod	.00169
25	c = 15	flat	sod	.00048
26	c = 15	flat	sod	.00120
27	c = 15	flat	sod	.00169
3-Dimensional				
28	water	flat	plywood	.00048
29	water	flat	plywood	.00108
30	water	flat	plywood	.0016
31	c = 9	flat	plywood	.00096
32	c = 9	flat	plywood	.00107
33	c = 60	flat	plywood	.00052
34	c = 60	flat	plywood	.00125
35	c = 60	flat	plywood	.0018
36	water	flat	sod	.0011
37	water	flat	sod	.0016
38	water	flat	sod	.0021

3.4 SUMMARY OF TEST METHODS

The following points describe the major steps necessary to prepare for, and complete, tests on the plywood and sod surfaces.

Plywood Surfaces

i) The chemical source was positioned and the appropriate flow rate set by adjusting the area of the discharge opening. A constant head tank was utilized to maintain a constant flow rate throughout the test.

ii) Flow depth markers positioned along the centre-line of the flow path were coated with a "water-indicating" paste. This paste changed colour when in contact with water and thus permitted the measurement of the "high-water" profile after the test was completed.

iii) The flow was then started and the chemical's spreading rate determined by timing the arrival of the chemical front at each of the flow-depth markers.

iv) When the chemical reached the end of the test bed, the flow was stopped.

v) The maximum water depth profile reached during the test was then measured from the flow depth markers and the test bed dried for the next test.

Sod Tests

i) Soil was placed in the test bed in 2 separate 7.5 cm lifts compacted each time by passing a 20 kg roller over the levelled surface (finished depth approximately 15cm).

ii) After the second layer was placed and rolled, the surface received a final levelling to ensure an even flow of chemical to either side of the source.

iii) The sod was placed over the soil and rolled in place to improve the contact between the sod and soil.

iv) A corner of the sod was then lifted and a core sample of soil was taken and weighed to provide a pre-test measure of the soil's bulk density and porosity.

v) The sod surface was "broomed" to create a consistent surface roughness between tests.

vi) Flow depth markers were placed in the sod and coated with water-indicating paste (as in the plywood tests).

vii) Electrical conductivity probes were placed at 1 metre intervals along the flow's path on the sod surface, in the centre of the soil layer and at the bottom of the soil layer. These were connected to a computer data acquisition system described elsewhere (Belore, 1981). The time at which chemical passed by each probe was measured and recorded by the computer. Surface spreading and infiltration rates were measured automatically by this system.

viii) The chemical source was positioned and adjusted for the appropriate flow rate, as in the plywood tests.

ix) The flow was started and the chemical spreading rate measured manually as a check of the automated system and also as a precaution in the event of a failure of the automated system.

x) The flow was stopped after 200 litres of chemical was applied.

xi) The water depth profile was measured from the depth markers.

xii) The quantity of water which ran out the ends of the test basin was measured, as was the quantity which infiltrated through the complete soil layer.

xiii) Finally, a second set of soil core samples were taken to determine post-test soil conditions.

xiv) The saturated soil was then discarded and a new soil layer placed in the test bed to ensure similar soil conditions between tests.

The results of the experiments are summarized in Section 4 along with those of the mathematical modelling component of this study.

4.0 COMPARISON OF COMPUTED AND PHYSICAL MODELLING PROFILES

4.1 INTRODUCTION

To a degree, a computer model can be calibrated to physical modelling data. For the spill model developed in this study, the "fitting" coefficients are:

(i) Manning coefficient - for the physical experiments carried out on the plywood; and,

(ii) Manning coefficient, initial infiltration and infiltration decay coefficients - for the sod experiments.

Maximum depth and location of the bore were used as the primary fitting parameters. However, in the calibration efforts for the various physical model runs, the focus was on obtaining representative behaviour while retaining consistency in the parameters from one run to another. "Over-calibration" is a potential problem particularly for the experiments using sod where there is variability between sod conditions (e.g., roughness and initial water content) and uncertainty in the measurements. This concern will be apparent in the results to follow.

Most of the plots showing the physical and computer modelling results are included as Appendix I rather than the main text itself, to enhance the readability of the text. Several results are included within the text to demonstrate the general nature of the findings.

In presenting the results, the run number has been employed throughout to relate to the original set of physical modelling experiments. The summary characteristics associated with each run were documented in Table 3.1.

4.2 TWO-DIMENSIONAL ANALYSES

4.2.1 Modelling Results Using Water

Twelve experiments involving water were carried out, with the results indicated in Table 4.1, and example plots as Figure 4.1 (for plywood) and 4.2 (for sod). Apparent from the results in Appendix I, not all results are as favourable as those illustrated in Figures 4.1 and 4.2. The input data values used for each of the computer modelling experiments, are summarized in Table III.1.

As summary comments, the following are appropriate:

(i) the modelling of the plywood spills was very successful. The modelling of spills on sod were more difficult due to variable infiltration rates. As expected, the Manning coefficient is very difficult to assign. This concern is particularly relevant for grassed areas (for flow between grass blades, the extent to which the grass blades bend, impacts on the frictional resistance). There is even some difficulty in assigning the Manning coefficient for plywood, in part because at low depths of flow, the coefficient is a function of depth.

(ii) with the sod, and under sloped conditions, the computer model underpredicts the velocity of the leading edge movement. This concern warranted an adjustment in the mathematical model, for the reasons outlined below.

4.2.2 Impact of Different Surface Slopes

When the surface slope is "sufficiently" large, a different profile results. This occurs when the so-called "normal depth" is smaller than the "critical depth". Pictorially, it is apparent when $Y_n > Y_c$, profile type M2 from Figure 4.3 occurs and when $Y_c > Y_n$, profile type S2 occurs. Therefore, depending on the initial depth, the flow assumes a different surface profile when the channel is sloping.

Table 4.1 Modelling Results of Water - Two-Dimensional Analyses

Run No.	Slope Condition	Surface Condition	Flow Rate(*) $m^3/s.m$	Manning Coefficient (best-fit value)	Infiltration Initial (m/hr)	Infiltration Decay Coeff. (1/hr)	Maximum Depths (mm) Measured	Maximum Depths (mm) Computed
1	flat	plywood	.00046	.01	0	0	9,8,8,10	7
2	flat	plywood	.0012	.005	0	0	10,9,9.5,10	9
3	flat	plywood	.0017	.005	0	0	9,12,11,13	10
4	10° slope	plywood	.0014(**)	.015	0	0	8,10,9	3
5	10° slope	plywood	.0031(**)	.015	0	0	11,10,10	4
6	10° slope	plywood	.0039(**)	.015	0	0	11,11,10	5
7	flat	sod	.00048	.75	1.3	.005	25,25	27
8	flat	sod	.0012	.65	2.5	.005	38,47,37,38	53
9	flat	sod	.0017	.65	2.5	.005	45,41,37,37,33,35	67
10	10° slope	sod	.00096(**)	.05	2.5	.007	25	79
11	10° slope	sod	.0024(**)	.05	2.5	.007	40	177
12	10° slope	sod	.0034(**)	.075	2.5	.007	34	219

Notes - all of the above-indicated results relate to water

- (*) l/min values from the experiments have been translated to $m^3/(sec.m)$. As well, these are flow rates at the location of the spill
- (**) these experiments have flow rates all in one direction, down the slope, as opposed to the experiments on the flat condition which have been presumed to have equal flow in each direction

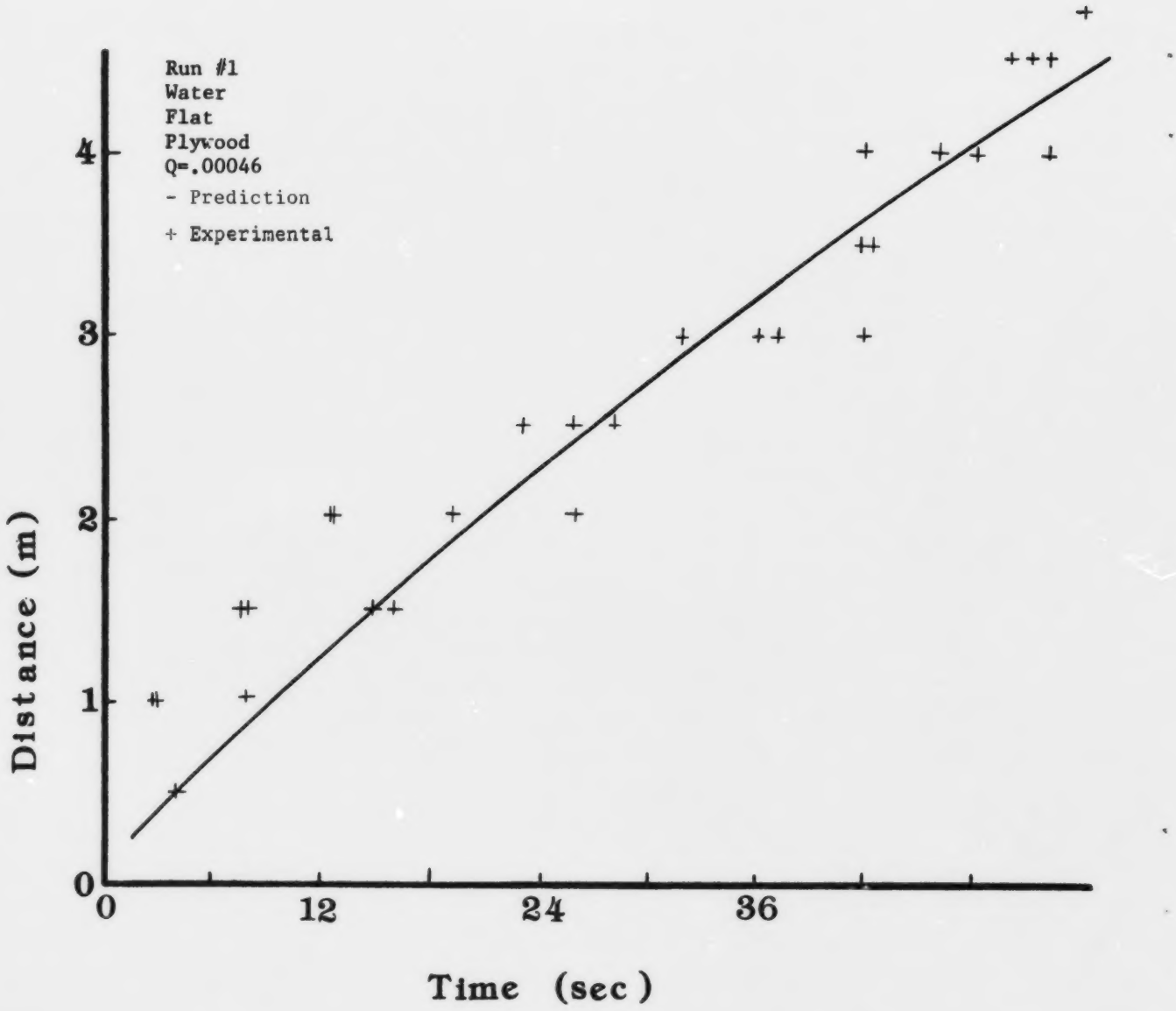

Figure 4.1 Example of Physical and Mathematical Results For Plywood Surface

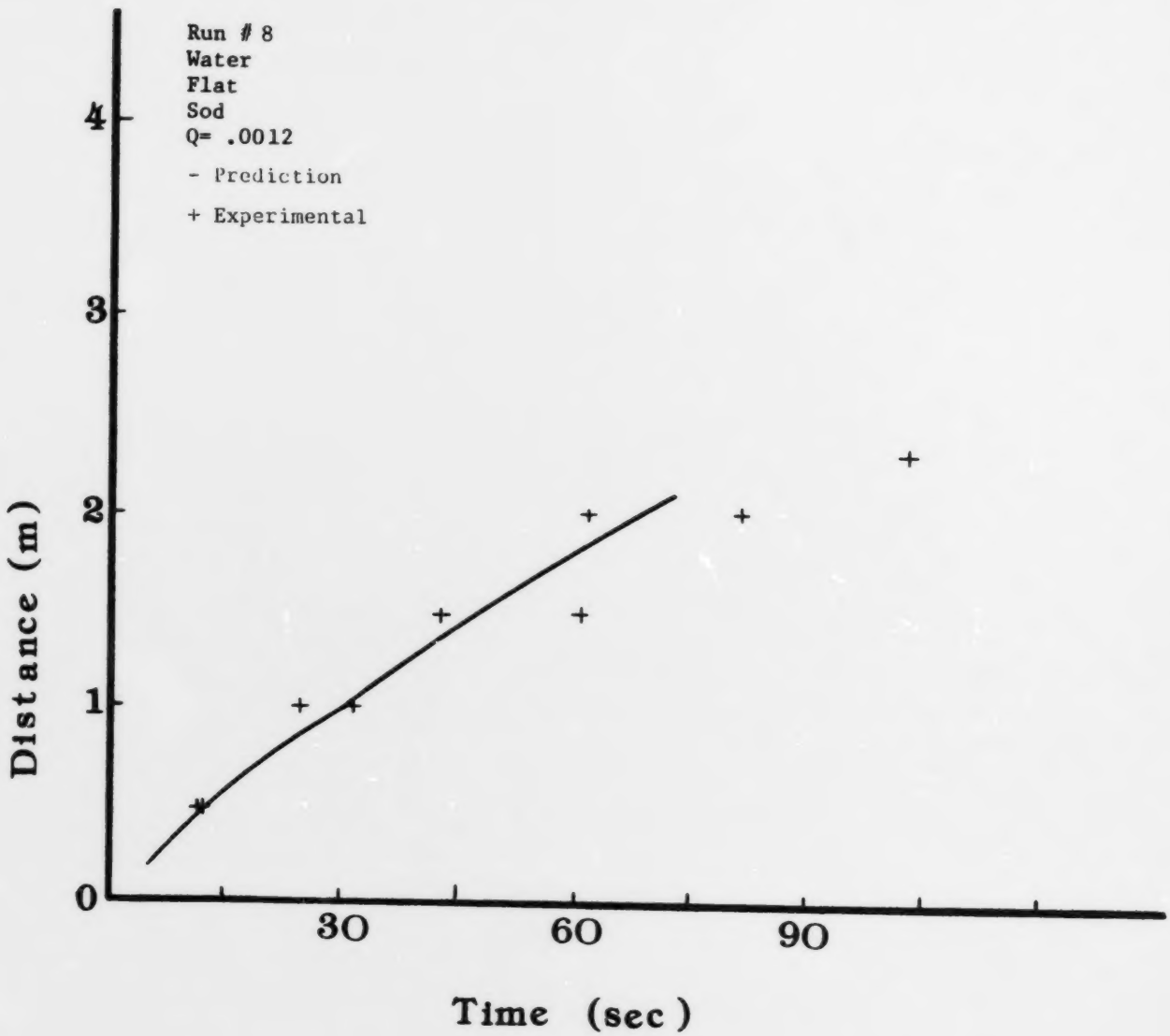

Figure 4.2 Example of Physical and Mathematical Results For Sod Surface

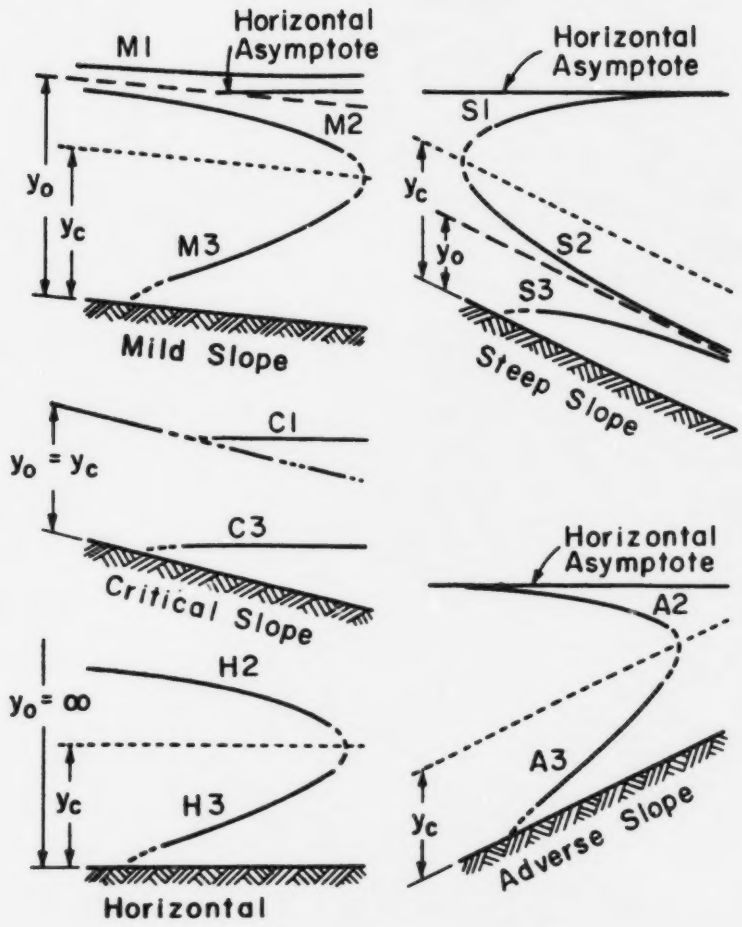

Figure 4.3 Standard Profile Types

The determination of the values for Y_n and Y_c (for a wide rectangular channel) are:

$$Y_c = \left(\frac{q^2}{g}\right)^{1/3} \qquad (4.1)$$

and

$$Y_n = \left(\frac{nq}{S_o^{1/2}}\right)^{3/5} \qquad (4.2)$$

In this formulation Y_n requires the specification of the Manning coefficient, but the Manning coefficient can vary based on both flow depth and liquid viscosity. This presents difficulties, therefore, when attempting to determine the magnitude of Y_n.

From the physical model experiments and calibration efforts, the discrimination to use profile of type "S" is based on $1.5\ Y_n \gtrless Y_c$. When this criteria implies an S-type profile, the model ignores the initial region and the larger of the normal depth or surface affinity depth is employed in determining the extent of excursion of the spill (i.e., a mass balance is employed and momentum, or force balances, are reflected only by the stipulation of the depth). This approach proved valid since the physical and mathematical modelling results compared favorably (e.g. see Figure 4.4 as an example run (which incidentally was developed without calibration of the computer model)).

4.2.3 Impact of Alternative Viscosities

As indicated in Chapter 3, a series of laboratory experiments were carried out using alternative viscosities. A summary of the characteristics of these runs is provided in Table 4.2. The initial five columns of this table summarize the input data to the model and are descriptive of the physical modelling experiments. Additional tabulated information includes:

(i) in column 6, the best-fit Manning coefficient. Recall this is a fitting coefficient, and the tabulated values indicate the results of the calibration;

(ii) columns 7 and 8 contain the infiltration model parameters, again fit to the physical modelling results;

(iii) columns 9 and 10 indicate the maximum depths for measured and computed results, respectively. Apparent from the results is that generally, the results on the plywood are very good. The results for the sod experiments, particularly for the higher viscosities, are not as comparable with respect to the maximum depths.

In the case of spills on a non-infiltrating surface, the only fitting parameter available is the friction coefficient. Engineers are most familiar with this measure and many sources of the coefficient (for water) are reported in the technical literature, providing a good data base. The question remains, however, as to how to reflect different fluid viscosities?

One approach involves use of the base relationship for Manning's friction coefficient (after Rouse (1967)) in which

$$\frac{R^{1/6}}{n} = 28.6\ Re^{1/8} \qquad (4.3)$$

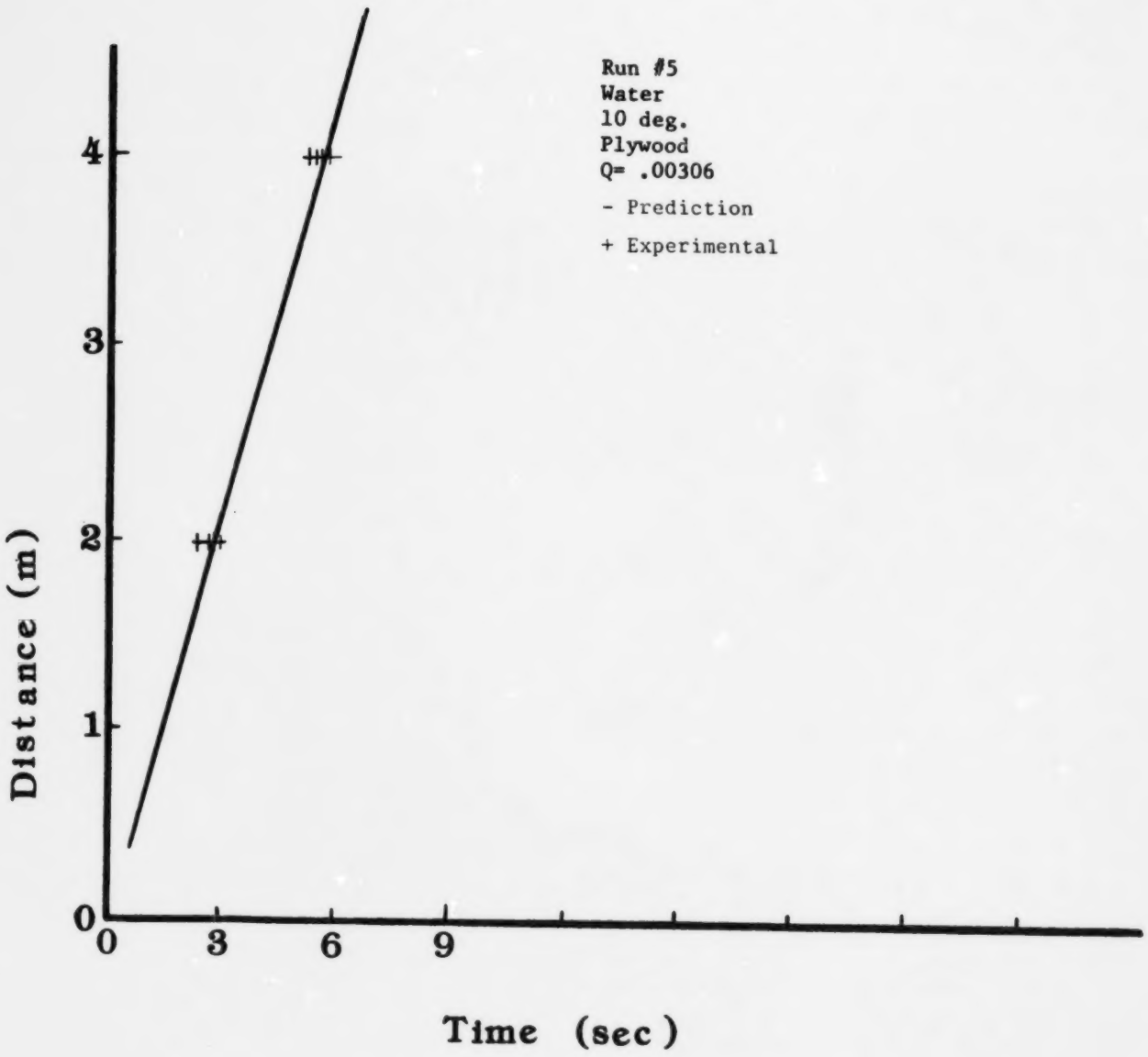

Figure 4.4 Example of Physical and Mathematical Results for Steep Slope Conditions ($Y_c > Y_n$)

Table 4.2 Impact of Alternative Viscosities - Two-Dimensional Analyses

Run No.	Viscosity (C_p)	Slope Condition	Surface Condition	Flow Rate(*) $m^3/s.m$	Manning Coefficient (best-fit value)	Infiltration Initial (m/hr)	Infiltration Decay Coeff (1/hr)	Maximum Depths (mm) Measured	Maximum Depths (mm) Computed
1	1.0	flat	plywood	.00046	.01	0	0	9,8,8,10	7
2	1.0	flat	plywood	.0012	.005	0	0	10,9,9.5,10	9
3	1.0	flat	plywood	.0017	.005	0	0	9,12,11,13	10
13	14.7	flat	plywood	.00038	.10	0	0	17,18,18,19	17
14	14.7	flat	plywood	.00187	.065	0	0	22,22	30
15	14.7	flat	plywood	.0020	.05	0	0	22,24	26
16	45.8	flat	plywood	.00032	.15	0	0	21,21,22,22	17
17	45.8	flat	plywood	.0015	.10	0	0	31,30,30	33
18	45.8	flat	plywood	.0018	.09	0	0	33,33	9(+)
4	1	10° slope	plywood	.00140(**)	.015	0	0	8,10,9	3
5	1	10° slope	plywood	.00306(**)	.015	0	0	11,10,10	4
6	1	10° slope	plywood	.00386(**)	.015	0	0	11,11,10	5
19	65	10° slope	plywood	.00061(**)	.13	0	0	7,7	6(+)
20	65	10° slope	plywood	.00300(**)	.06	0	0	15,15	10(+)
21	65	10° slope	plywood	.00368(**)	.055	0	0	16,13	10(+)
7	1	flat	sod	.00048	.75	1.3	.005	25,25	27
8	1	flat	sod	.0012	.65	2.5	.005	38,47,37,38	53
9	1	flat	sod	.0017	.65	2.5	.005	45,41,37,37,33,35	67
22	5	flat	sod	.00038	1.55	1.25	.003	25,30	51
23	5	flat	sod	.00118	.65	1.25	.003	38,46,38,45	53
24	5	flat	sod	.00169	.65	1.25	.003	42,47	65
25	15	flat	sod	.00048	1.75	1.50	.02	35,35	59
26	15	flat	sod	.00120	.65	1.50	.02	45,47,40,45	55
27	15	flat	sod	.00169	.65	1.3	.02	50,40	65

Notes - (*) L/min values from the experiments have been translated to $m^3/(sec.m)$
As well, these are flow rates at the location of the spill

- (**) These experiments have flow rates all in one direction, down the slope, as opposed to the experiments on the flat condition which have been presumed to have equal flow in each direction
- (+) encountered critical flow condition

where R = hydraulic radius, Re = Reynolds number, and "28.6" is a coefficient, the result of fitting to experimental data. Rewriting Equation (4.3), but expanding the terms and setting the initial constant as c = 28.6, provides

$$\frac{1}{n}\left(\frac{bd}{b+2d}\right)^{1/6} = c\left(\frac{vd}{\nu}\right)^{1/8} \qquad (4.4)$$

Using the equation of continuity and rewriting (4.4) gives

$$n = \frac{1}{c}\left(\frac{\nu b}{Q}\right)^{1/8}\left(\frac{bd}{b+2d}\right)^{1/6} \qquad (4.5)$$

A change in n due to a change in fluid viscosity, ν , then may be determined by the ratio

$$\frac{n'}{n} = \frac{\left(\frac{\nu'}{Q'}\right)^{1/8}\left(\frac{d'}{b+2d'}\right)^{1/6}}{\left(\frac{\nu}{Q}\right)^{1/8}\left(\frac{d}{b+2d}\right)^{1/6}} \qquad (4.6)$$

where the prime(') indicates modified values due to the new flow conditions (viscosity, flow rates, hydraulic radius). (Note, the 'c' and 'b' cancel because they were not changed during the physical modelling experiments).

Investigations using Equation (4.6) proved that n' was consistently being underpredicted; nevertheless, the general form of the equation provides interesting variable ratios. Consequently, an equation of the form

$$\frac{n'}{n} = \left(\frac{\nu'_0}{\nu_0}\right)^{1/x} \left(\frac{\frac{d'}{b+2d'}}{\frac{d}{b+2d}}\right)^{1/6} \qquad (4.7)$$

is proposed where the computer output results were used to estimate 'x'. The results of the 'curve-fitting' are contained in Table 4.3. The similarity in magnitudes of x as computed from the various combinations of runs indicates the procedure has utility.

It is to be noted that there is an unknown magnitude of uncertainty in the physical experimental results because of potential changes in the viscosity. The viscosity of water was changed, as noted in Chapter 3, by the addition of carboxy methyl cellulose. During the progress of the experiment the viscosity potentially changes as the grass blades tend to "strip" away some of the cellulose additive used in doping the water.

4.2.4 Characterization of Infiltration and Evaporation Rates

The computer model contains both an infiltration and an evaporation component. However, none of the physical experiments focussed on the evaporative flux component since, for the liquids considered, this component is negligible during the period of the experiment. As well, there is a significant technical literature available dealing with the evaporation of highly volatile liquids under free surface conditions. Consequently, all of the following discussion relates only to the infiltration component.

Table 4.3 Estimates of Exponent for Predicting Manning's Coefficient for Variations in Viscosity

Run Numbers	Fitted Value of 'x'
1 and 13	1.19
1 and 16	1.50
2 and 14	.91
2 and 17	1.23
3 and 15	1.11
3 and 18	1.23

Notes The fitted values of x used Equation (4.7) and input values in accord with the Q, b, d, d' and v and v'. It is to be noted, that Q and Q' were retained in Equation (4.7) as a means of reflecting the variations in flows between laboratory experiments.

A comparison of the infiltration results of the mathematical and physical modelling are contained in Table 4.4. Several explanatory points are appropriate:

(i) the initial infiltration levels and exponential die-offs for the infiltration used in the mathematical model are higher than those generally reported in the technical literature. The magnitudes used in the modelling were necessary, to provide reasonable comparisons with the physical modelling results. This may be due to the substantial volume of fluid flowing over the sod (much more so than with rainfall, which is the basis for the reported technical literature values), and the relatively dry and loosely-compacted initial conditions present in the physical modelling work.

(ii) there are many values of parameters which would have provided comparable curves (i.e., the results are not overly sensitive to variable input parameters, at least within engineering judgement). On the other hand, there are insufficient data to warrant a continued refinement of the data. As well, on individual plots, the fit between physical and mathematical results could have been improved, but the input values corresponding from run to run would have become inconsistent;

(iii) the infiltration representation is at a relatively simple level to keep the model easy to use. During the use of the mathematical model, if the infiltration rates were set too high, the leading edge of the spill "ran out of water" and the execution of the model terminated; and,

(iv) the final comment is that detailed data for use in real-world applications is unlikely to be extensive; of primary interest, therefore, is the ability to calculate the behaviour and to provide the opportunity for easy sensitivity testing.

Table 4.4 Comparison of Mathematical and Physical Modelling Results for Infiltration Prediction

Run No.	Slope Condition	Viscosity	Flow Rate (*) (l/min)	Infiltrate. Rate Initial (m/hr)	Infiltrate. Rate Decay (l/hr)	Infiltration Volume as a Percent of Spilled Fluid Calculated (percent)	Infiltration Volume as a Percent of Spilled Fluid Measured (percent)
7	flat	C=1	.00048	1.3	.005	79	nm
8	flat	C=1	.0012	2.5	.005	59	76
9	flat	C=1	.0017	2.5	.005	48	nm
22	flat	C=5	.00038	1.25	.003	57	nm
23	flat	C=5	.00118	1.25	.003	28	48
24	flat	C=5	.00169	1.25	.003	22	nm
25	flat	C=15	.00048	1.50	.02	69	26
26	flat	C=15	.00120	1.50	.02	24	35
27	flat	C=15	.00169	1.3	.02	27	30

Notes: 'nm' refers to not measured

4.3 THREE-DIMENSIONAL ANALYSES

4.3.1 Modelling Results Using Water

In theory, the equations used in Section 4.2 for the two-dimensional model are directly translatable to the three-dimensional model. The major, necessary change, involves usage of an assumption of axisymmetry which assumes that all spill-related concerns radiate away from the spill location in all directions with no changes (as a function of direction). Nevertheless, it was found that the numerical aspects of such a complicated formulation (because of the losses to infiltration and evaporation) are substantial, in both extent of computational effort and in resulting numerical convergence problems (use of successive substitutions often produced spurious answers). As a consequence, the decision was made to utilize a simpler theoretical basis for the three-dimensional model than employed in the two-dimensional model, as will be indicated below.

Use is made of two depths of flow:

i) the surface affinity depth; and,
ii) critical depth.

Both of these depths are approximate measures of flow depths that may exist within the spill (although, as apparent from the two-dimensional analyses, they are shallower than the average depth of the spill profile). With the estimated depths, and knowledge of the duration and flow rate of the spill, the extent of excursion of the spill can be obtained. Given the extent of excursion, estimates of the evaporative and infiltrative fluxes are obtained; these calculations must be done in a second step since they are surface-area related. Given the removal fluxes due to infiltration and evaporation, modifications of the areal extent of excursion of the spill profile are then undertaken.

The resulting model preserves the principle of continuity and reflects the principle of momentum (or force balances) by including only the surface affinity effect. The result of the simplification of the momentum is that the resistance to spill migration is underpredicted and, thus, the predicted extent of the spill migration is overpredicted, i.e., the model predictions are on the conservatively high side, as will be apparent from the comparisons with experimental results. Examples of the model predictions and experimental findings are summarzied in Figures 4.5 and 4.6 for experiments on plywood and sod, respectively.

A summary comparison of the depths of the computed and experimentally-measured results is presented in Table 4.5; the differences in maximum depths are apparent and indicate why the model overpredicts the lateral excursion of the spill. (It is to be noted that there also exists a considerable variation in the experimental findings).

4.3.2 Impact of Alternative Viscosities

The only "fitting" coefficient currently available in the model to reflect alternative viscosities is Manning's coefficient; however, this coefficient is only active in the simple, three-dimensional model formulation, when the slope is nonzero (Manning's coefficient is active in the two-dimensional model through the more detailed mathematical representation of the momentum equation). Nevertheless, the resulting comparisons between measured and computed depths are summarized in Table 4.6; the results are seen to be quite similar and the comparison of computed and measured estimates will improve as the duration of the spill increases

4.4 SENSITIVITY ANALYSES USING THE SPILL MODEL

A series of analyses were carried out to explore the characteristics of the computer model and the spill processes.

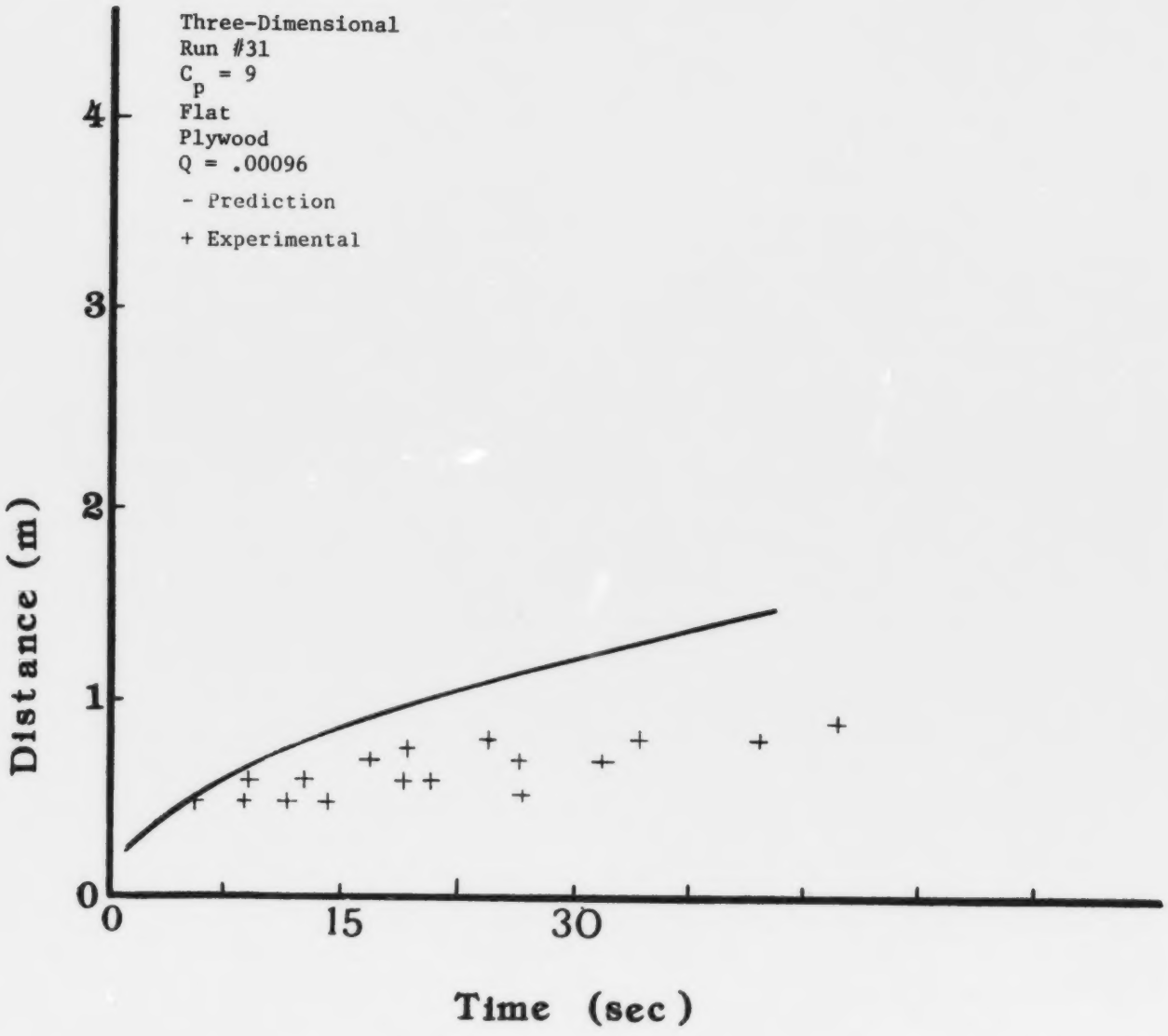

Figure 4.5 Example Prediction by Three Dimensional Model: Plywood

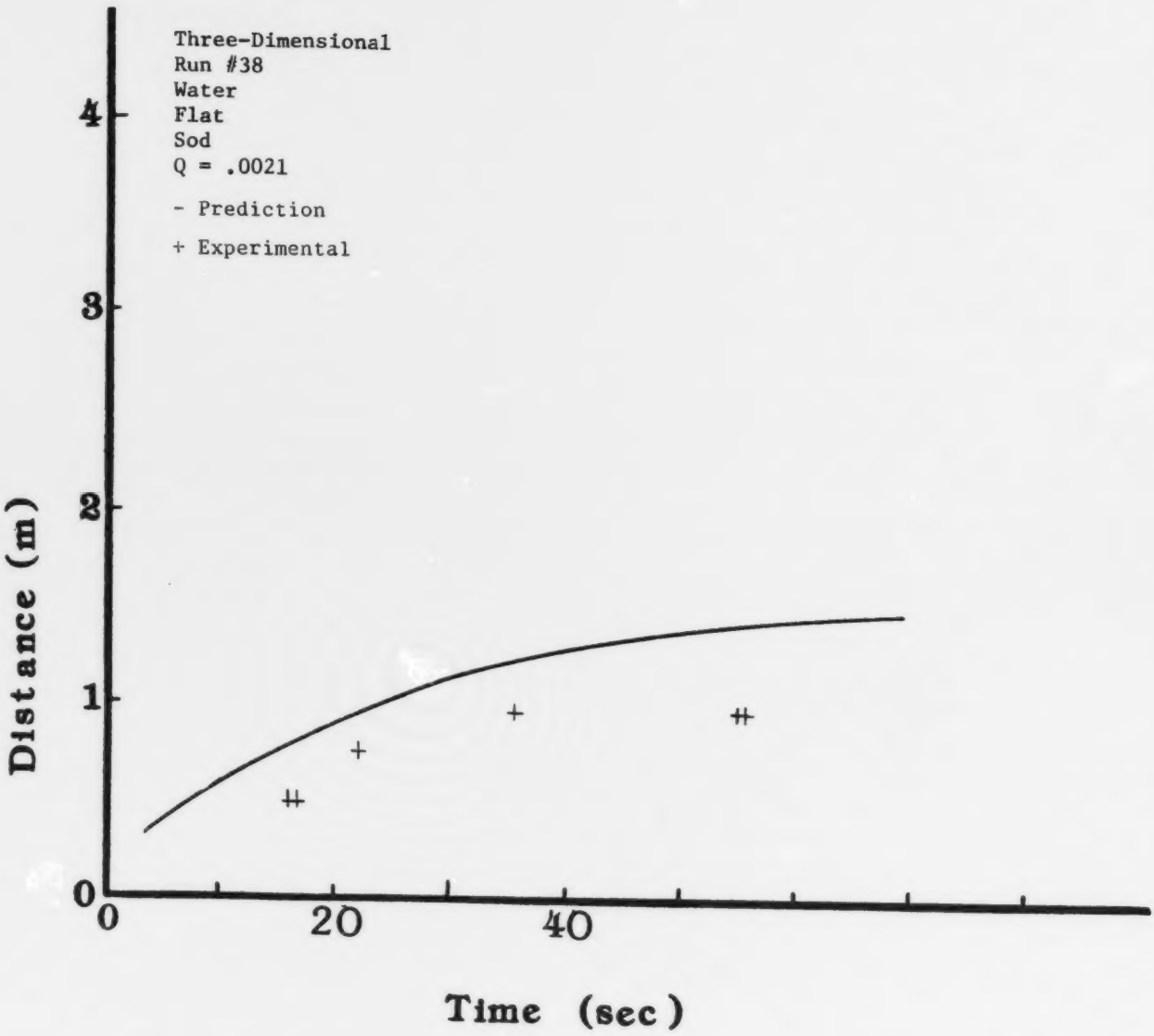

Figure 4.6 Example Prediction by Three Dimensional Model: Sod

Table 4.5 Modelling Results of Water: Three-Dimensional Analyses

Run No.	Surface Condition	Flow Rate (l/min)	Infiltration Initial (m/hr)	Infiltration Decay (l/hr)	Maximum Depths (mm) Measured	Maximum Depths (mm) Computed
28	Plywood	22.04	0	0	6, 11, 9, 8, 7, 7, 8, 6, 6, 6, 3, 3	3
29	Plywood	49.25	0	0	7, 5, 11, 9	5
30	Plywood	73.1	0	0	8, 10, 8, 11, 8, 10, 7, 14	6
36	Sod	49	.7	.005	21,20	5
37	Sod	73.1	.5	.005	20, 30	6
38	Sod	95.	.5	.005	5, 17, 22, 26	8

Table 4.6 Impact of Alternative Viscosities: Three Dimensional Analyses

Run No.	Viscosity (C_p)	Surface Condition	Flow Rate (l/min)	Infiltration Initial (m/hr)	Infiltration Decay Coeff. (l/hr)	Maximum Depths (mm) Measured*	Maximum Depths (mm) Computed
28	1.0	Plywood	22.04	0	0	6, 11, 9, 8, 7, 7, 8, 6, 6, 6, 3, 3	3
29	1.0	Plywood	49.25	0	0	7, 5, 11, 9	5
30	1.0	Plywood	73.1	0	0	8, 10, 8, 11, 8, 10, 7, 14	6
31	8.98	Plywood	22	0	0	9, 9, 10, 9	3
32	8.89	Plywood	49	0	0	10, 10, 11 13	5
33	59.8	Plywood	23.72	0	0	11, 13, 13,	3
34	59.8	Plywood	56.92	0	0	12, 15, 14 16	5
35	59.8	Plywood	82.32	0	0	13, 23, 16 16	7

Notes * Depths taken as the maximum on each surface profile

These analyses include:

i) The computed results arising from alternative infiltration rates in the two-dimensional model (see Figure 4.7). The values used in the model are tabulated below (other input values are associated with Run #7):

Run Designation	Infiltration Rate (m/hr)	Decay Rate (1/sec)	Evaporation Rate (m/hr)
A	1.7	.005	0
B	2.7	.005	0
C	3.7	.005	0

The excursion of the leading edges for the three runs are essentially identical; however, as indicated by the symbols B and C the exhaustion of the spill processes for the higher infiltration rates occurs (i.e., with 3.7 m/hr, the leading edge excursion only over .64 m distance).

ii) The computed results for the 2.7 m/hr infiltration rate, in combination with nonzero evaporation rates (see Figure 4.8). The values used in the model are tabulated below (other input values are associated with Run #7):

Run Designation	Infiltration Rate (m/hr)	Decay Rate (1/sec)	Evaporation Rate (m/hr)
A	2.7	.005	0
B	2.7	.005	.05
C	2.7	.005	1

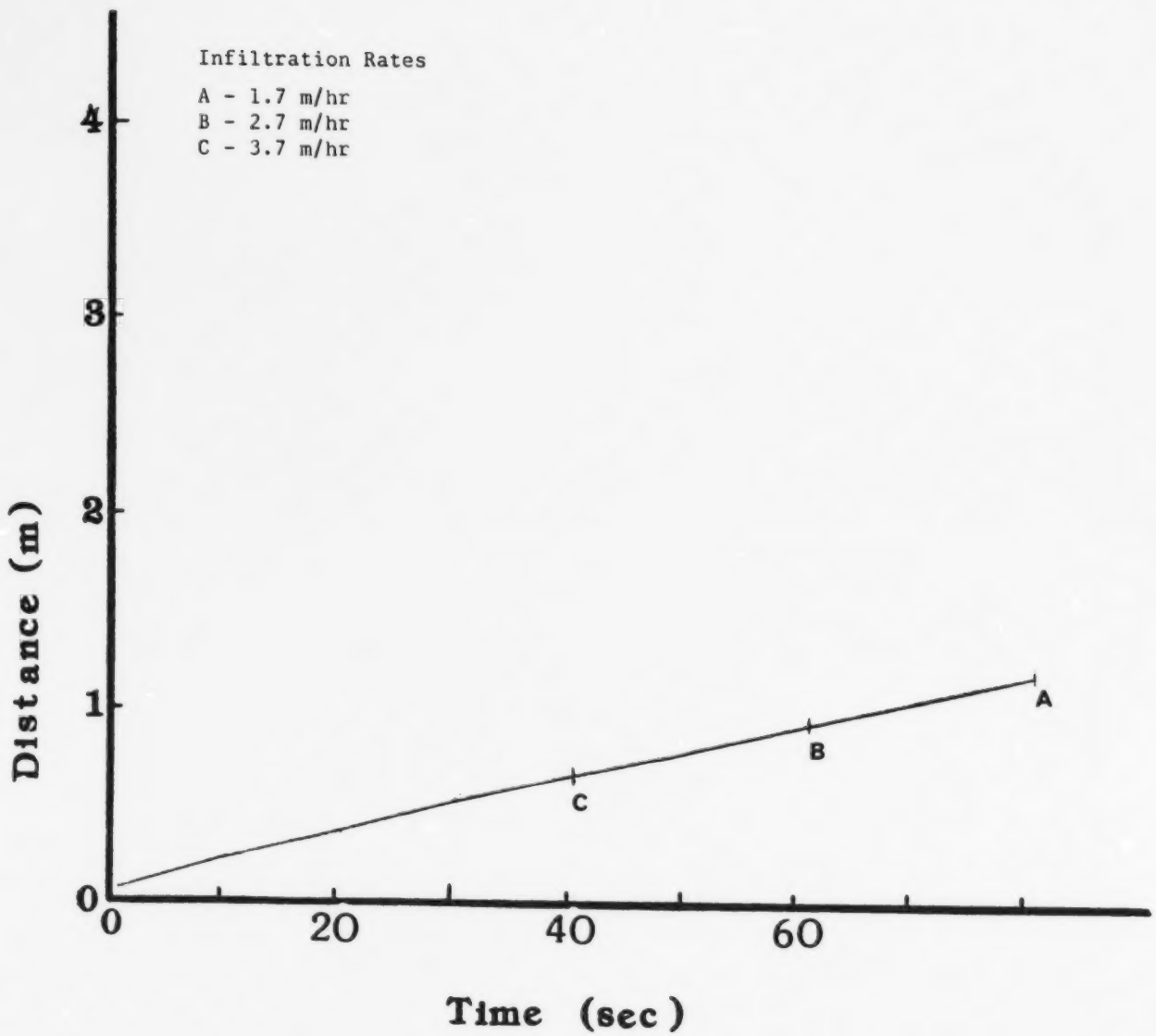

Figure 4.7 Sensitivity of Two-Dimensional Modelling Results to Alternative Infiltration Rates

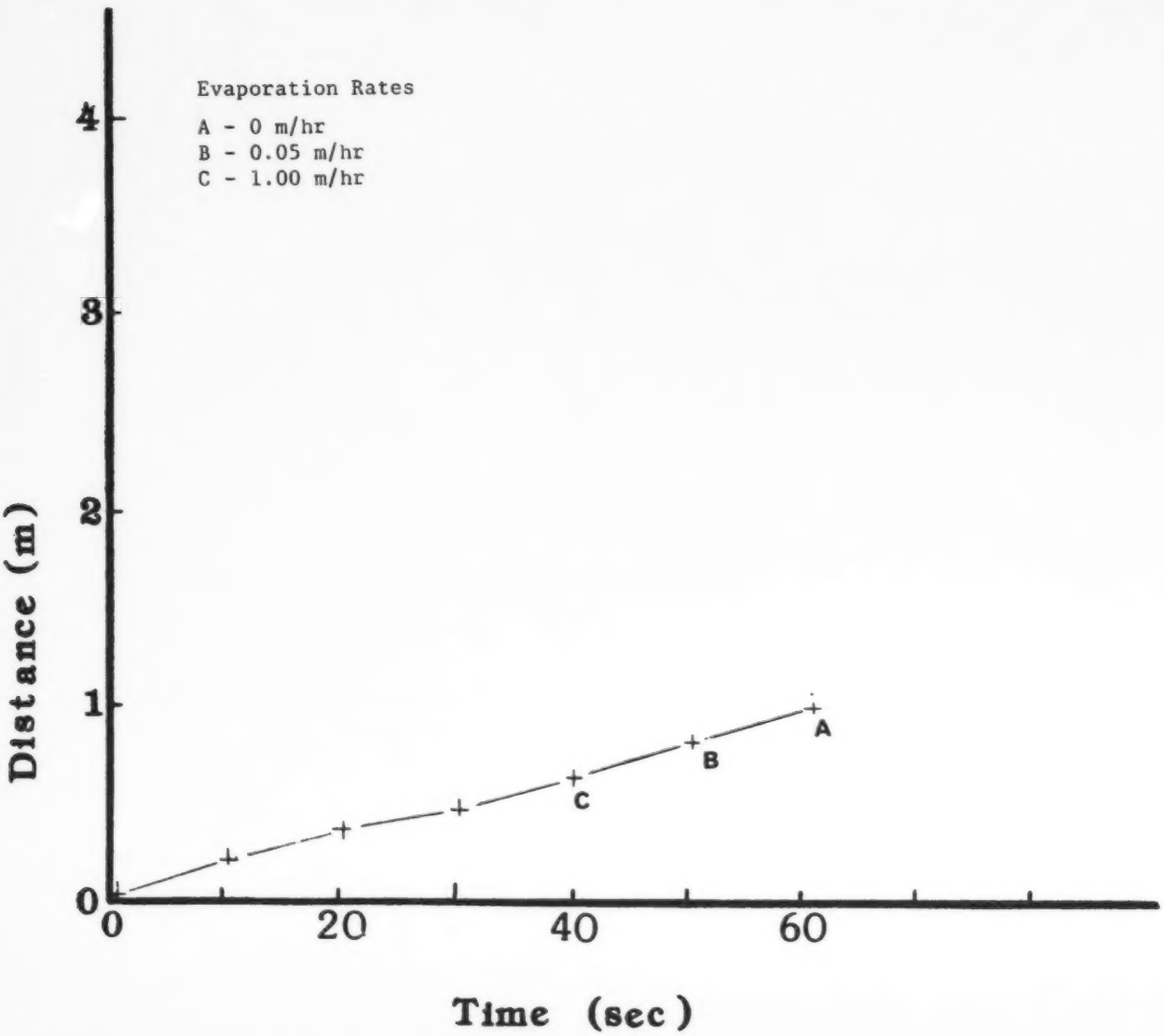

Figure 4.8 Sensitivity of Two-Dimensional Modelling Results to Alternative Evaporation Rates

In a similar manner to i) above, the excursion of the leading edges for the three runs are essentially identical; however, the symbols A, B and C indicate the times and locations of exhaustion of the spill processes for the different combinations of model parameters.

iii) The computed results arising from alternative infiltration rates in the three-dimensional (see Figure 4.9). The values used in the model are tabulated below (other input values relate to Run #36):

Run Designation	Infiltration Rate (m/hr)	Decay Rate (1/sec)	Evaporation Rate (m/hr)
A	.7	.005	0
B	.5	.005	0
C	.3	.005	0
D	.1	.005	0

The curves for A and B show a stoppage of flow (the infiltration volumes exhaust the flow) at the end of curves. In the case of Runs C and D, the infiltration rate is such that the leading edge continues to migrate away from the source of the spill, although for Run C the point of exhaustion is just after 91 seconds.

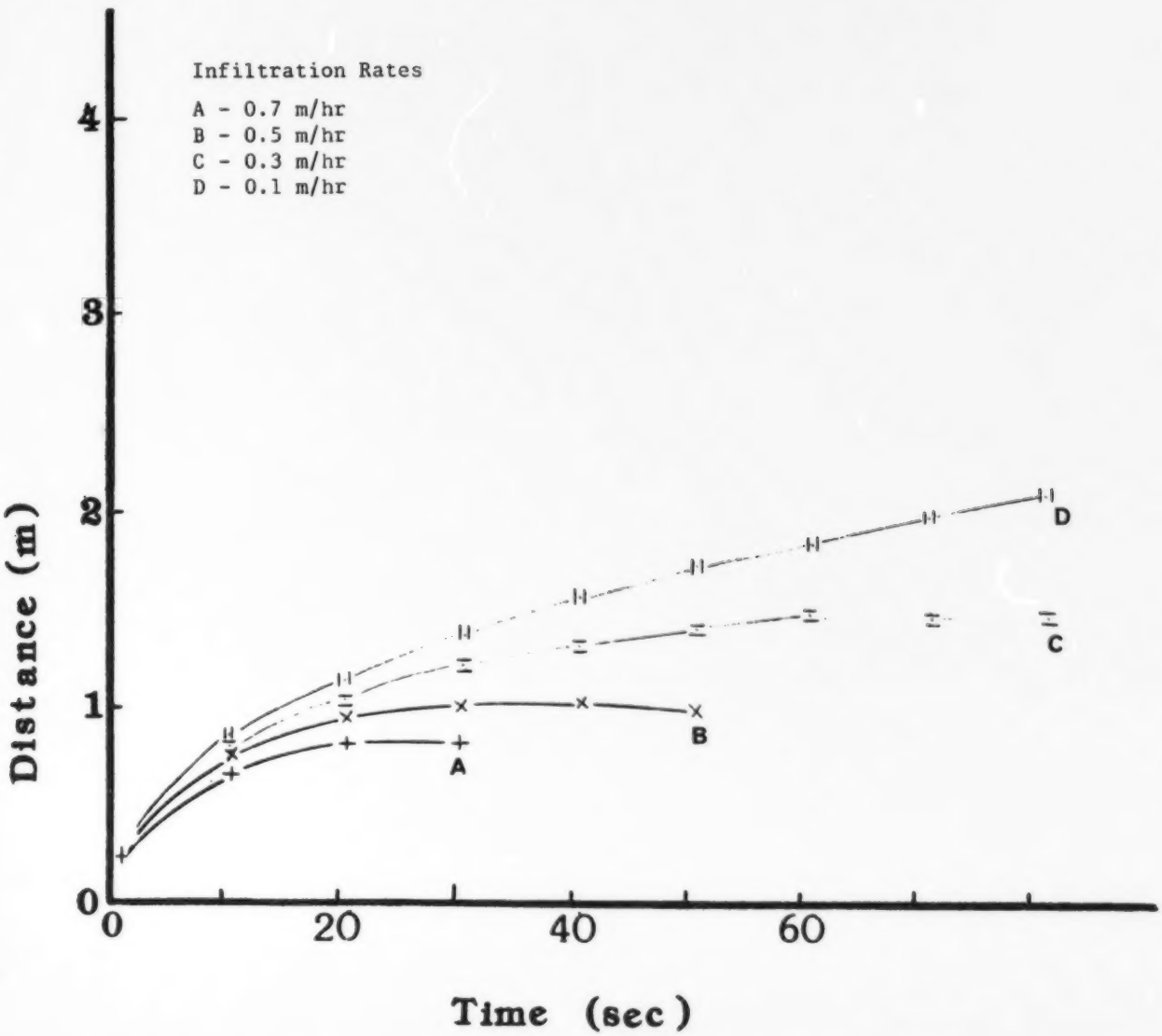

Figure 4.9 Sensitivity of Three-Dimensional Modelling Results to Alternative Infiltration Rates

iv) The computed results for moderate infiltration rates (Run C from above) but with nonzero evaporation rates (see Figure 4.10). The values used in the model are tabulated below (other input values relate to Run #36):

Run Designation	Infiltration Rate (m/hr)	Decay Rate (1/sec)	Evaporation Rate (m/hr)
A	.3	.005	0
B	.3	.005	.1
C	.3	.005	.2

As expected, as the evaporation rate is increased the excursion of the spill is decreased.

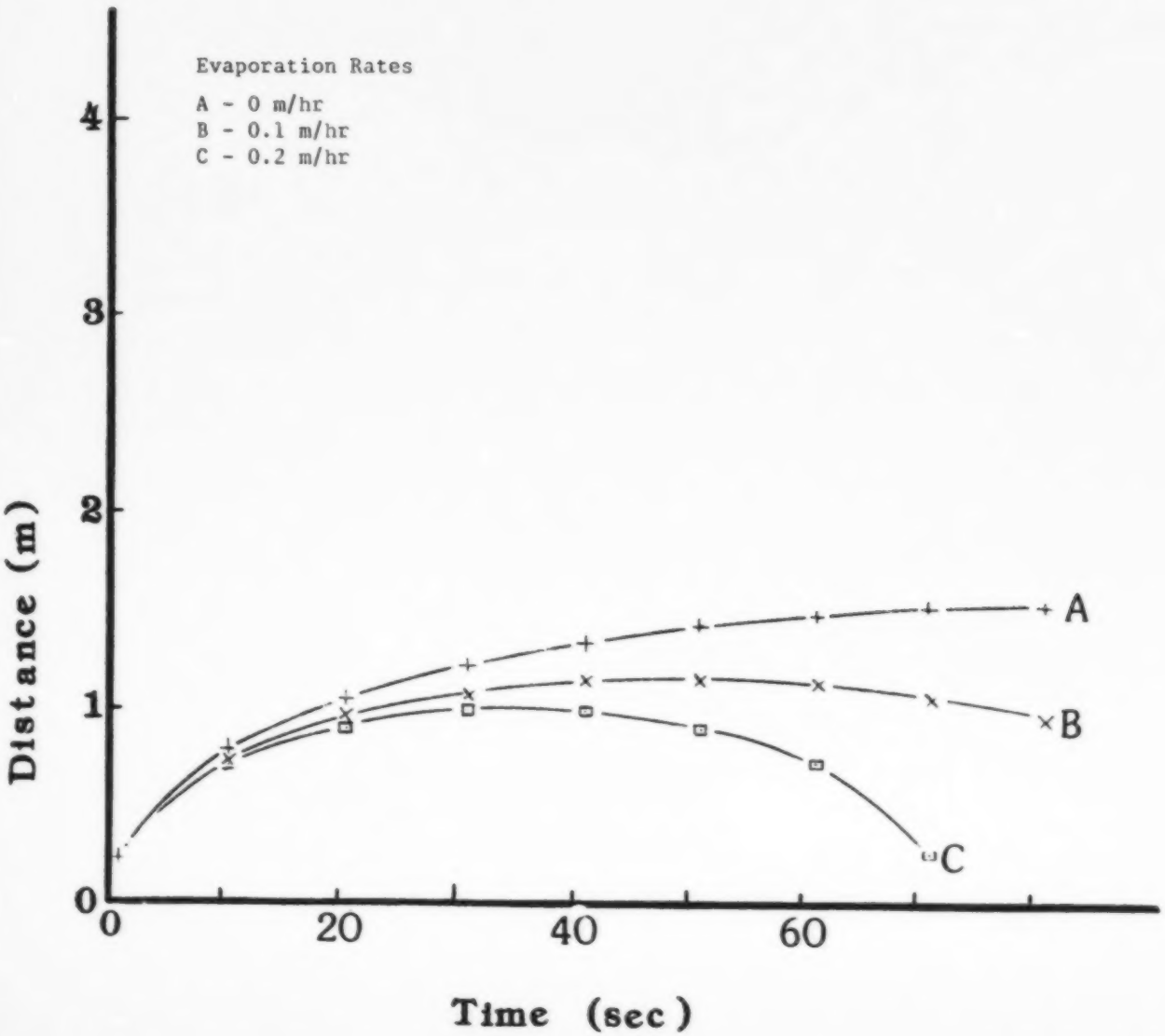

Figure 4.10 Sensitivity of Three-Dimensional Modelling Results to Alternative Evaporation Rates

4.5 COMPARISON OF MODEL OUTPUTS TO EXISTING METHODS OF CHEMICAL POOL SIZE PREDICTION

As was outlined in the Introduction to this report, this research was necessary due to the lack of confidence in existing methods to predict the pool size of chemical spills on land. The methods used in the existing EnviroTIPS manuals include equating the extent that the liquid would spread on water to its potential worst-case size on land or arbitrarily assuming a final pool thickness and estimating the pool area given the volume of chemical spilled.

A comparison of these methods with the 3-dimensional mathematical model's predictions has been made for examples illustrated in the Ethylbenzene and Sulphuric Acid EnviroTIPS manuals (February, 1984). The example spills are 20 tonne discharges on flat ground. The model predictions noted below included no infiltration or evaporation and are therefore conservative (i.e., actual spill radius could be smaller by incorporating these components).

Chemical Spilled	Tips Prediction Method	Tips Estimate of Spill Radius (m)	Model's Estimate of Spill Radius (m)
Ethylbenzene	Equivalent to Spreading on Water	250	18
Sulphuric Acid	Arbitrary Assignment of Spill Depth	40	15

The assumption of similar spreading on land to that which would occur on water resulted in more than an order of magnitude over-estimate of pool size when compared to the more rigorous mathematical modelling results. For the case where the final spill thickness was estimated in order to predict the pool size a closer agreement is evident in this particular case. However, this method relies on a guess of the chemical's thickness and so the results can not be used with any degree of confidence.

While these spreading models require further field-scale verification and the development of necessary input data for a wider range of chemicals they already provide a more confident estimate of the spreading rate and ultimate pool size of chemicals spilled on land when compared to the methods presently in use.

5.0 CONCLUSIONS AND RECOMMENDATIONS

5.1 CONCLUSIONS

Two computer models for quantifying the spread of fluids over surfaces have been developed. The models are general in that a number of aspects of the fluid being spilled, and the characteristics of the receiving surfaces, are input data to models. Both models are relatively simple, mechanistic models. The differences between the models is with respect to their dimensionality, and thus, the situations for which they can be applied.

5.1.1 Two-Dimensional Model

This model is applicable to the most common spill situations such as roadside ditch analyses. As a result, this model was the major focus of the model development work within the study.

The model entails some numercial convergence requirements which necessitates careful selection of the input data. A primary example of the problem of the numerical aspects of the model is related to the need to quantify the leading edge of the spill to allow quantification of evaporative and infiltrative fluxes but, alternatively, the location of the leading edge cannot be quantified without knowledge of the evaporative and infiltrative fluxes. The model must therefore iterate to determine the solution. As a consequence, a smoothing of the calculated profile occassionally is necessary since the solutions are calculated at specified increments. The validity of the predictions of the two-dimensional model was demonstrated in application to a variety of laboratory experiments with very good results. A procedure to modify the model for different fluid viscosities was developed that is a mechanistic model which should greatly assist in the use of the model for situations for which experimental data do not exist.

5.1.2 Three-Dimensional Model

This model is considerably simpler in its numerical aspects, in comparison with the two-dimensional model. The simplicity of the model arises because of the treatment of momentum; the result of the simplification of the model is that the model predictions are conservative solutions (the extent of the spill excursion is consistently overpredicted).

The predictions of the three-dimensional model were good in comparison with the laboratory data. The predictors were consistently larger than the laboratory experiments and, therefore, may be used as an indication of the maximum extent of the excursion. As well, the shape of the curve of leading edge versus time as predicted, compared favourably with the experimental data. The inclusion of the surface affinity force component as the only force will make the model predictions of the three-dimensional model most accurate for liquids which are highly viscous.

5.1.3 General Comments

The primary goals in the development of the model was to represent the spill processes in as general a form as possible while maintaining a level of simplicity which would permit them to be operated on a micro-computer. This provides the opportunity for easy testing of the sensitivity of the model's output to changes in the model's various input parameters. It also makes the models accessible to a greater number of end users.

The two and three-dimensional models' abilities to accurately speading rates on two very different surface conditions have been demonstrated by comparison to large scale laboratory tests. However, the accuracy of the model is tied to several input parameters which are not well defined for different chemicals or terrain types. The more important of these parameters are the surface contact angles of the chemicals and the Mannings roughness coefficient of various terraines for each of these chemicals. Even

with our limited knowledge of these types of parameters estimates of pool size an order of magnitude better than existing prediction methods is possible. More confidence in these models' predictive capabilities will come with further study of their essential input parameters and the application of the models to full-scale chemical spill occurrences.

5.2 RECOMMENDATIONS

Several aspects of the study are particularly worthy of closer examination.

i) Several parameters needed for the model use are not currently available, the most noteworthy being the surface contact angles of various chemicals which are a function of both the fluid and the surface, and the Manning's roughness coefficients for these chemicals over various surface types;

ii) further validation of the models by comparison to measurements at spills of opportunity or at controlled field-scale tests would increase confidence in the models' abilities;

iii) the models are not difficult to use but they are numerical models which always provide some difficulties to the uninitiated. A useful analysis would, therefore, be to use the models to develop a series of nomographs which would allow quick access to spill excursion, for a variety of specified conditions.

REFERENCES

Abbott, M.B. 1966. An Introduction to the Method of Characteristics, Thames and Hudson, American Elsevier N.Y.

Allan, R., G.J. Farquhar, and E.A. McBean. 1985. "Modelling the Movement of Vapours from Hazardous Liquids in Soil", presented at Technology Transfer Conference No. 6, Ontario Ministry of the Environment, Toronto, Ontario.

Anderson, D.C. and S.G. Jones. 1984. "Fate of Organic Liquids Spilled on Soil", presented at Hazardous Wastes and Environmental Emergencies, Houston, Texas.

Belore, R.C. 1981. The Physical Modelling of a Thermal Discharge Under a Salt Water Ice Layer. Masters Thesis. University of Waterloo, Waterloo, Ontario.

Fannelop, T.K. and G.D. Waldman. 1971. "Dynamics of Oil Slicks", AIAA Journal, Vol. 10, No. 4, pp 506-510.

Farquhar, G.J. and E.A. McBean. 1984. "Assessing the Behaviour of Hazardous Liquids Spilled Onto Soils", presented at Technology Transfer Conference No. 5, Ontario Ministry of the Environment, Toronto, Ontario.

Fay, J.A. 1969. "The Spread of Oil on a Calm Sea", in Oil on the Sea, ed. D.P. Hoult, Plenum Press, N.Y.

Henderson, F.M. 1966. Open Channel Flow, MacMillan Series in Civil Engineering

Holtan, H.N. 1961. "A Concept for Infiltration Estimates in Watershed Engineering", U.S. Dept. of Agriculture, Agricultural Research Service, ARS 41-51.

Holtan, H.N., G.J. Stiltner, W.H. Hensan and N.C. Lopeg. 1975. "USDAHL -74 Revised Model of Watershed Hydrology", U.S. Department of Agriculture, ARS Tech. Bulletin No.1518, Washington, D.C.

Horton, R.E. 1935. "Surface Runoff Phenomena; Part I, Analyses of the Hydrograph", Horton Hydrol. Lab. Pub.101, Ann Arbor Michigan.

Hoult, D.P. and W. Suchan. 1970. "The Spread of Oil in a Channel", Report Two Fluid Mechanics Lab., Dept. of Mechanical Engineering, M.I.T., Massachusetts.

Huggins, L.F. and E.J. Monke. 1966. "The Mathematical Simulation of the Hydrology of Small Watersheds", Tech. Report 1, Purdue Unversity, Water Resources Center, Lafayette, Indiana.

Mackay, D. and R.S. Matsugn. 1973. "Evaporation Rates of Liquid Hydrocarbon Spills on Land and Water", Canadian Journal of Chemical Engineering, Vol. 51, pp 434-439.

McBean, E.A. and F.E. Perkins. 1970. "Error Criteria in Water Surface Profile Computations", Hydrodynamics Laboratory Report No. 124, M.I.I., Cambridge, Massachusetts.

Raisbeck, J.M. and M.F. Mohtadi. 1974. "The Environmental Impacts of Oil Spills on Land in Arctic Regions", Water, Air and Soil Pollution, 3, pp 195-208.

Raj, P.P.K. and A.S. Kalelkar. 1974. "Assessment Models in Support of the Hazard Assessment Handbook", U.S. Coast Guard Report No. CC-D-6574.

Rouse, H. 1967. Engineering Hydraulics, McGraw-Hill Book Co., N.Y.

Streeter, V.L. and E.B. Wylie. 1981. Fluid Mechanics, McGraw-Hill Ryserson Ltd., Toronto.

Tanner, L.H. 1979. "The Spreading of Silicone Oil Drops on Horizontal Surfaces", J. Physics D: Applied Physics, Vol. 12, pp 1473-1484.

Thibeaux, L.J. 1977. "Mechanics and Idealized Dissolution Modes for High Density (p 1), Immiscible Chemicals Spilled in Flowing Aqueous Environments", AICHE Journal, Vol. 23, No. 4, pp 544-554.

Wall, R. 1984. "Numerical Modelling of the Spill of Volatile Toxic Liquids over Porous Media", M.A. Sc. thesis, Dept. of Civil Engineering, University of Waterloo, Waterloo.

Viessman, W., J.W. Knapp, G.L. Lewis, and T.E. Harbaugh. 1977. Introduction to Hydrology, Harper & Row Publishers, New York.

APPENDIX I

Graphs of Location of the Leading Edge of the Spill
as a Function of Time, Computed and Laboratory Measuremets

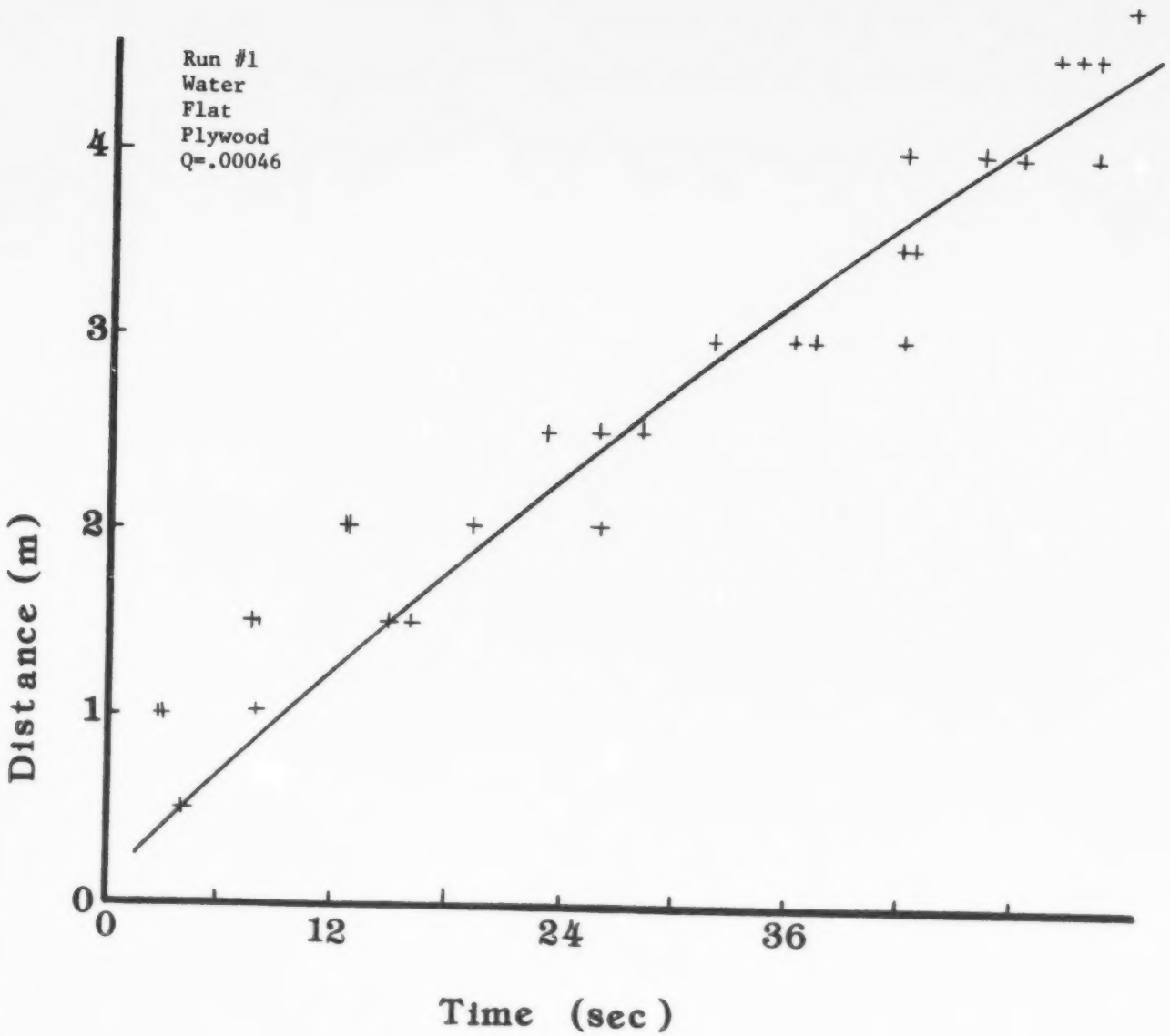
Run #1
Water
Flat
Plywood
Q=.00046
Distance (m)
0
1
2
3
4
0
12
24
36
Time (sec)

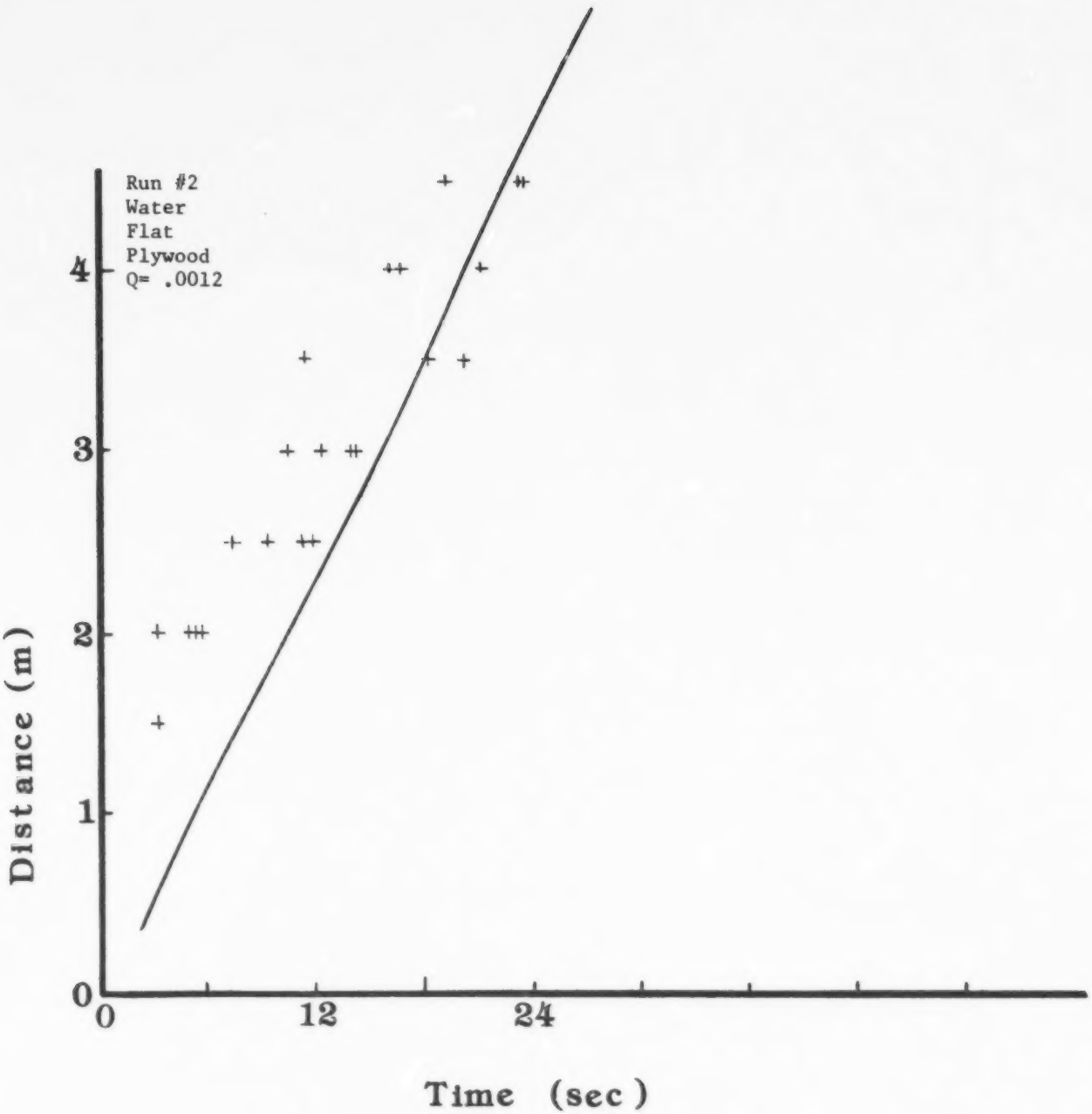
Run #2
Water
Flat
Plywood
Q= .0012
Distance (m)
0
1
2
3
4
0
12
24
Time (sec)

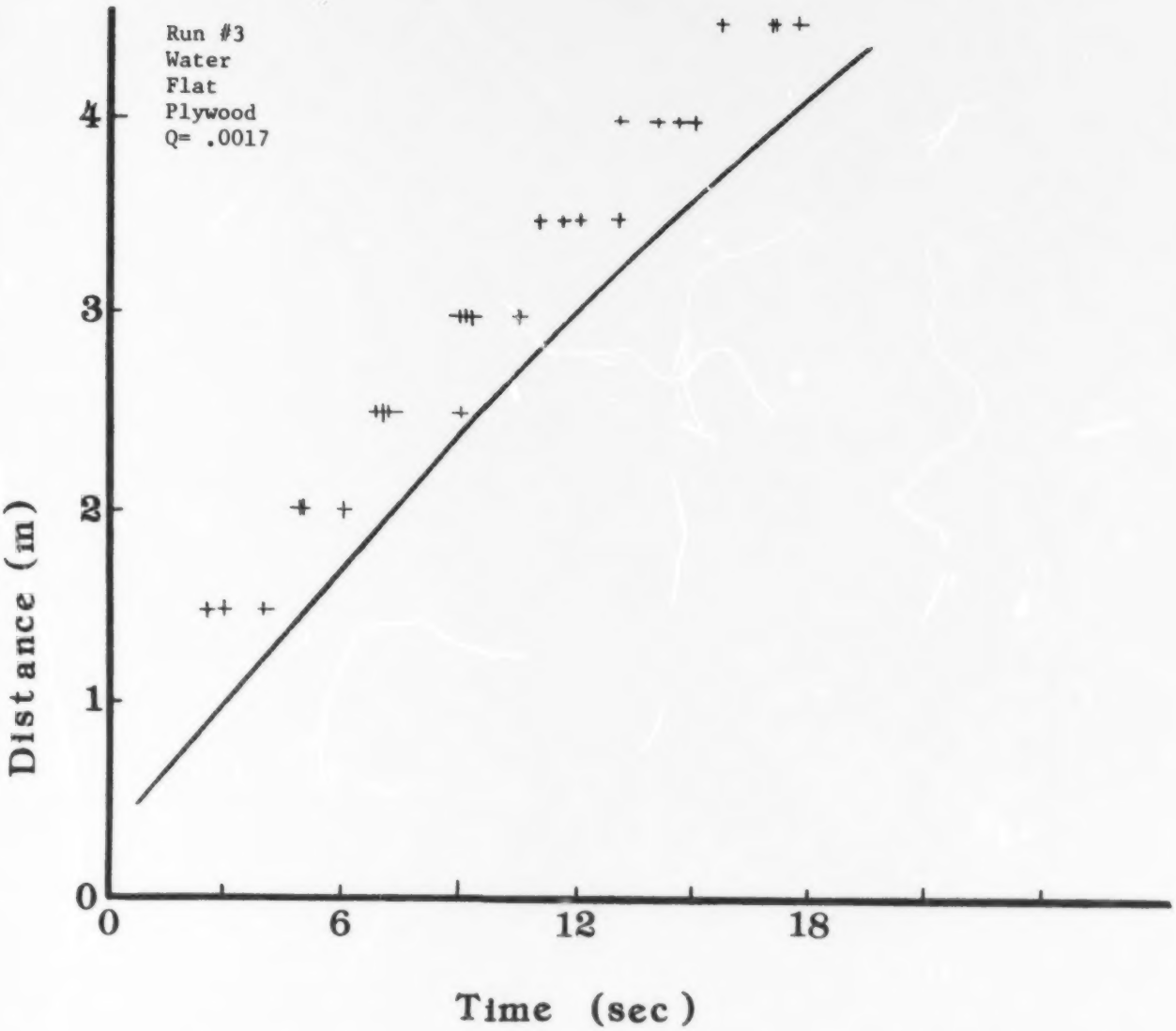
Run #3
Water
Flat
Plywood
Q= .0017
Distance (m)
0
1
2
3
4
0
6
12
18
Time (sec)

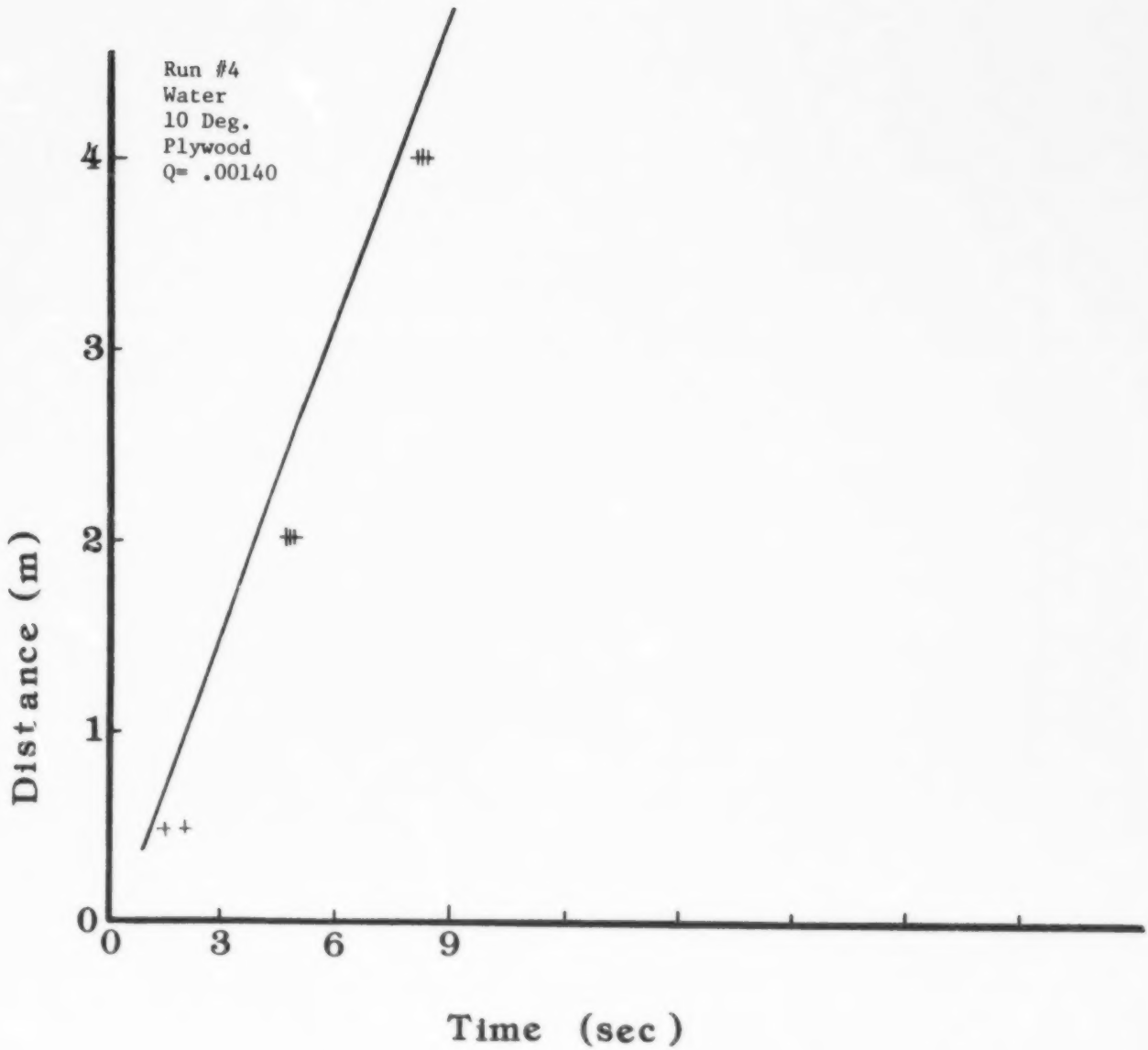
Run #4
Water
10 Deg.
Plywood
Q= .00140
Distance (m)
0
1
2
3
4
0
3
6
9
Time (sec)

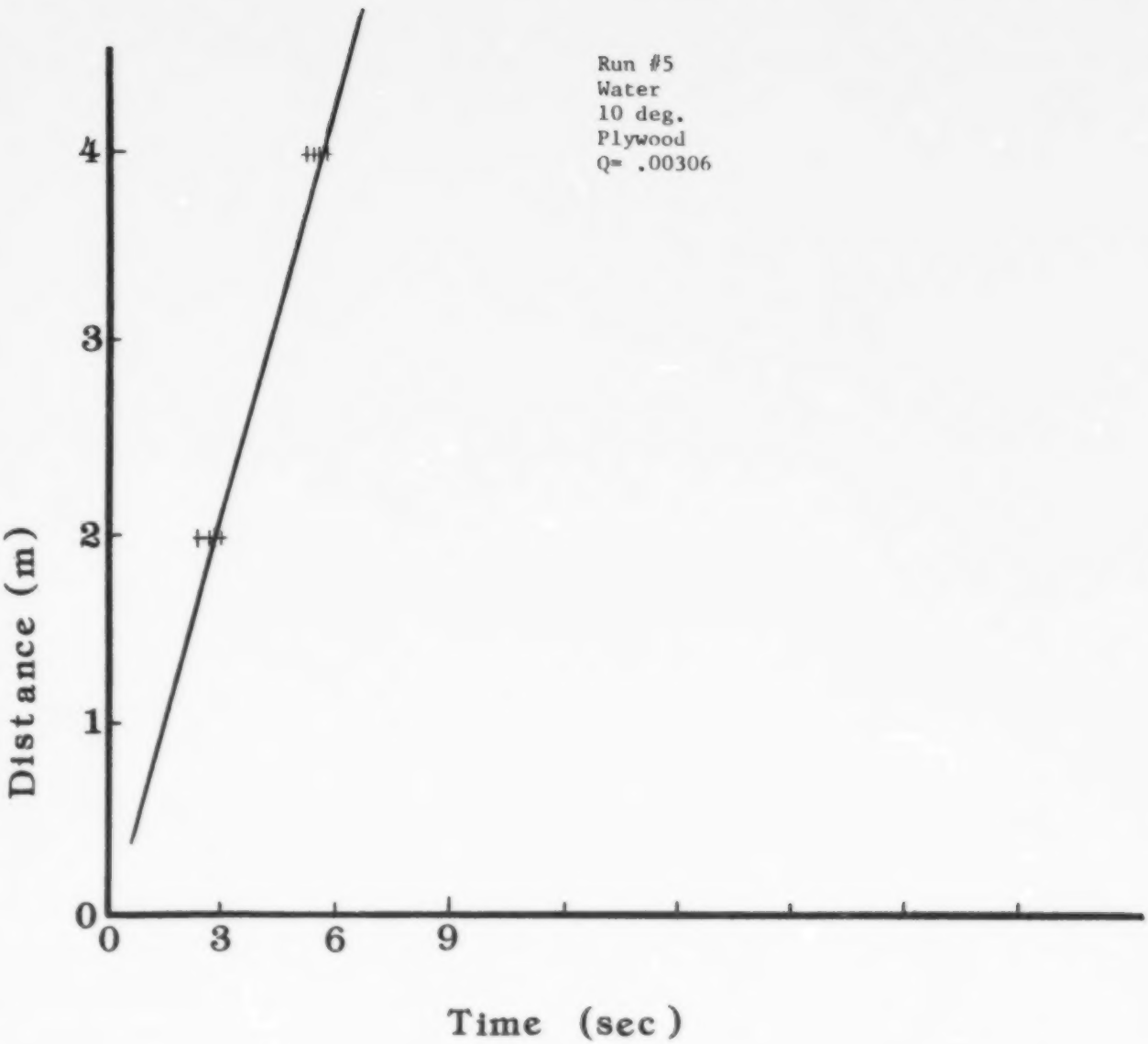
Run #5
Water
10 deg.
Plywood
Q= .00306
Distance (m)
0
1
2
3
4
0
3
6
9
Time (sec)

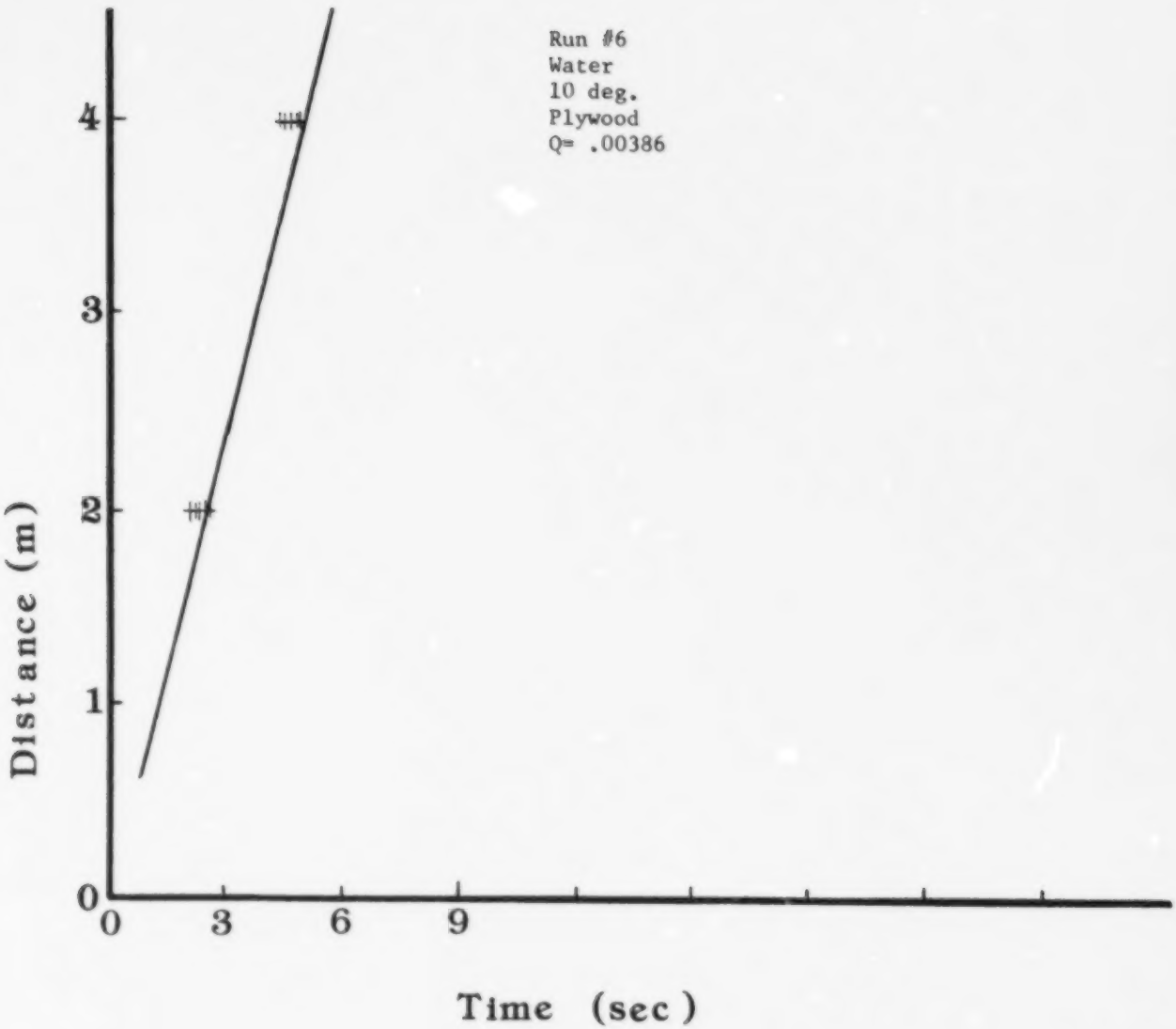
Run #6
Water
10 deg.
Plywood
Q= .00386
Distance (m)
0
1
2
3
4
0
3
6
9
Time (sec)

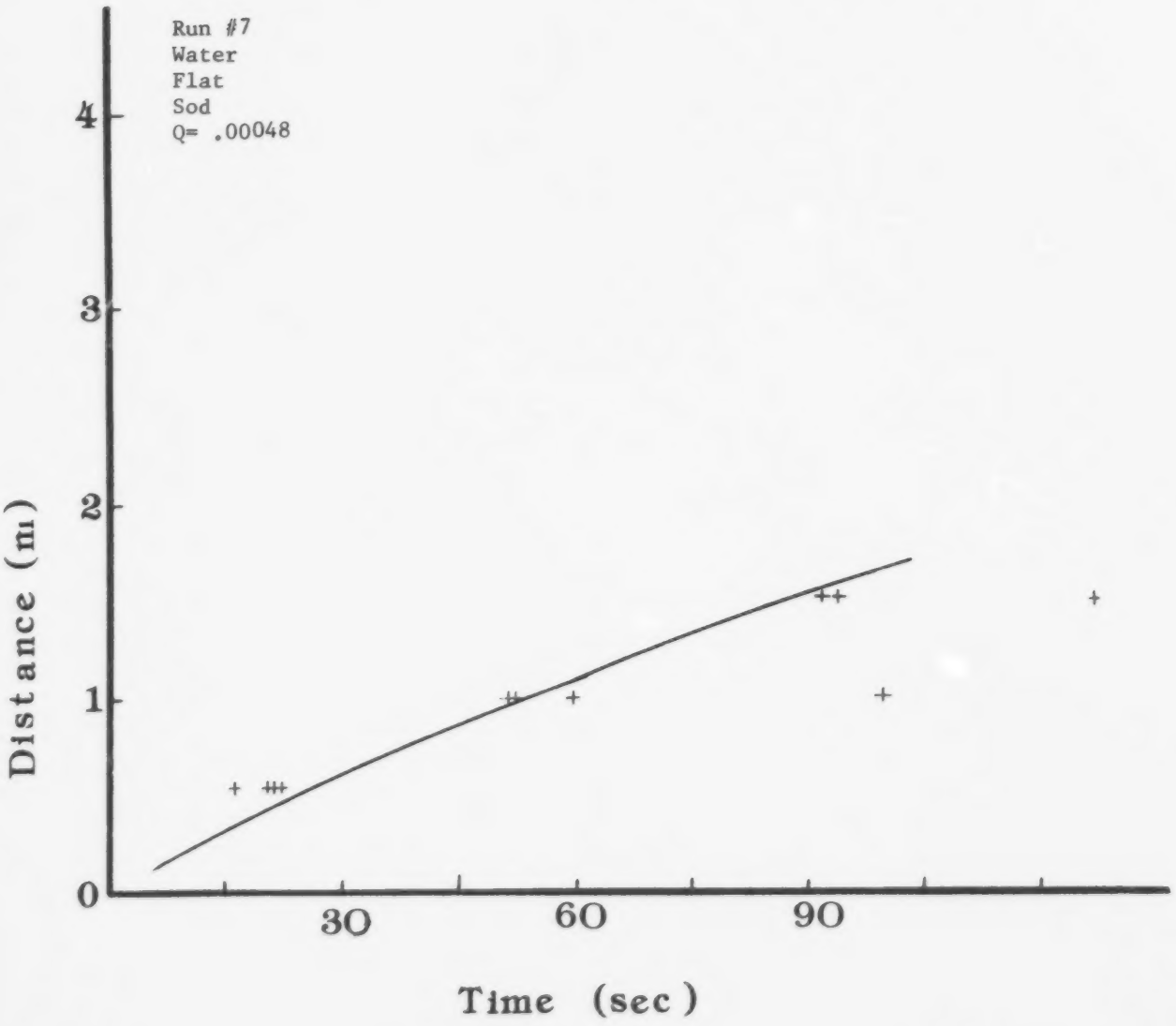
Run #7
Water
Flat
Sod
Q= .00048
4
3
2
1
0
Distance (m)
30
60
90
Time (sec)

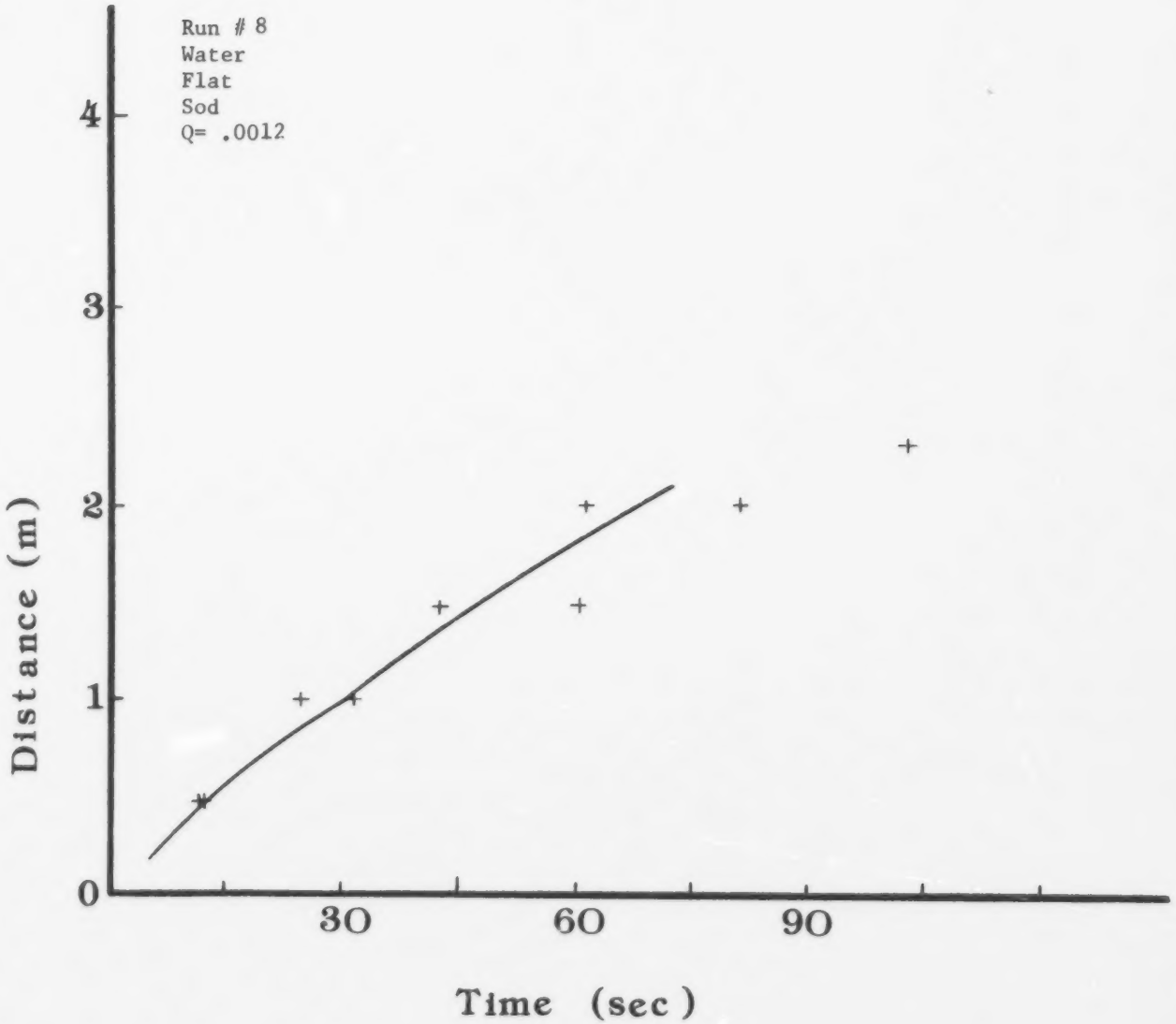
Run # 8
Water
Flat
Sod
Q= .0012
Distance (m)
0
1
2
3
4
30
60
90
Time (sec)

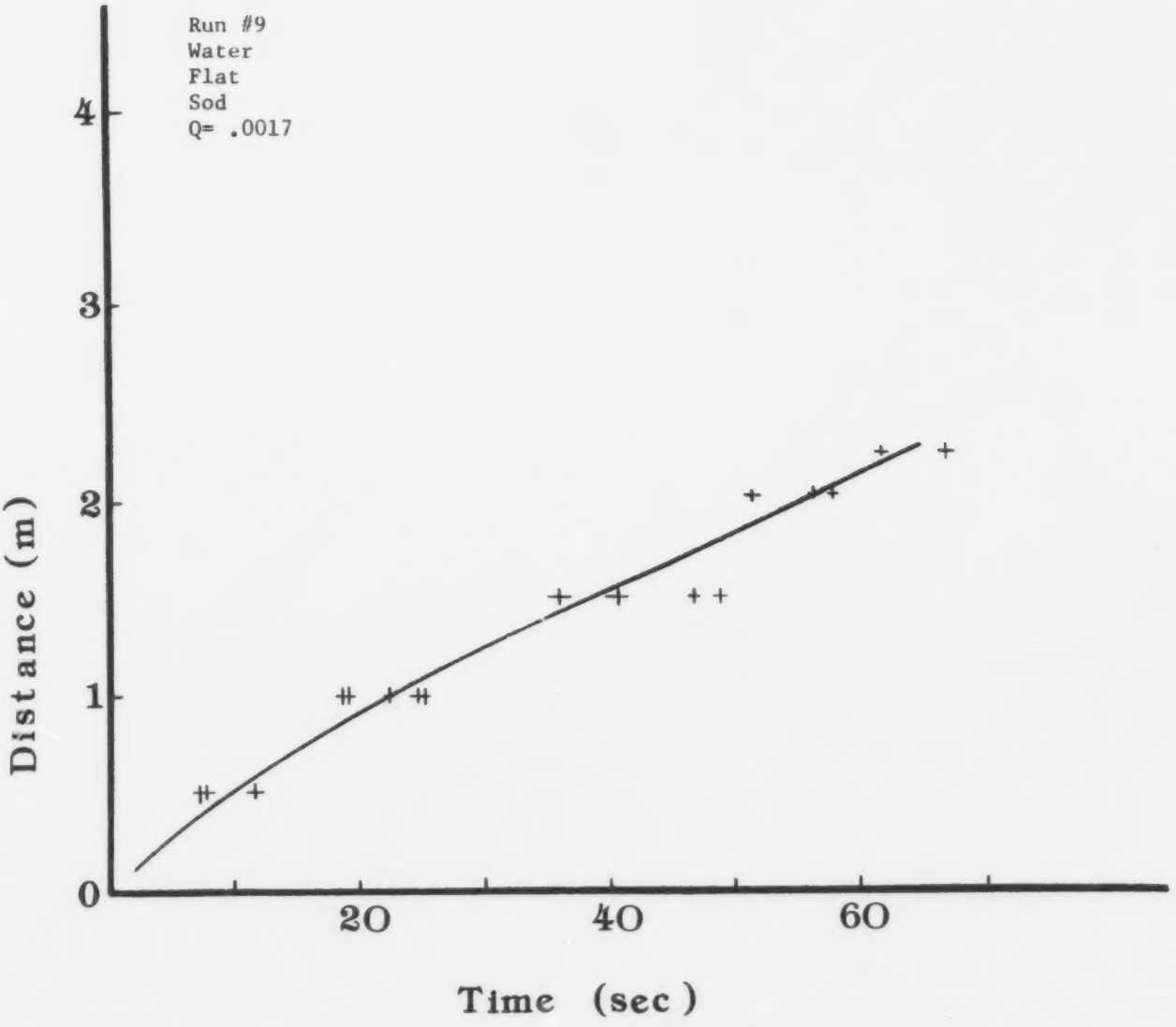
Run #9
Water
Flat
Sod
Q= .0017
4
3
2
1
0
Distance (m)
20
40
60
Time (sec)

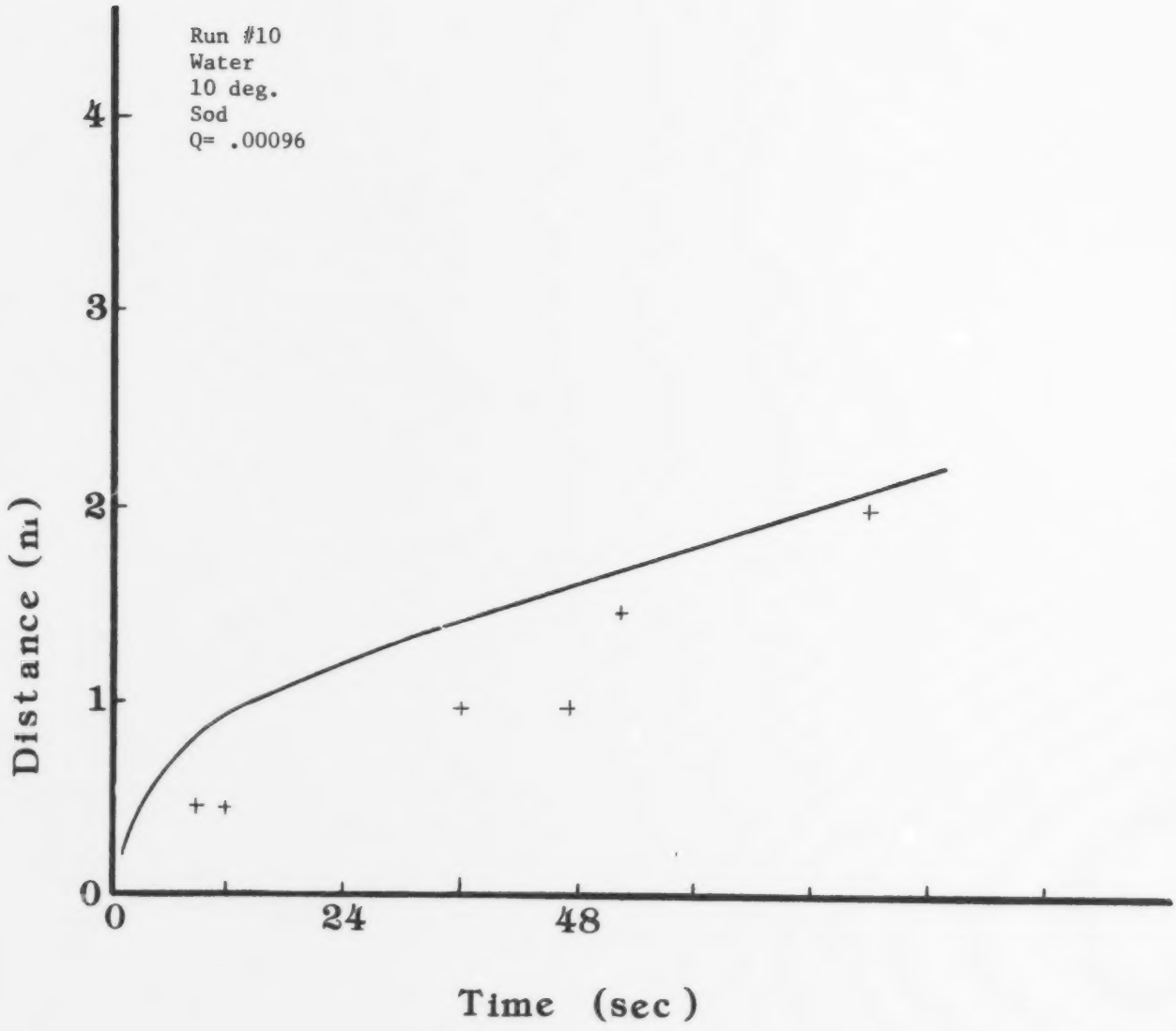
Run #10
Water
10 deg.
Sod
Q= .00096
Distance (ft)
0
1
2
3
4
0
24
48
Time (sec)

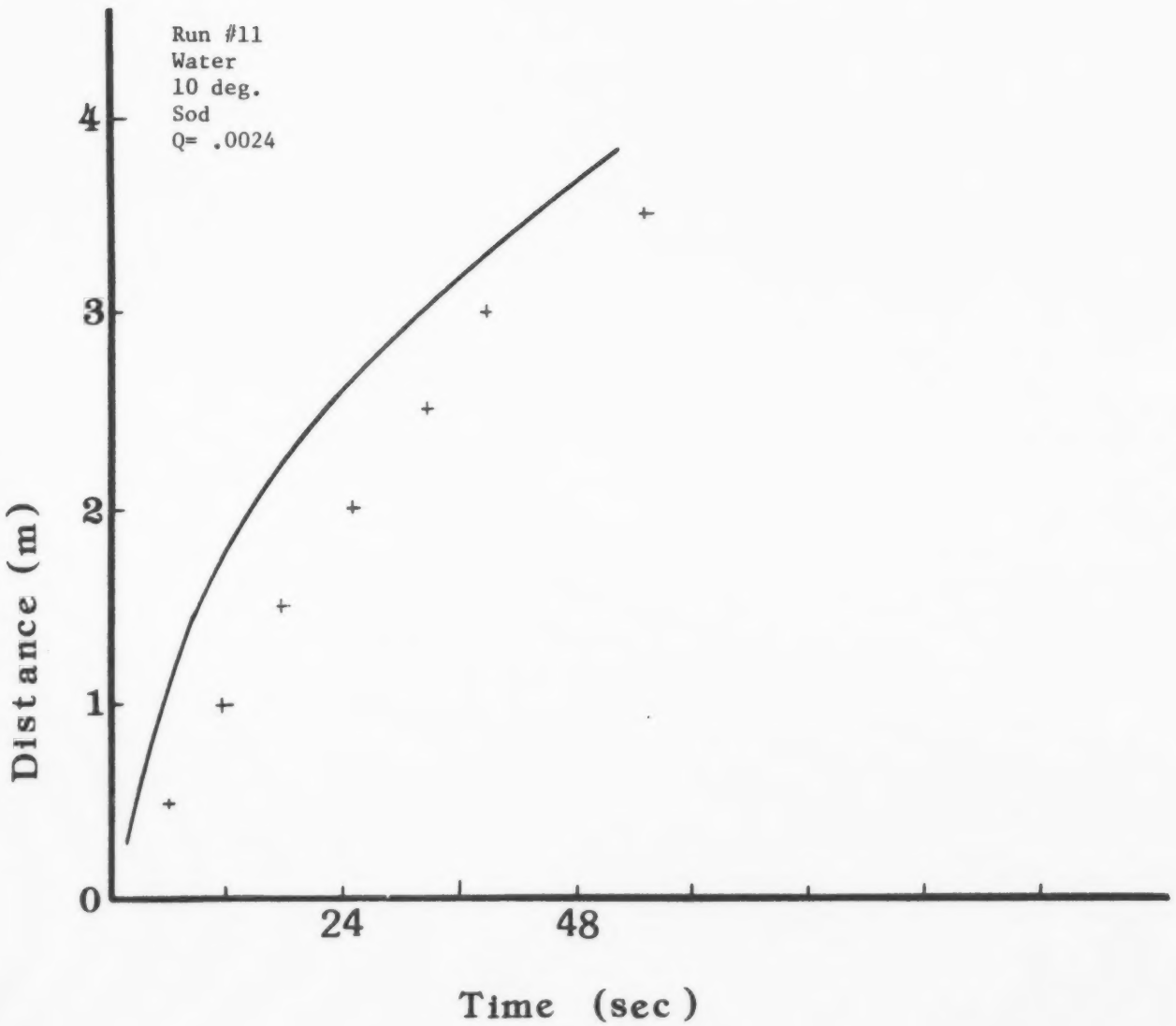
Run #11
Water
10 deg.
Sod
Q= .0024
4
3
2
1
0
Distance (m)
24
48
Time (sec)

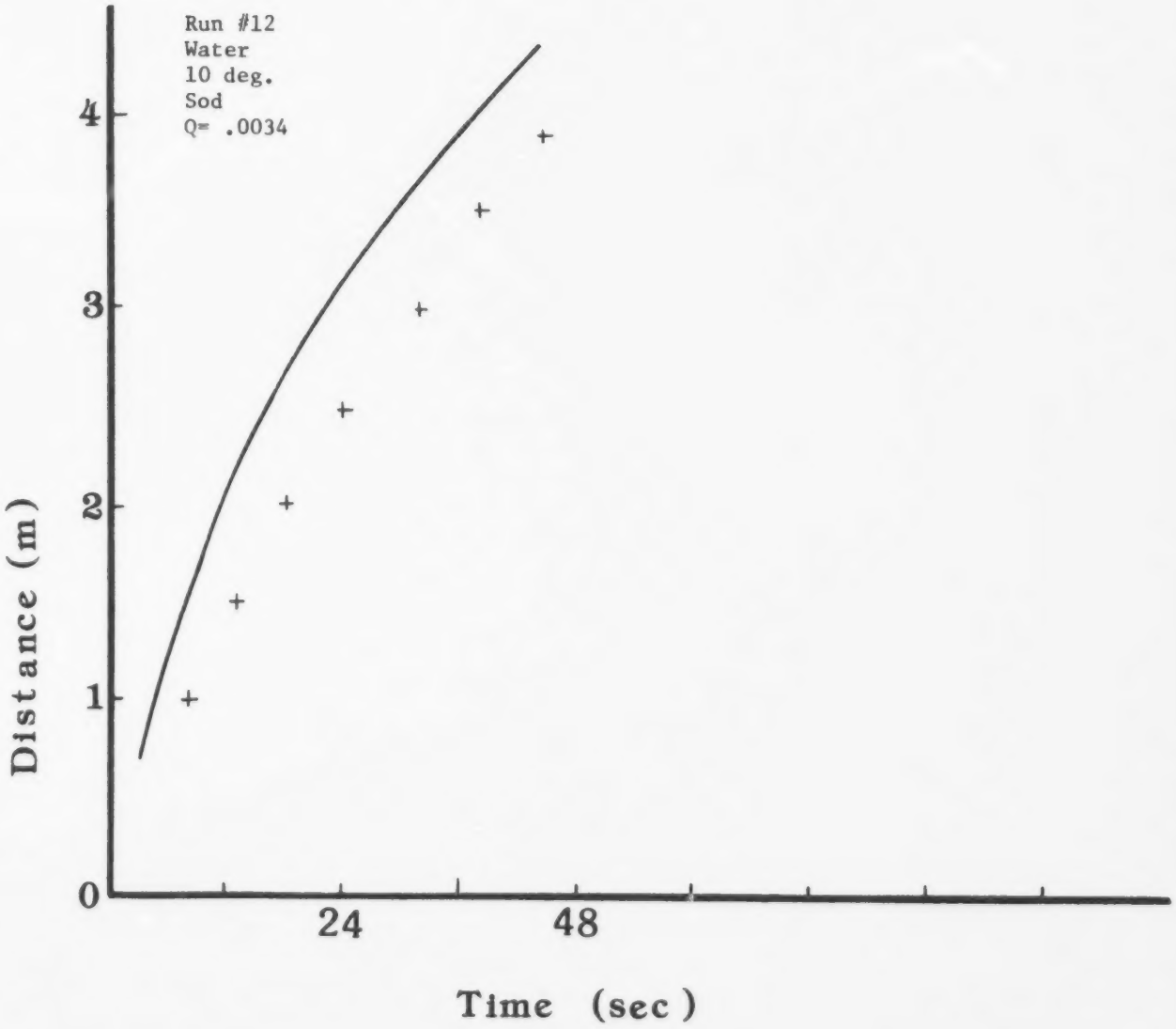
Run #12
Water
10 deg.
Sod
Q= .0034
4
3
2
1
0
Distance (m)
24
48
Time (sec)

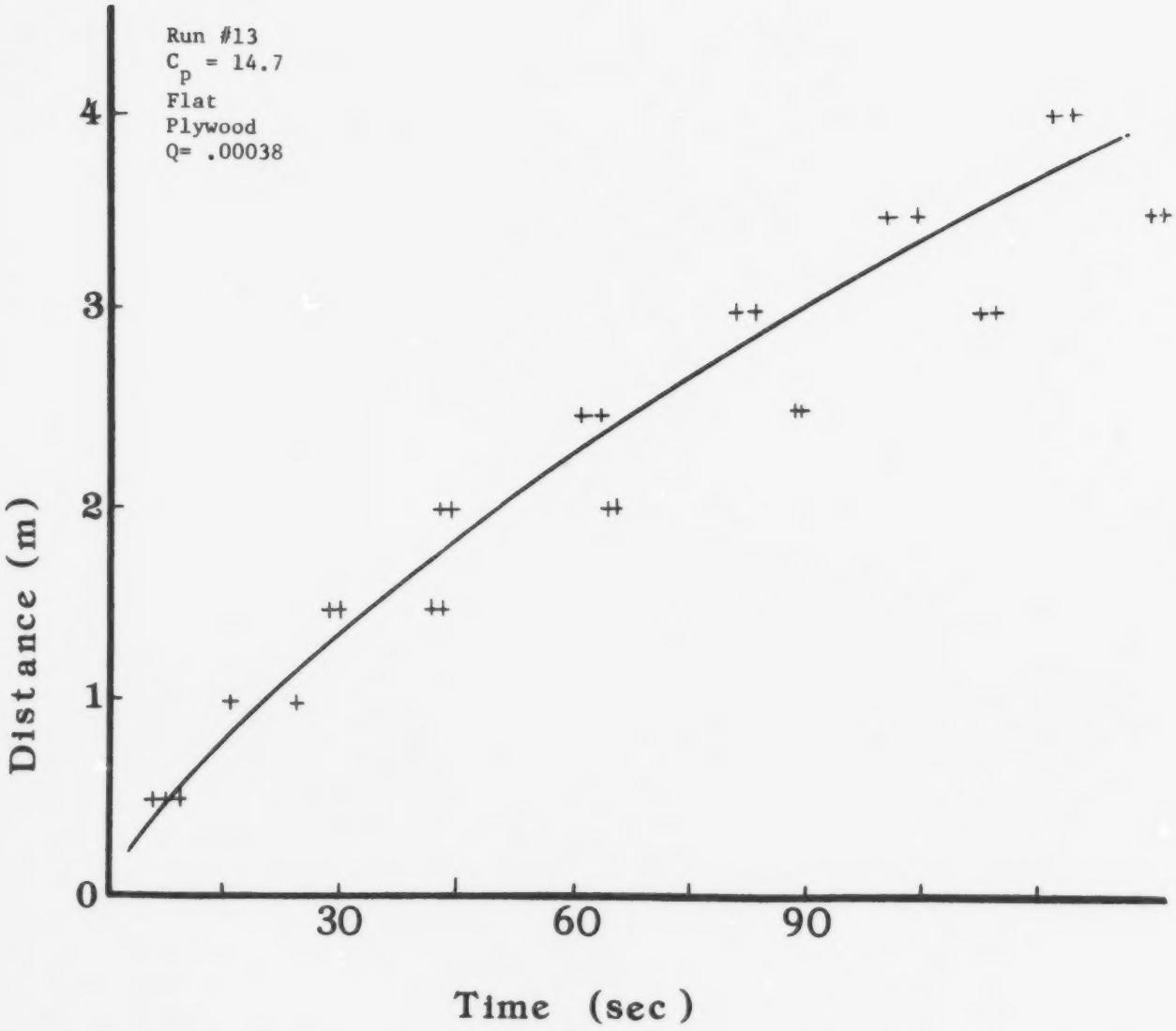
Run #13
C_p = 14.7
Flat
Plywood
Q= .00038
Distance (m)
0
1
2
3
4
30
60
90
Time (sec)

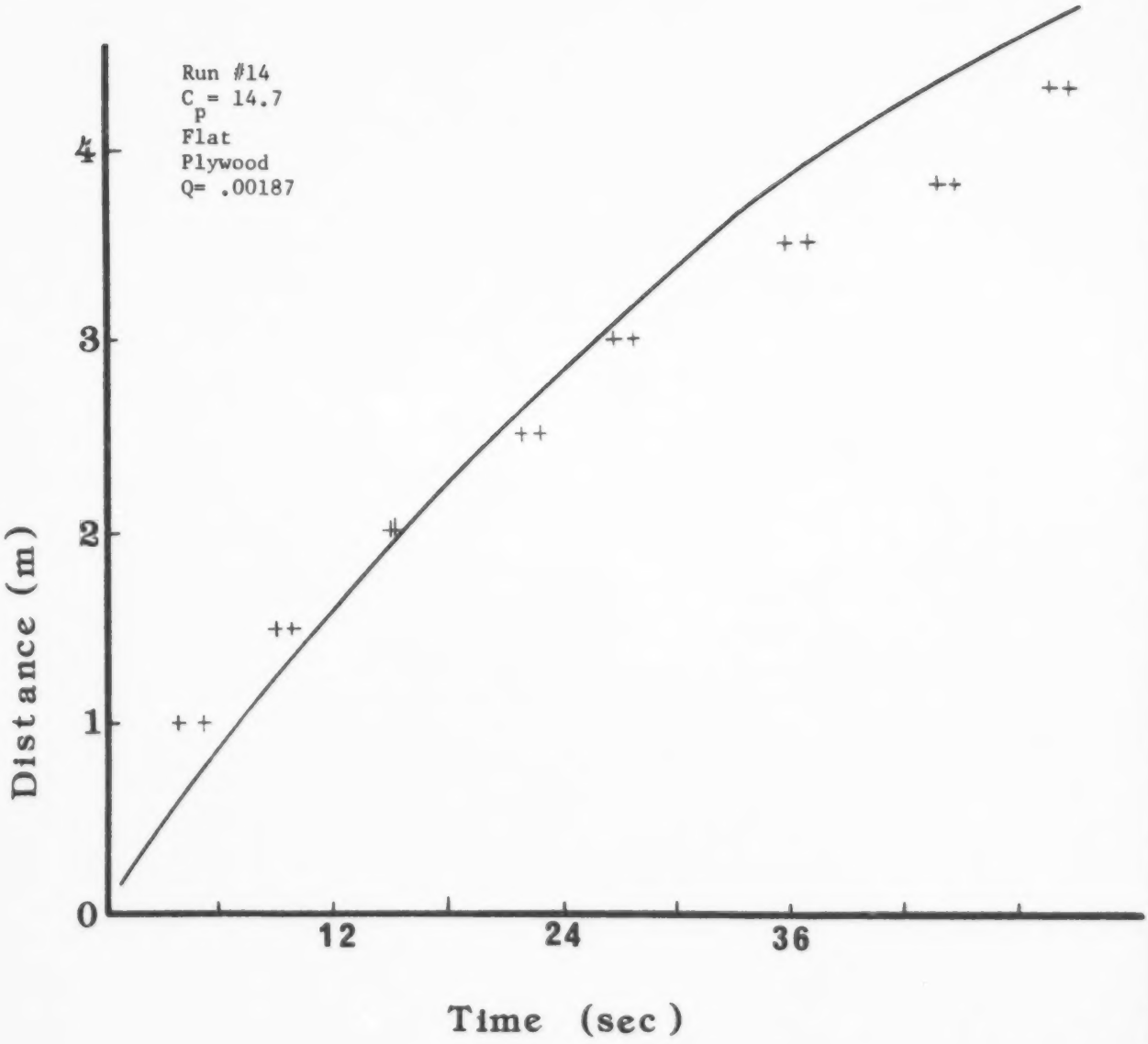
Run #14
C p = 14.7
Flat
Plywood
Q= .00187
Distance (m)
0
1
2
3
4
12
24
36
Time (sec)

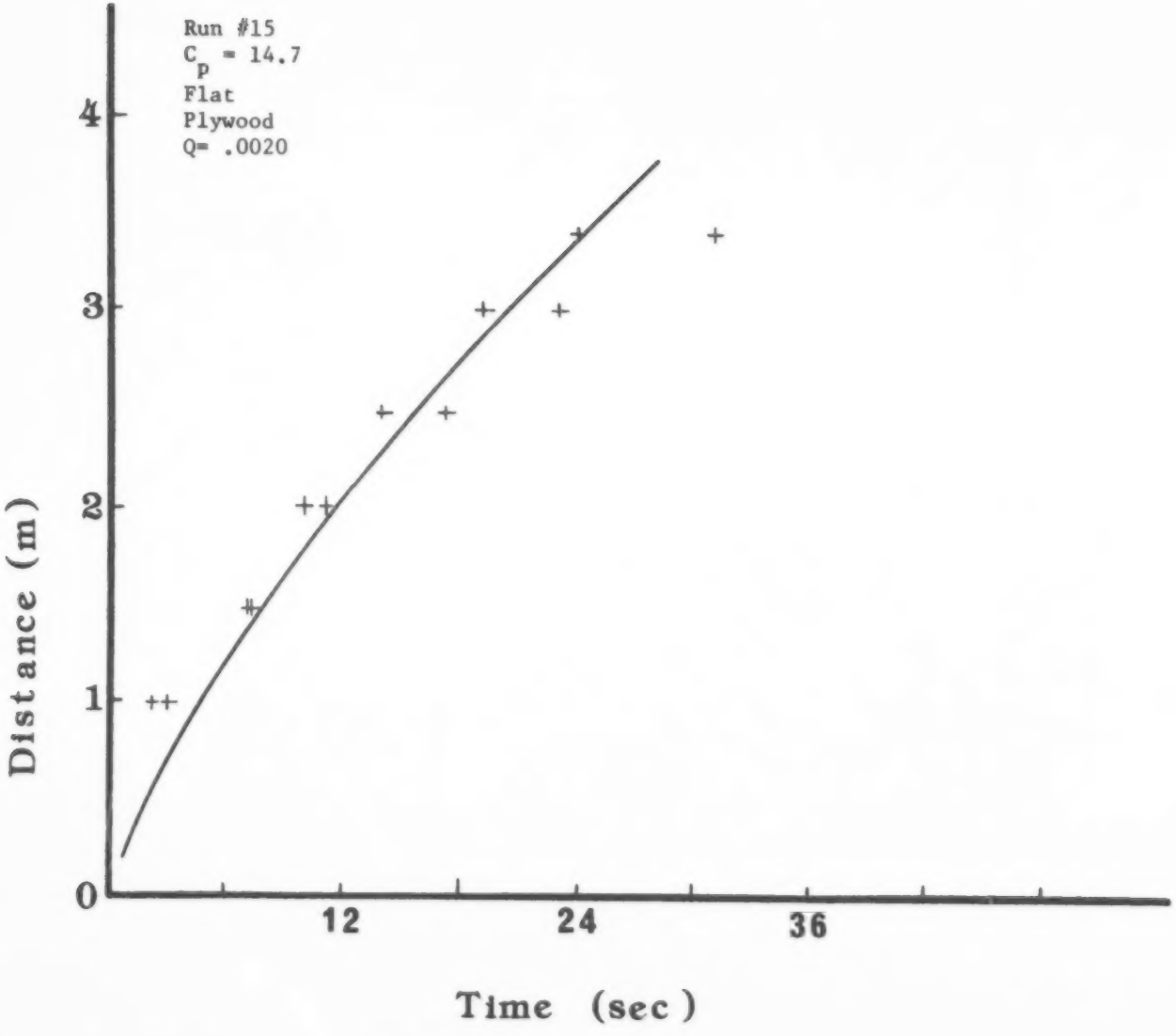
Run #15
C_p = 14.7
Flat
Plywood
Q= .0020
4
3
2
1
0
Distance (m)
12
24
36
Time (sec)

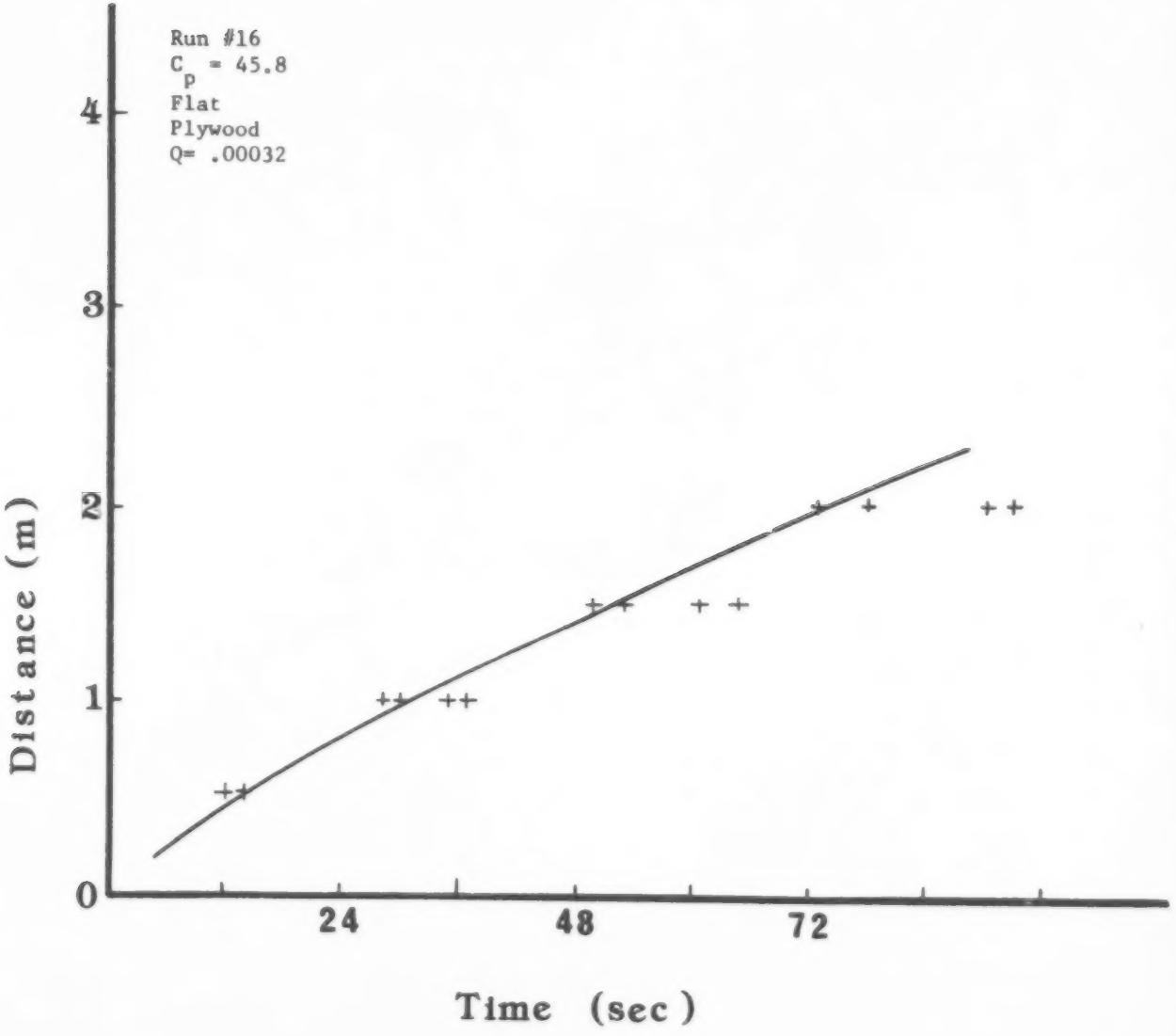
Run #16
C_p = 45.8
Flat
Plywood
Q= .00032
Distance (m)
0
1
2
3
4
24
48
72
Time (sec)

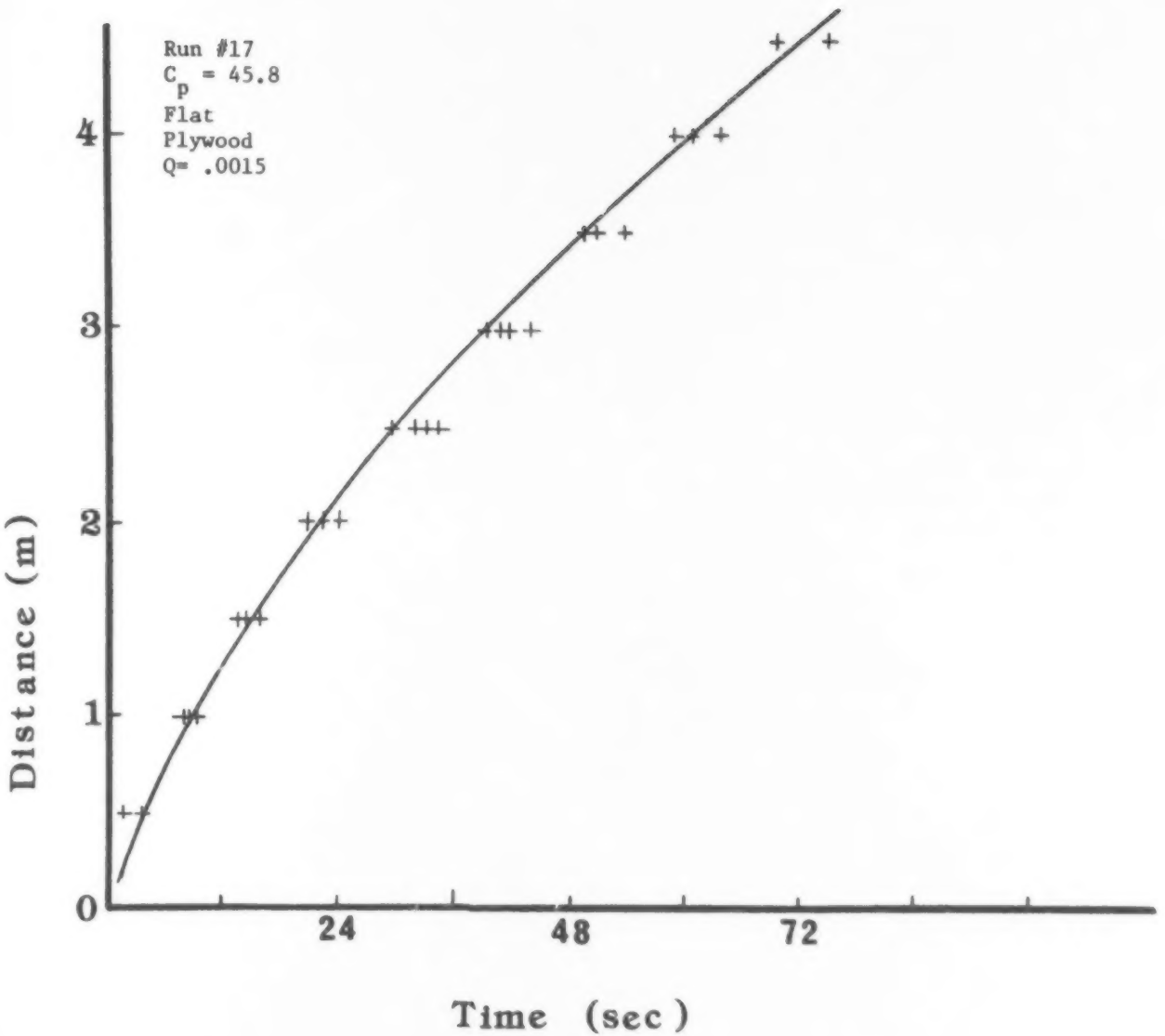
Run #17
C_p = 45.8
Flat
Plywood
Q= .0015
Distance (m)
0
1
2
3
4
24
48
72
Time (sec)

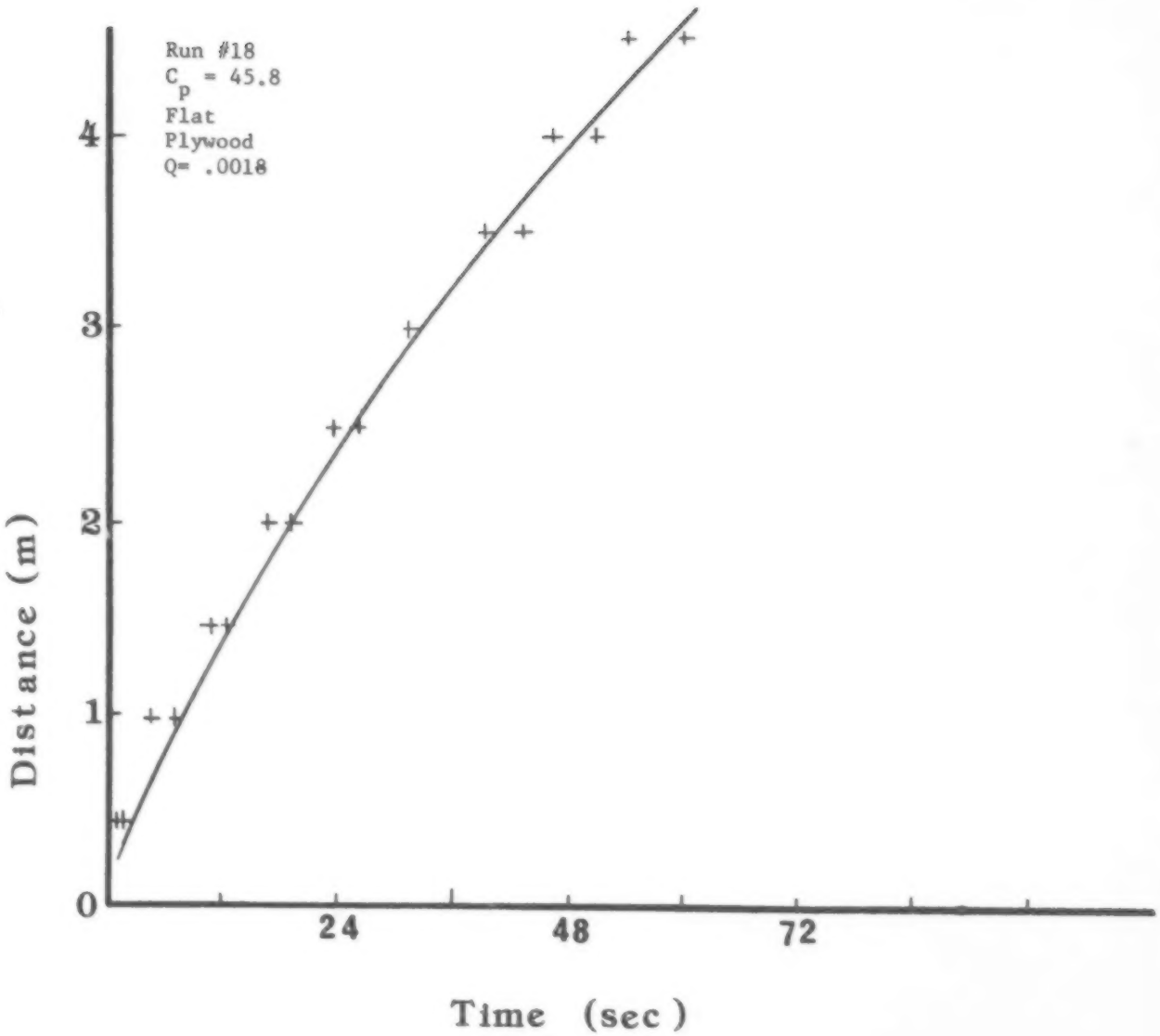
Run #18
C_p = 45.8
Flat
Plywood
Q= .0018
Distance (m)
0
1
2
3
4
24
48
72
Time (sec)

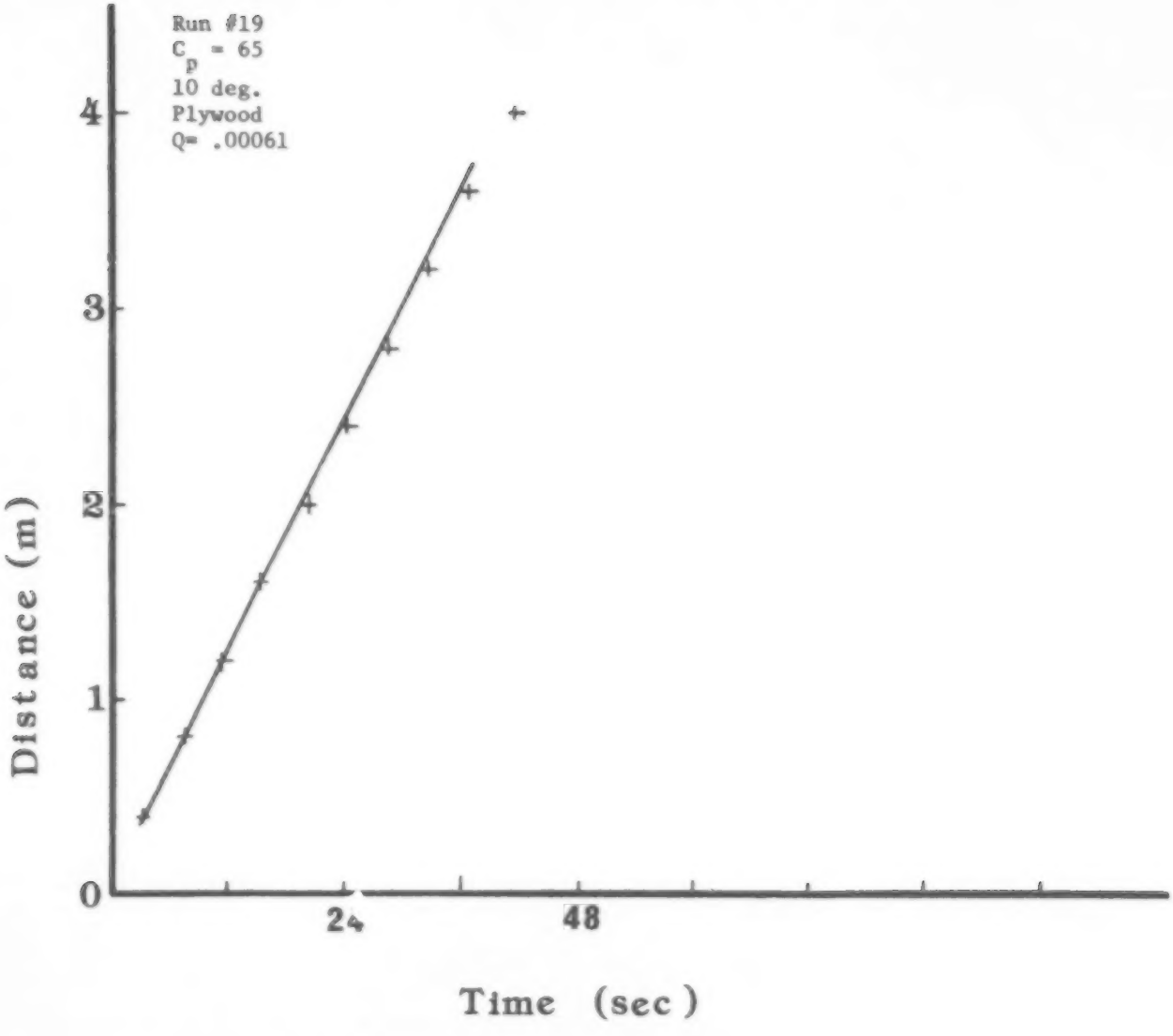
Run #19
C_p = 65
10 deg.
Plywood
Q= .00061
4
3
2
1
0
24
48
Distance (m)
Time (sec)

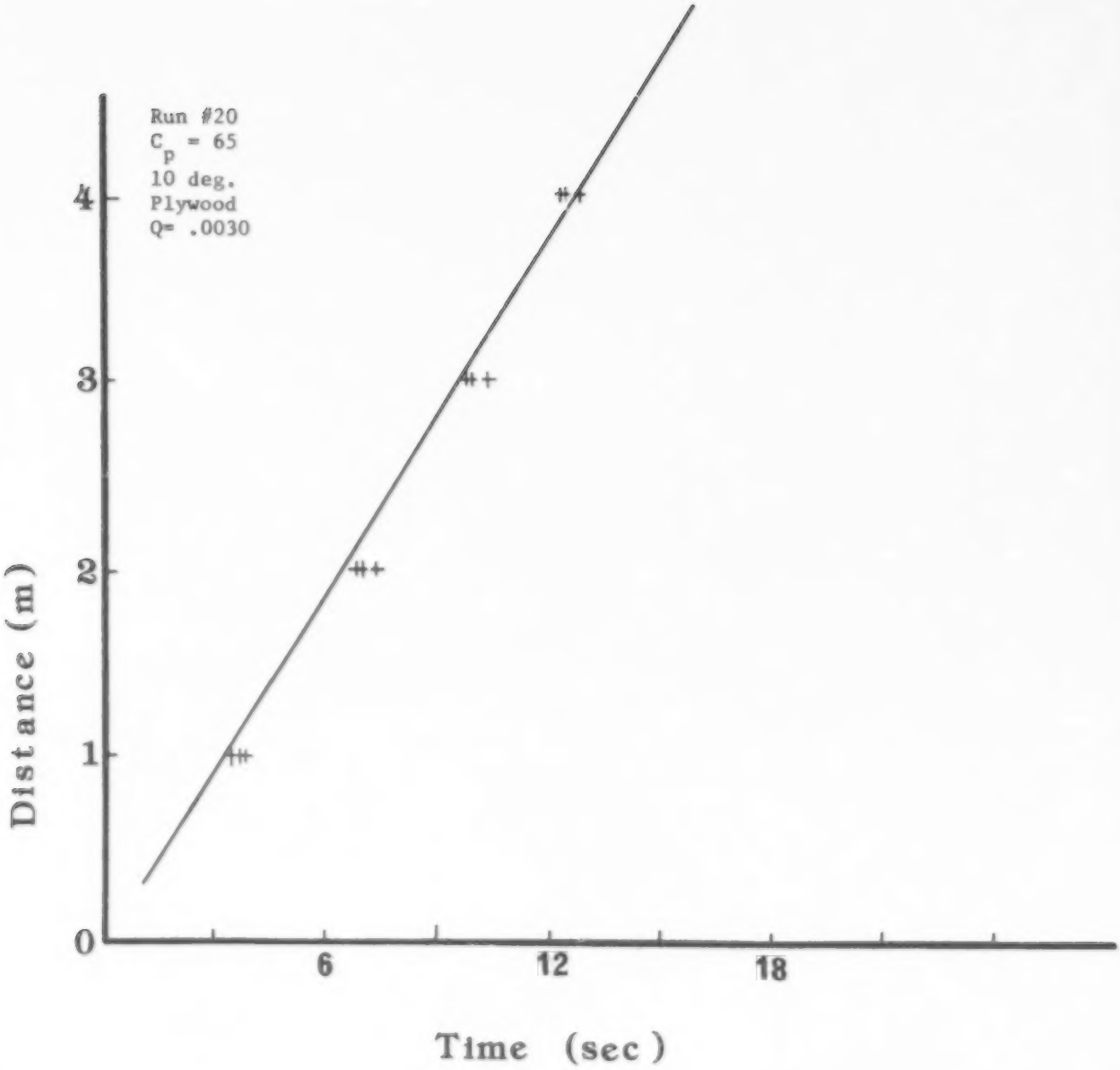
Run #20
C_p = 65
10 deg.
Plywood
Q= .0030
Distance (m)
0
1
2
3
4
6
12
18
Time (sec)

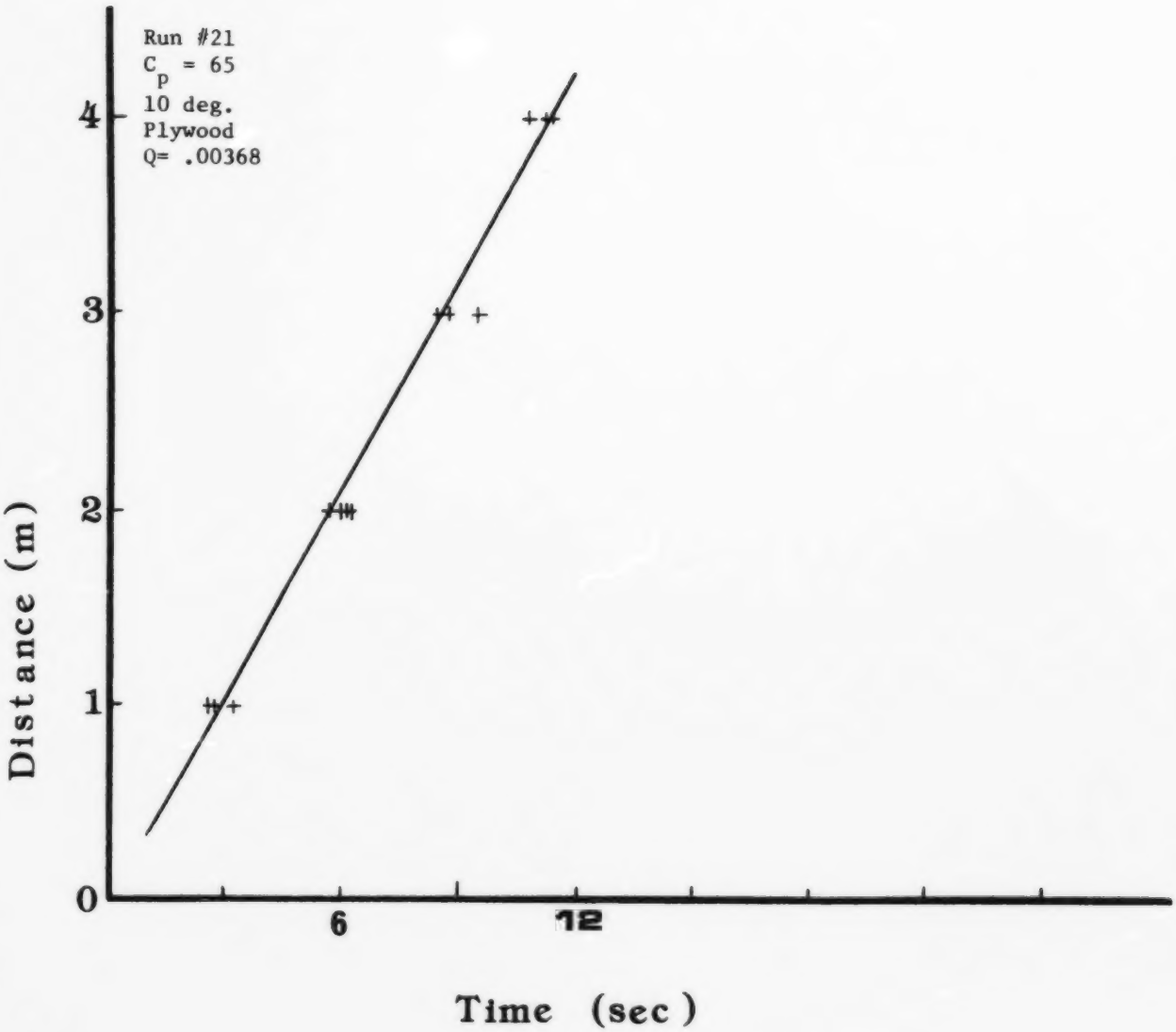
Run #21
C_p = 65
10 deg.
Plywood
Q= .00368
4
3
2
1
0
6
12
Distance (m)
Time (sec)

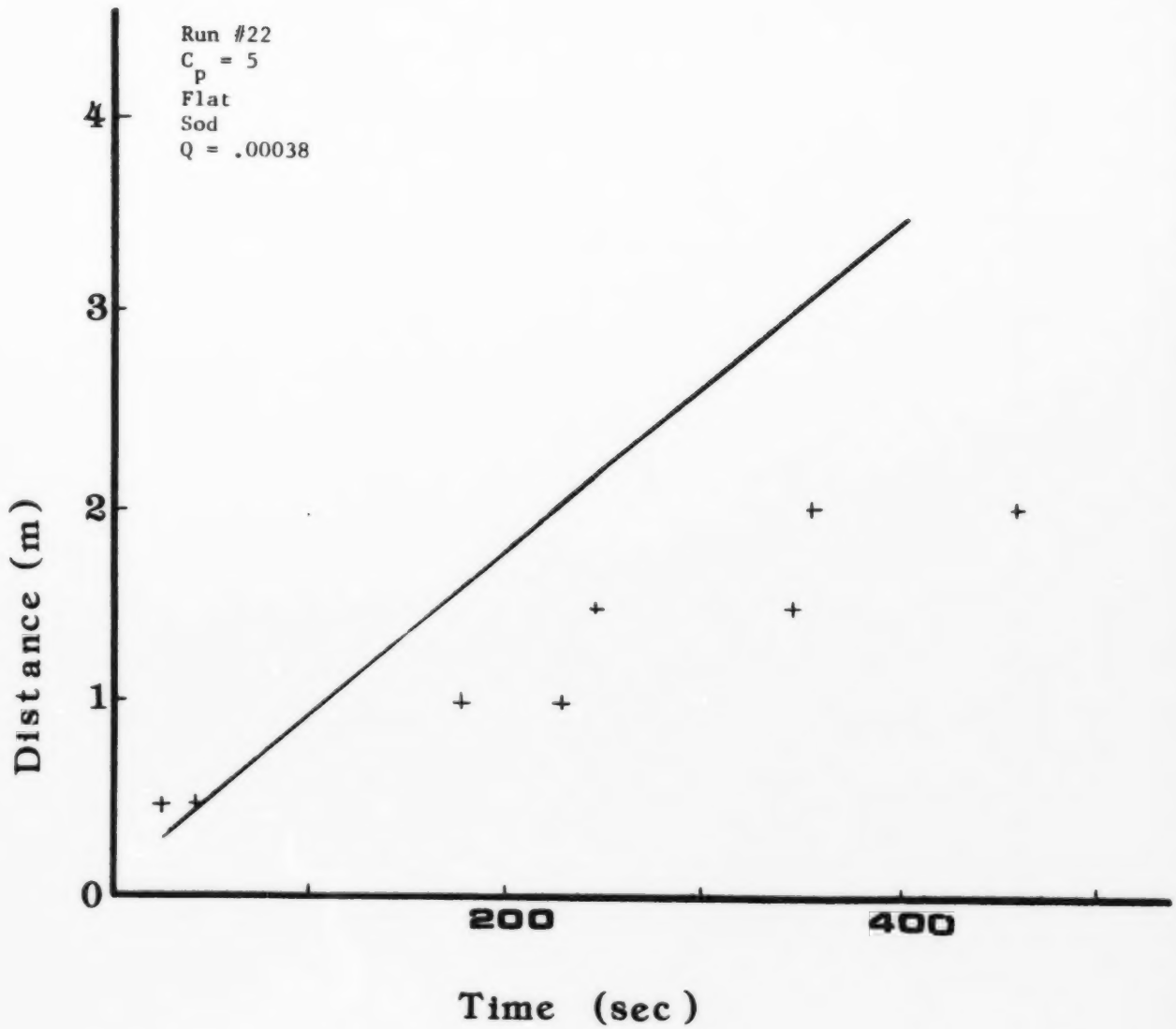
Run #22
C_p = 5
Flat
Sod
Q = .00038
4
3
2
1
0
Distance (m)
200
400
Time (sec)

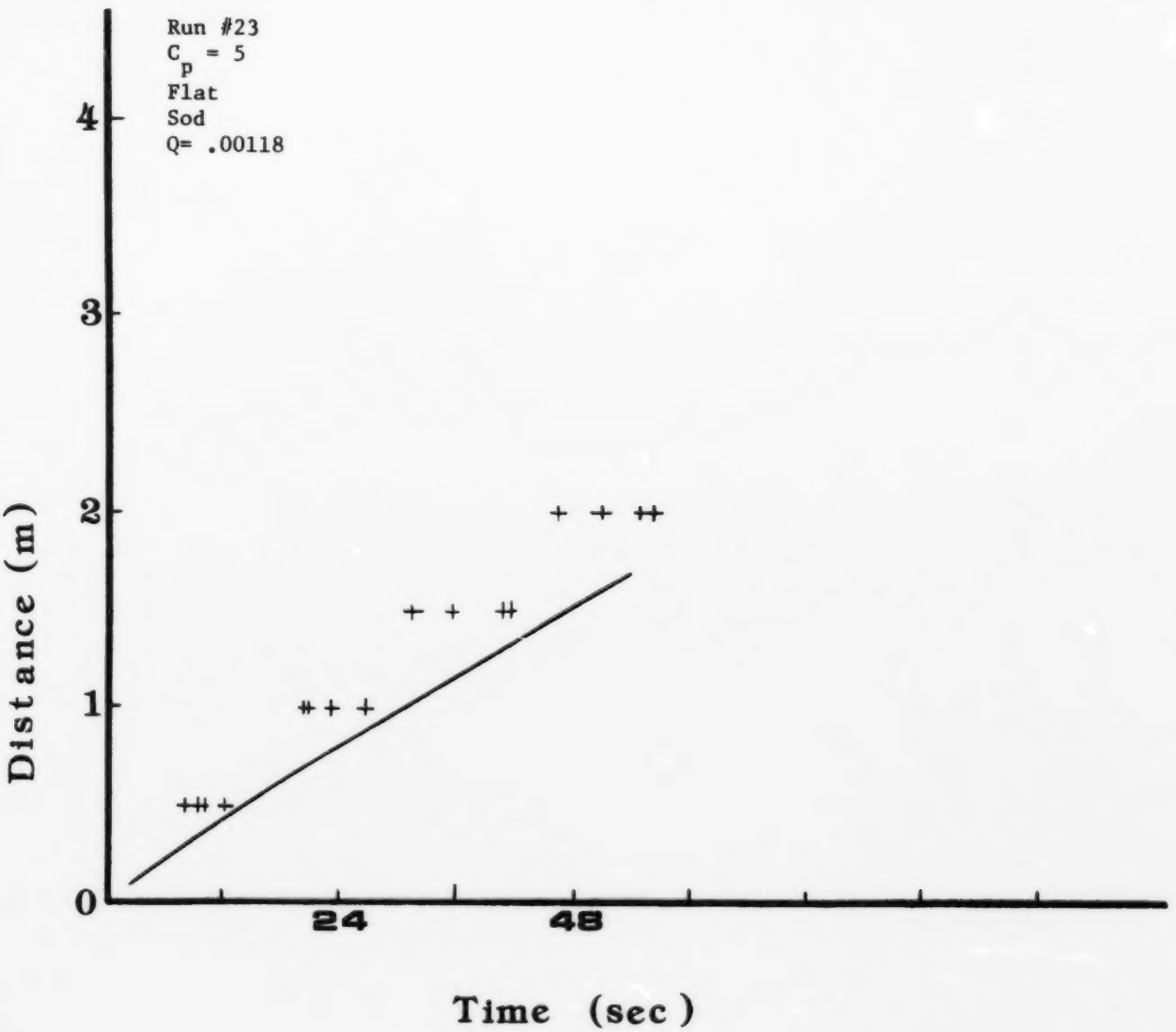
Run #23
C_p = 5
Flat
Sod
Q= .00118
4
3
2
1
0
Distance (m)
24
48
Time (sec)

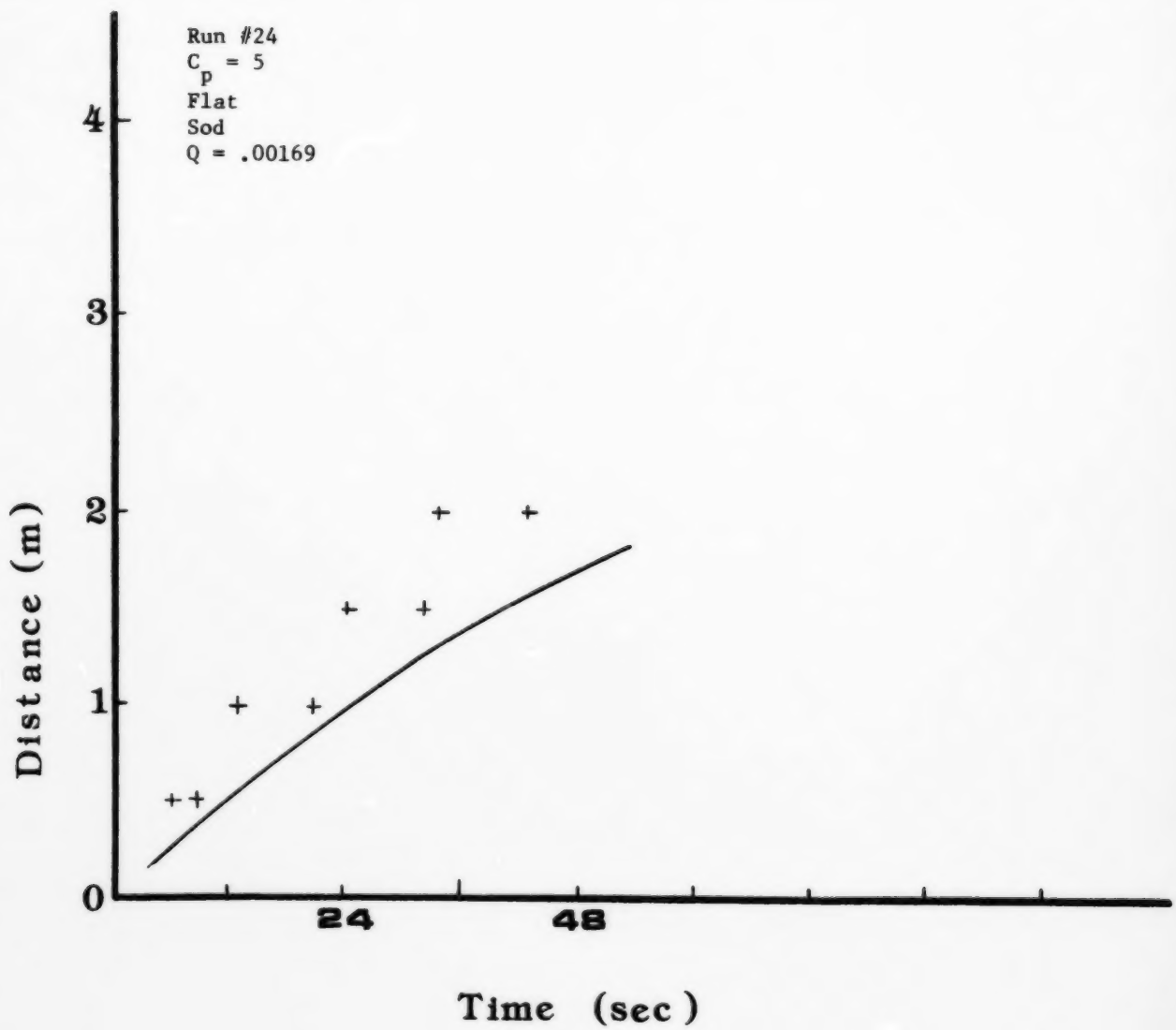
Run #24
C_p = 5
Flat
Sod
Q = .00169
4
3
2
1
0
Distance (m)
24
48
Time (sec)

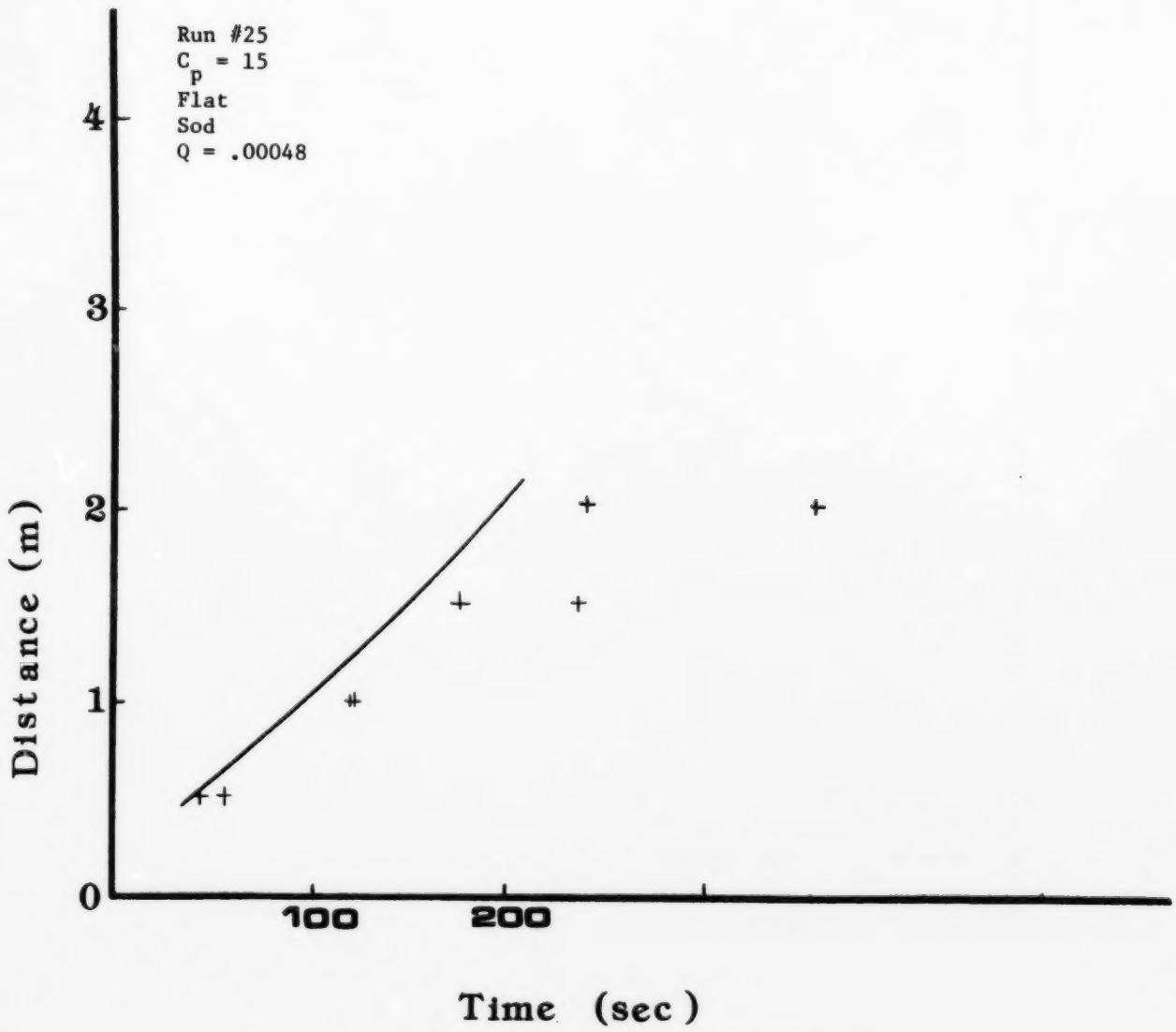
Run #25
C_p = 15
Flat
Sod
Q = .00048
4
3
2
1
0
100
200
Distance (m)
Time (sec)

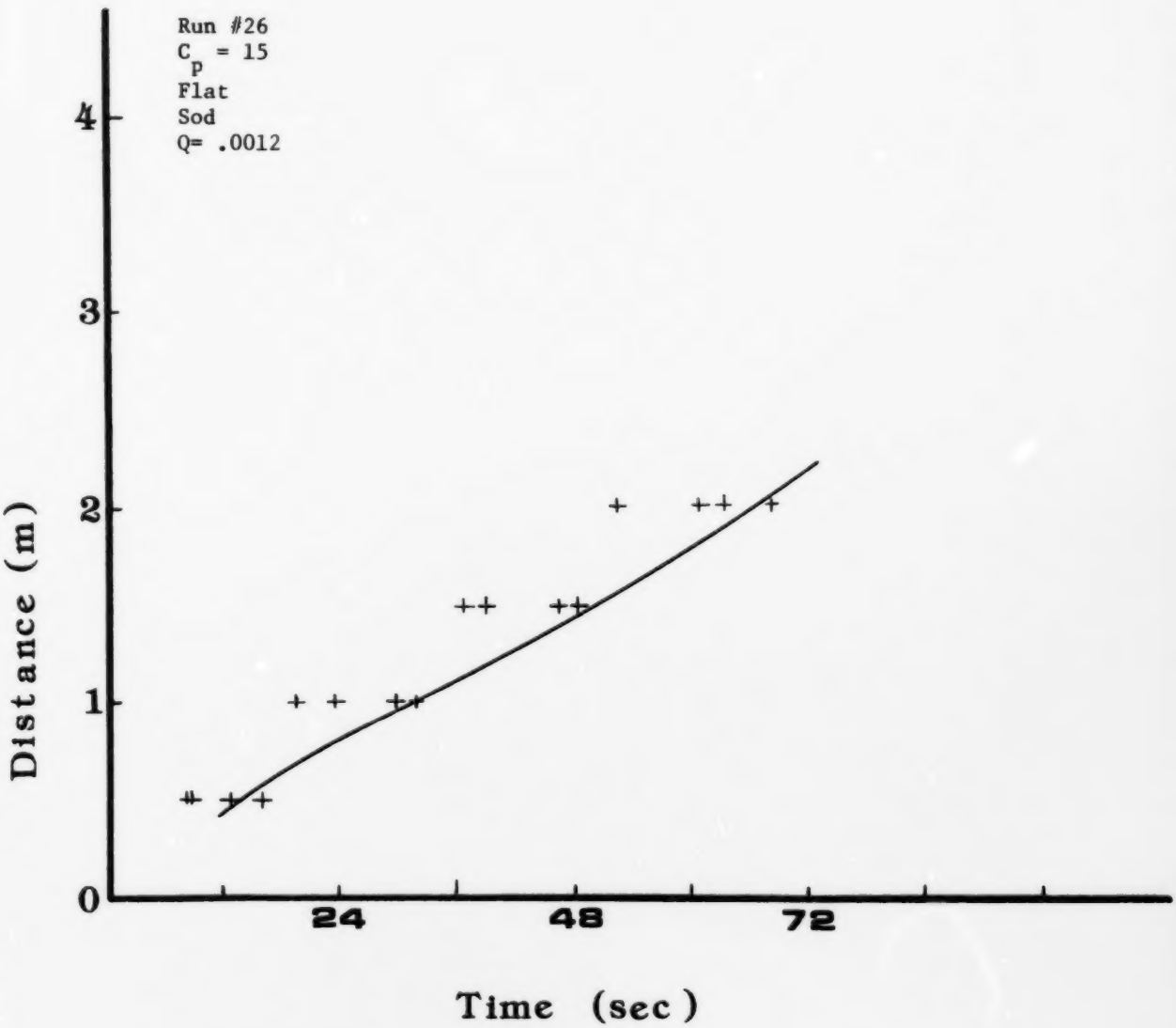
Run #26
C p = 15
Flat
Sod
Q= .0012
4
3
2
1
0
Distance (m)
24
48
72
Time (sec)

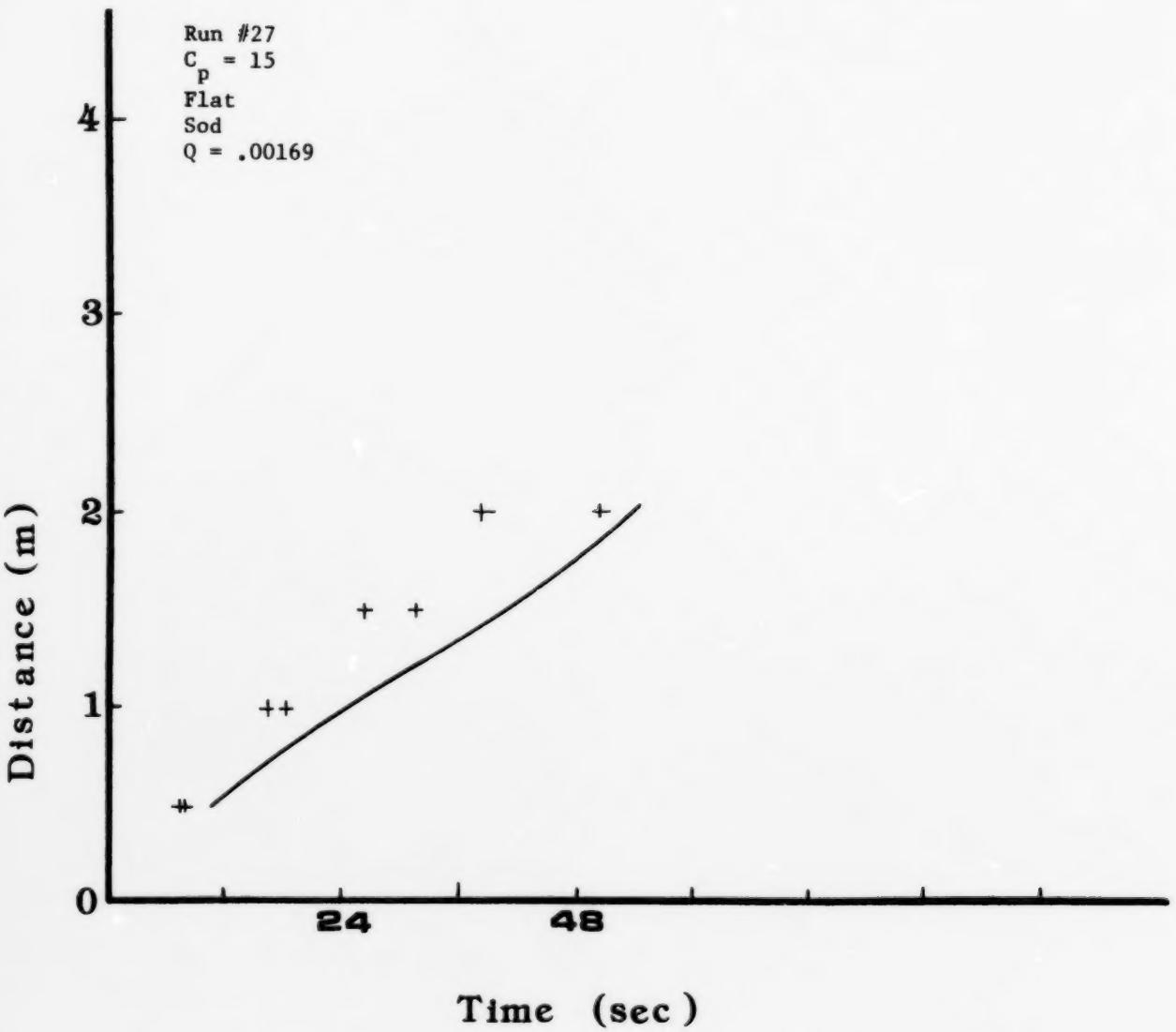
Run #27
C_p = 15
Flat
Sod
Q = .00169
4
3
2
1
0
Distance (m)
24
48
Time (sec)

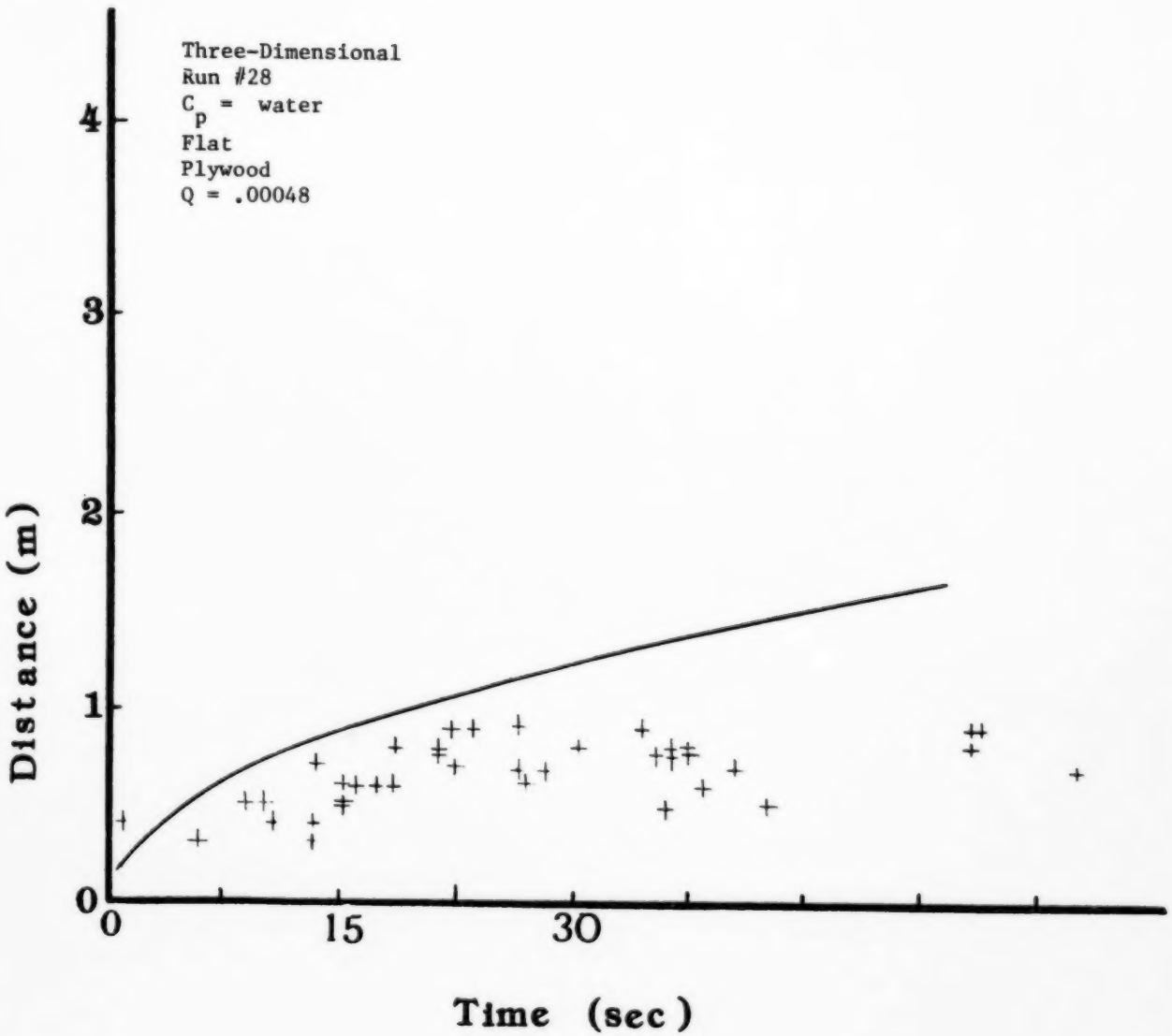
Three-Dimensional
Run #28
C_p = water
Flat
Plywood
Q = .00048
Distance (m)
0
1
2
3
4
0
15
30
Time (sec)

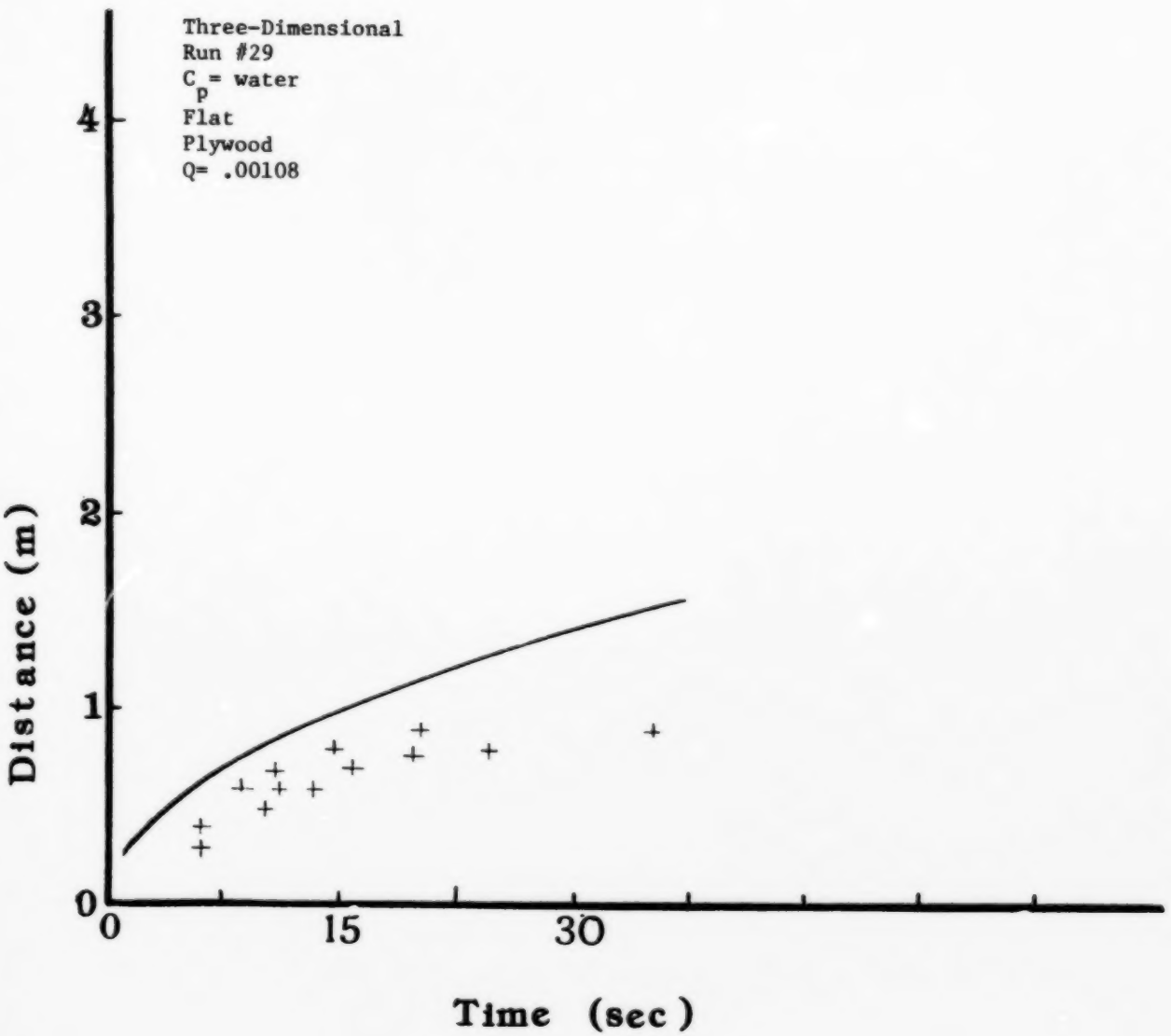
Three-Dimensional
Run #29
C_p = water
Flat
Plywood
Q= .00108
Distance (m)
0
1
2
3
4
0
15
30
Time (sec)

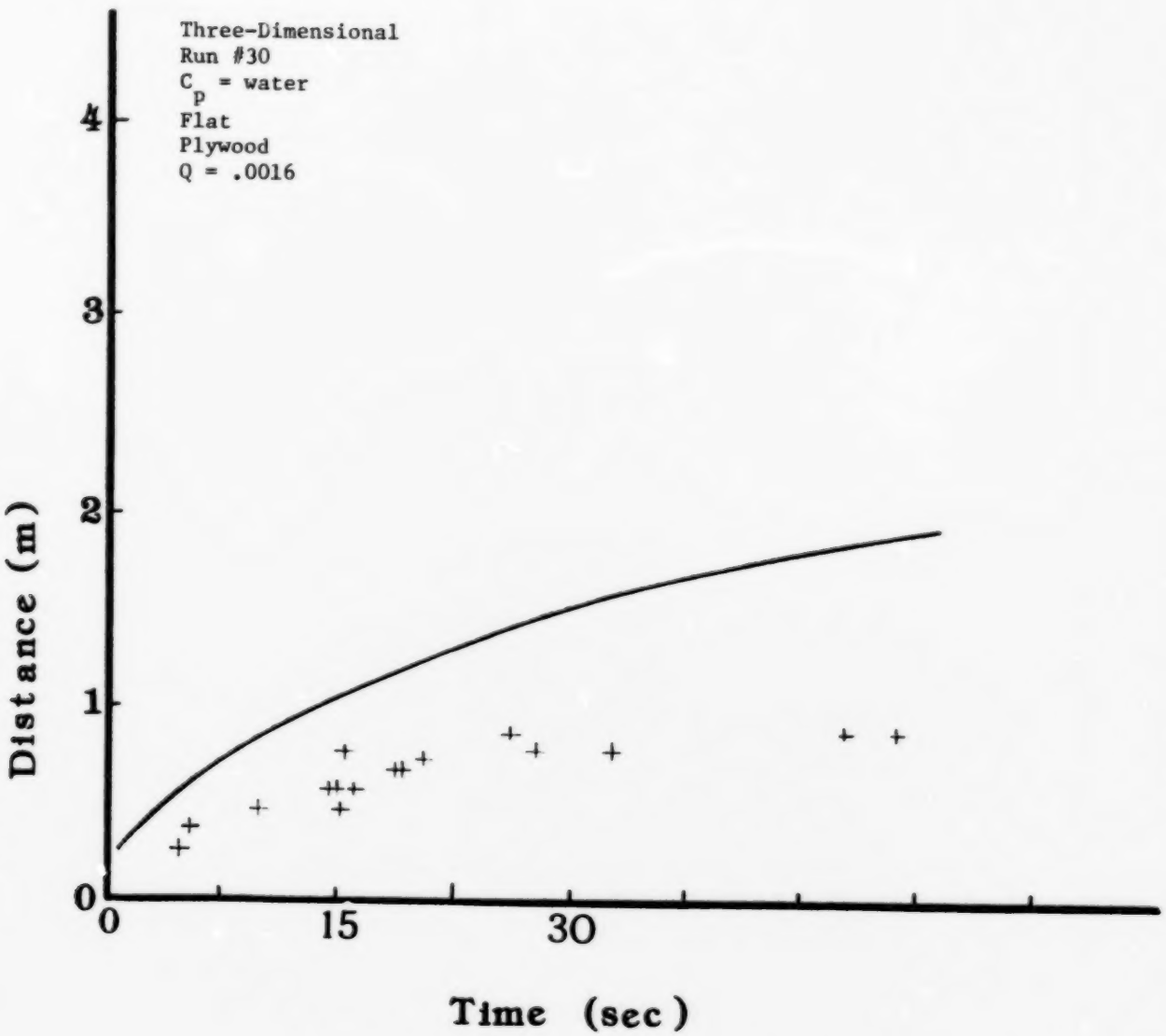
Three-Dimensional
Run #30
C_p = water
Flat
Plywood
Q = .0016
Distance (m)
0
1
2
3
4
0
15
30
Time (sec)

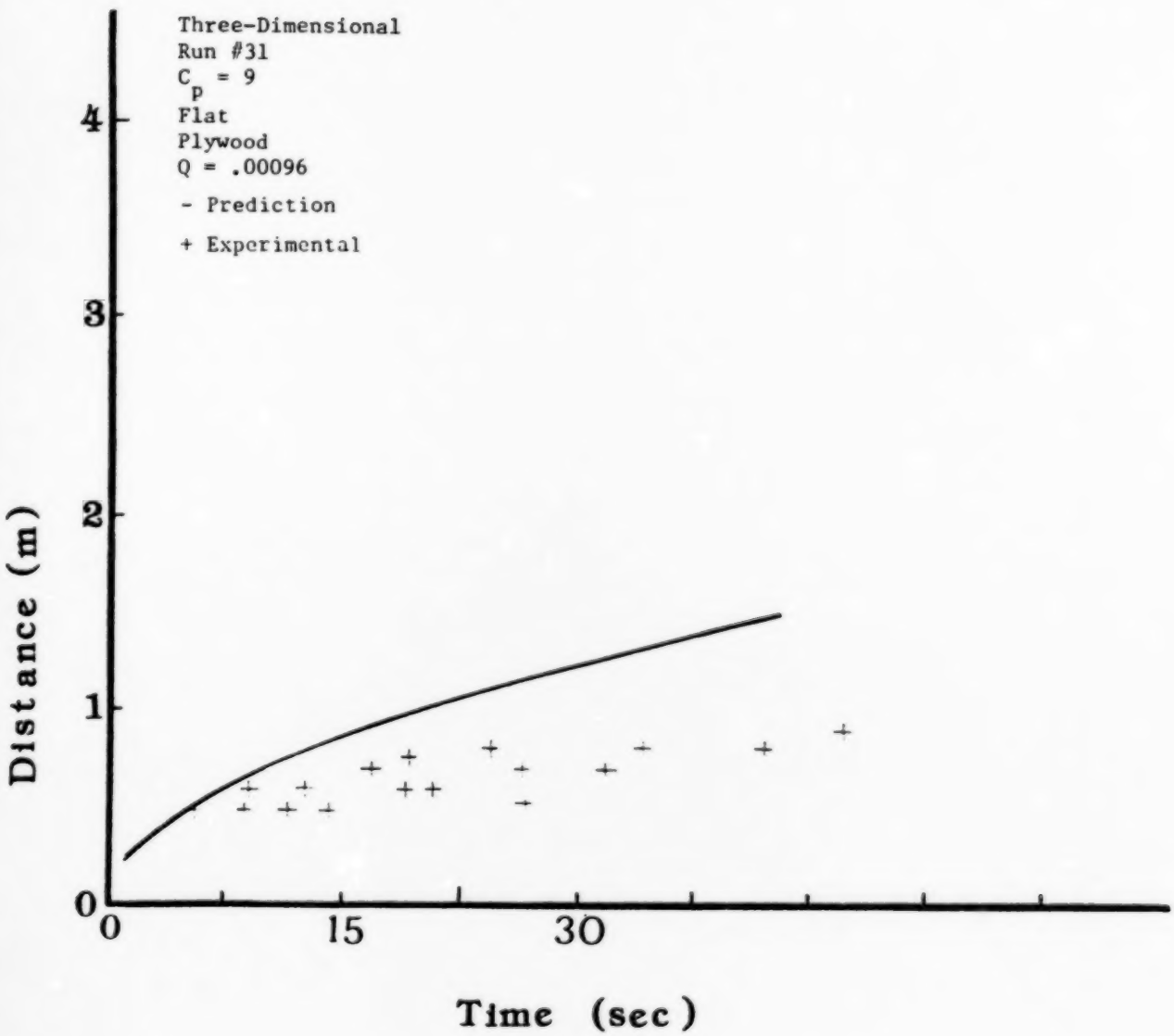
Three-Dimensional
Run #31
C_p = 9
Flat
Plywood
Q = .00096
- Prediction
+ Experimental
Distance (m)
0
1
2
3
4
0
15
30
Time (sec)

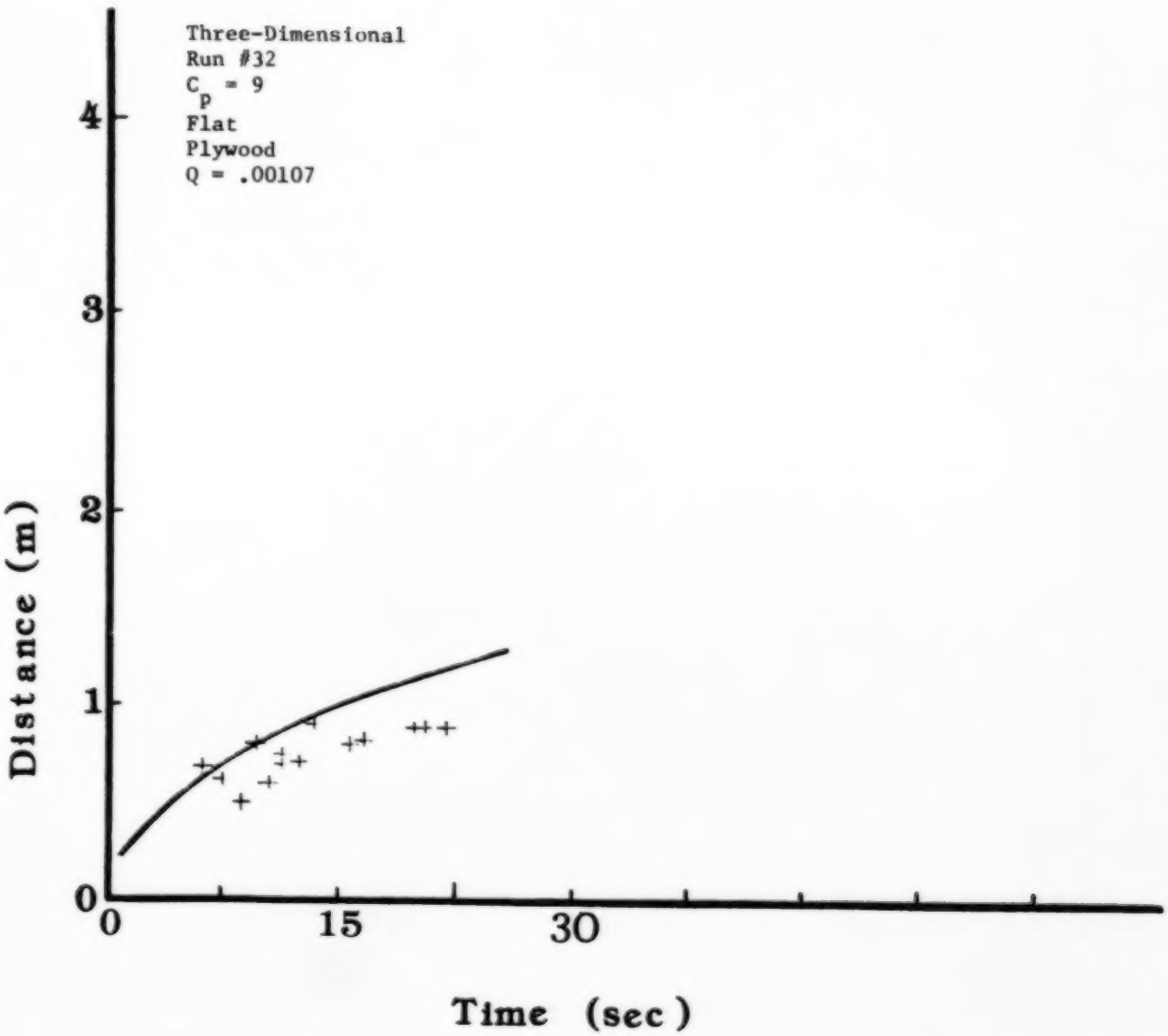
Three-Dimensional
Run #32
C_p = 9
Flat
Plywood
Q = .00107
Distance (m)
0
1
2
3
4
0
15
30
Time (sec)

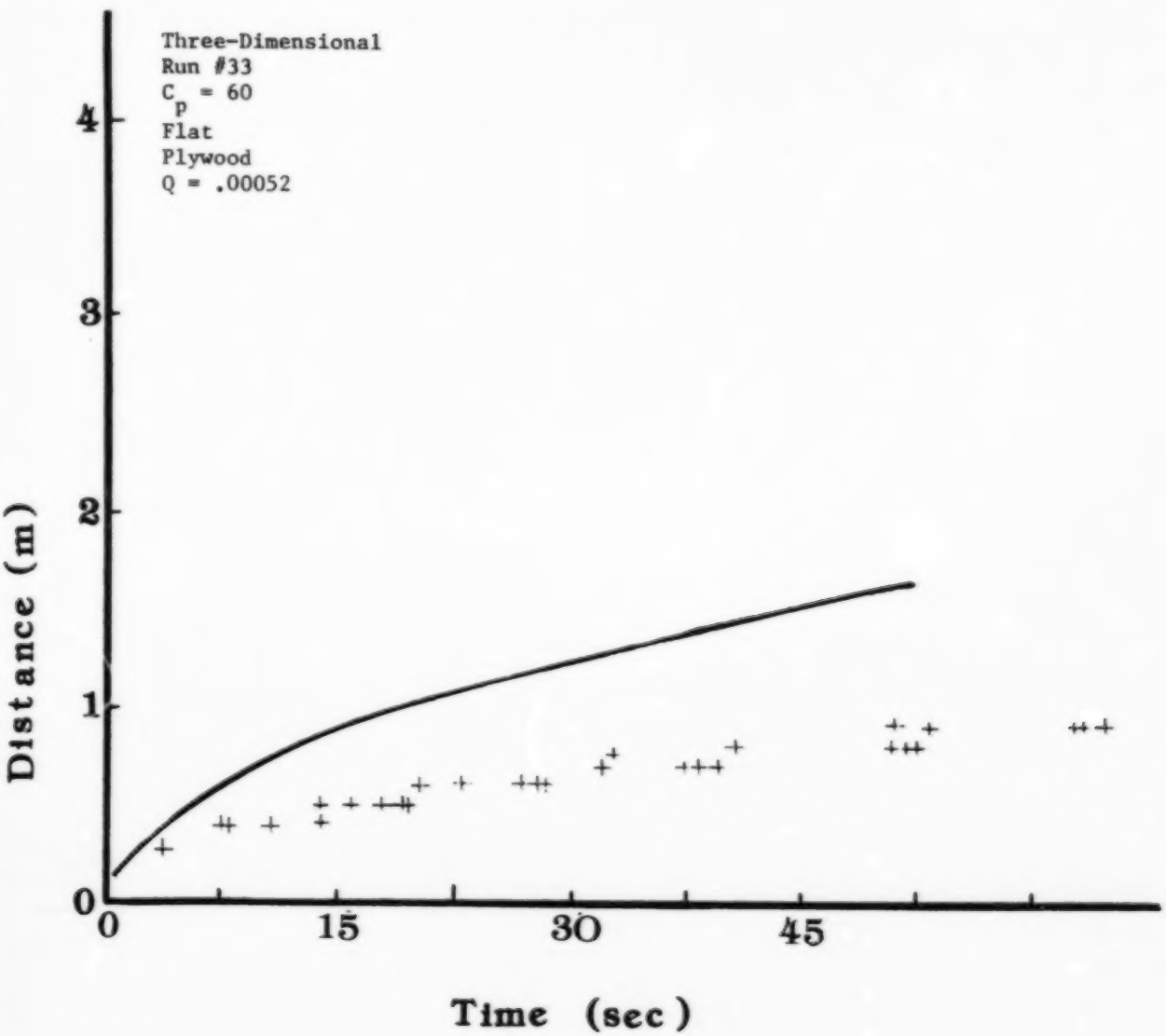
Three-Dimensional
Run #33
C_p = 60
Flat
Plywood
Q = .00052
Distance (m)
0
1
2
3
4
0
15
30
45
Time (sec)

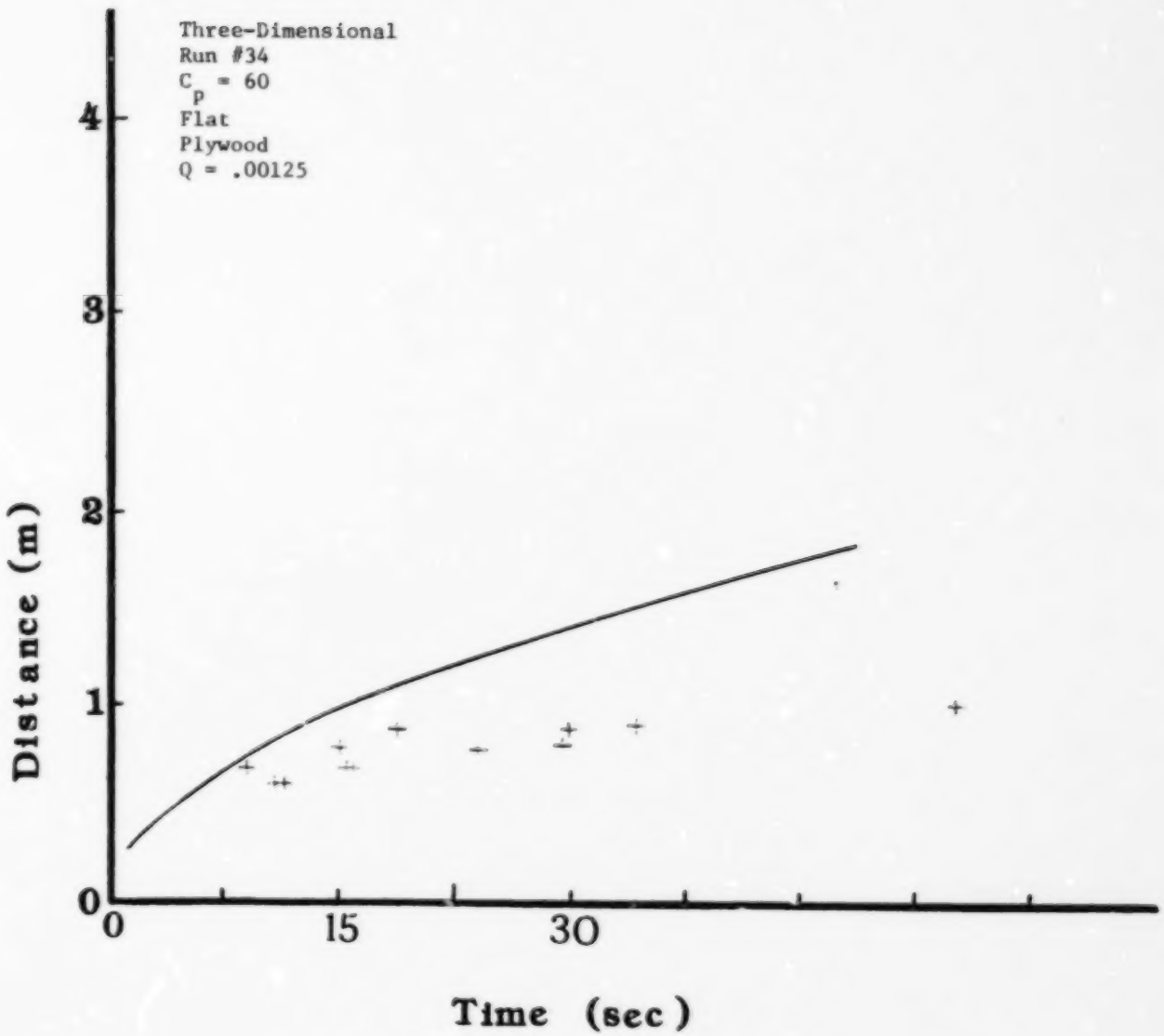
Three-Dimensional
Run #34
C_p = 60
Flat
Plywood
Q = .00125
Distance (m)
0
1
2
3
4
0
15
30
Time (sec)

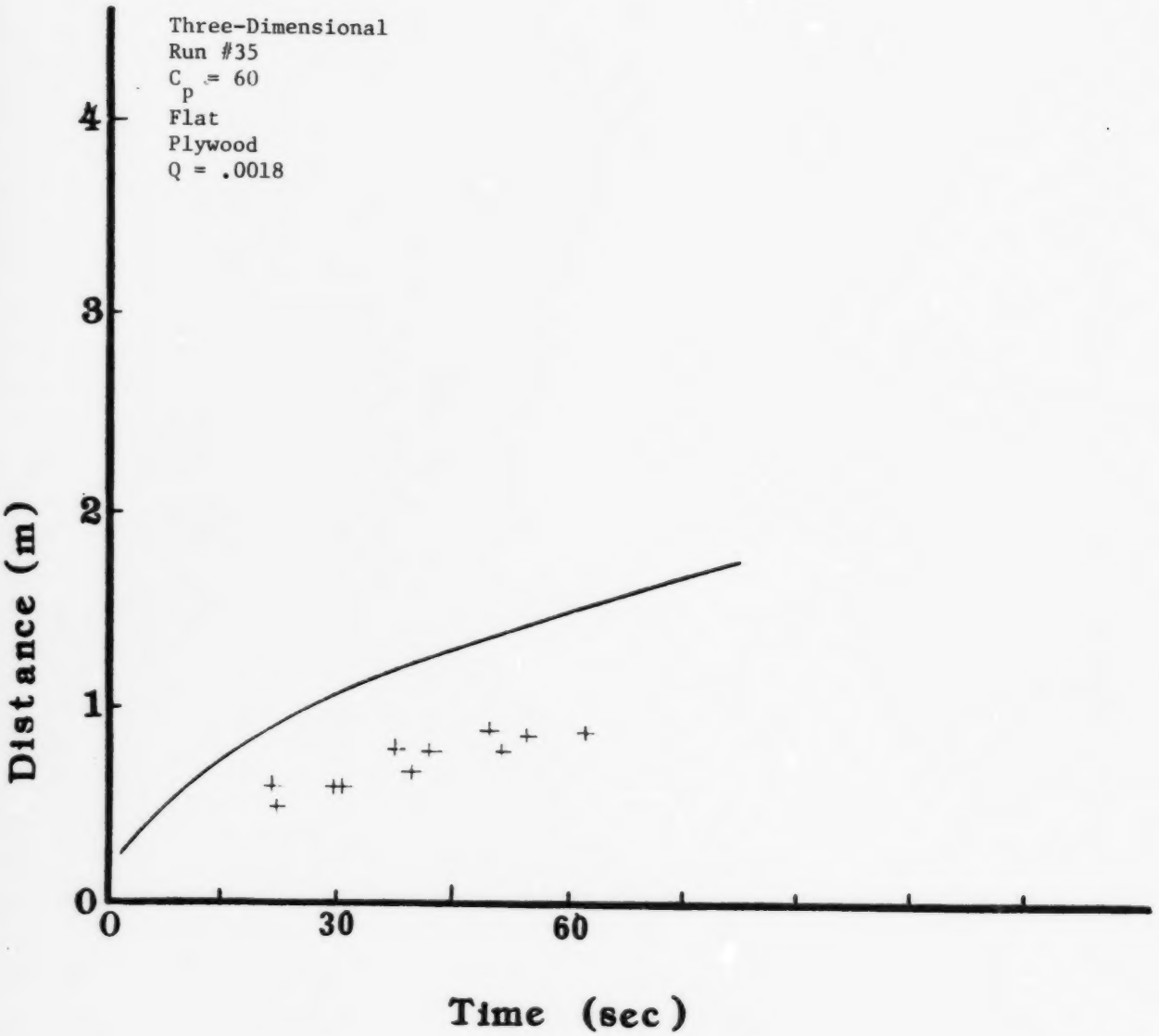
Three-Dimensional
Run #35
C_p = 60
Flat
Plywood
Q = .0018
Distance (m)
0
1
2
3
4
0
30
60
Time (sec)

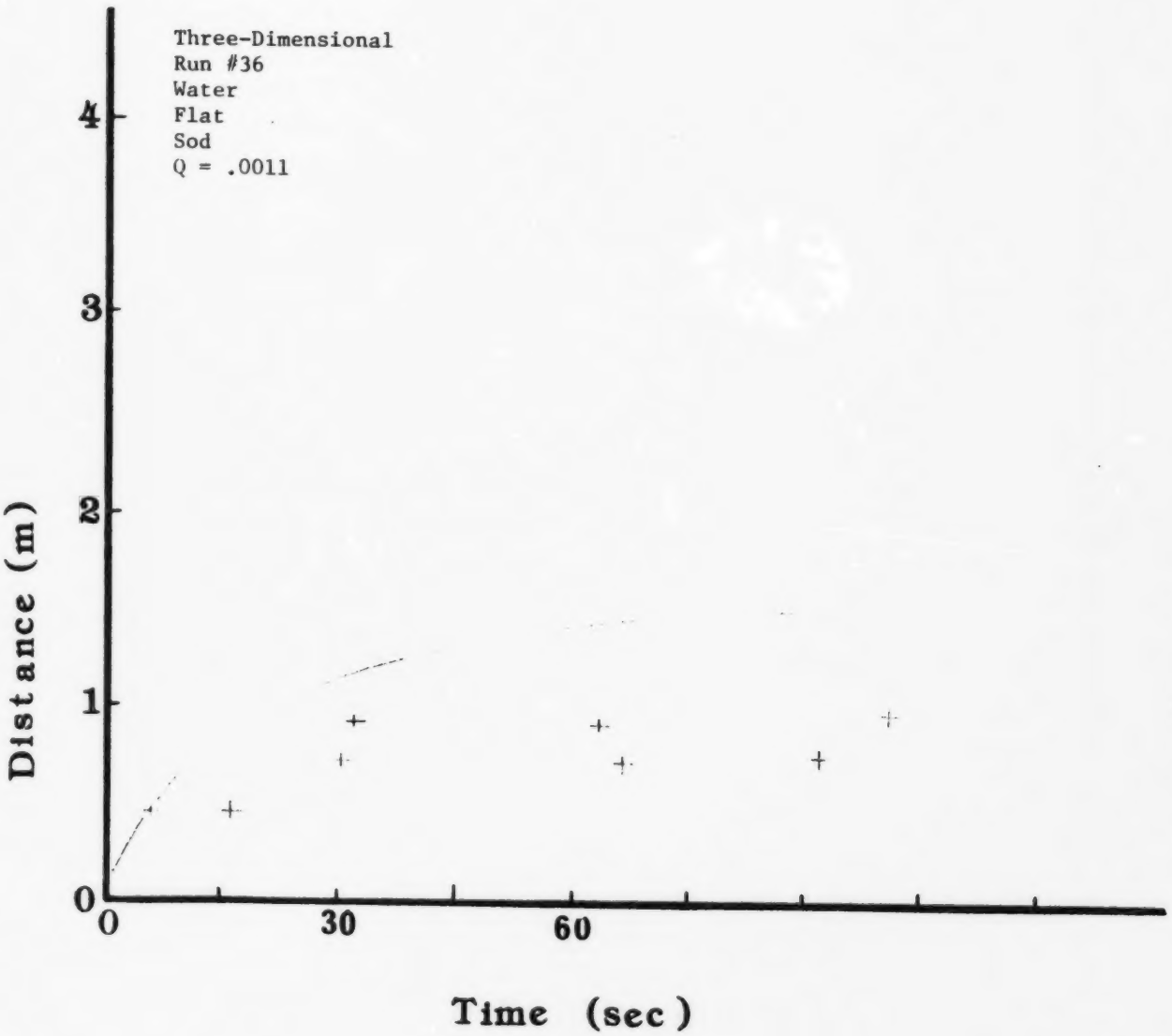
Three-Dimensional
Run #36
Water
Flat
Sod
Q = .0011
Distance (m)
0
1
2
3
4
0
30
60
Time (sec)

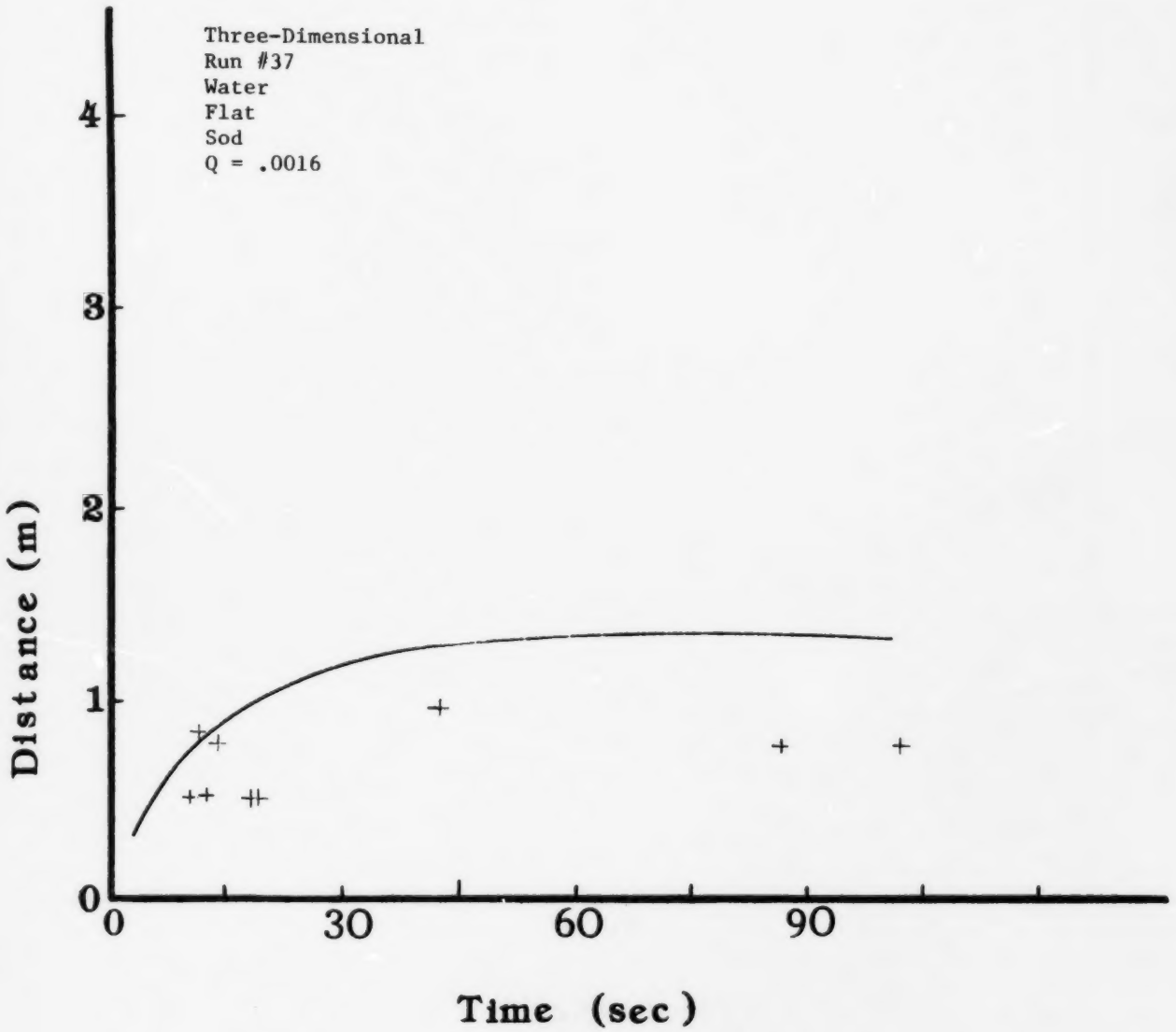
Three-Dimensional
Run #37
Water
Flat
Sod
Q = .0016
Distance (m)
0
1
2
3
4
0
30
60
90
Time (sec)

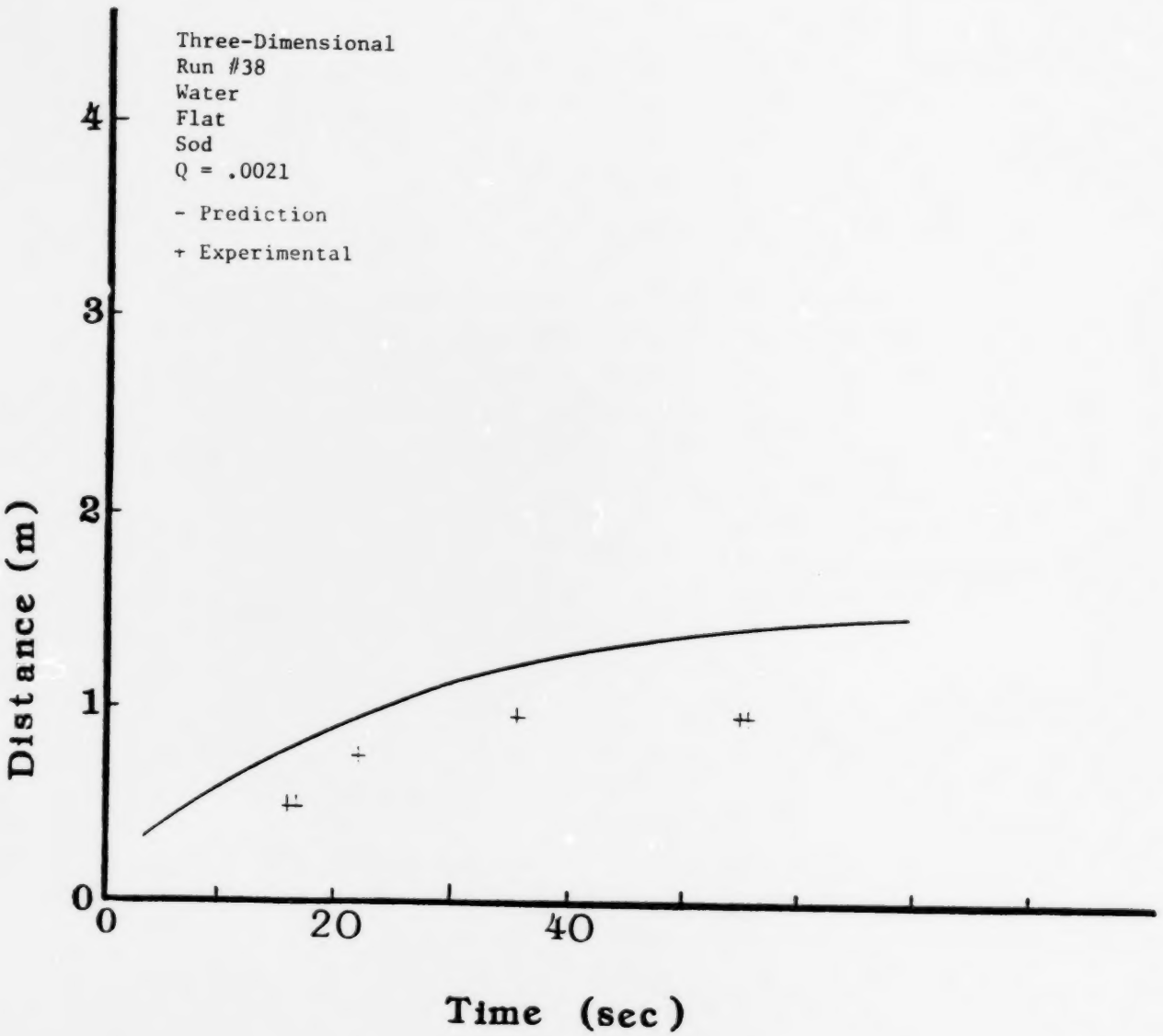
Three-Dimensional
Run #38
Water
Flat
Sod
Q = .0021
- Prediction
+ Experimental
Distance (m)
0
1
2
3
4
0
20
40
Time (sec)

APPENDIX II

Listing of Computer Model

I.1 Spill Model for Two-Dimensions

As a general guideline, when detailed calculations are desired, use small y's; this inceases the computational effort involved in the model use but the accuracy of the model is improved. As well, when the bed slope is relatively small, the surface profile will also be quite small and thus y should be kept small. However, if the frictional resistance to flow is high, then a relatively large y should be used.

```
5 REM *** *** *** *** *** *** *** *** *** *** *** *** *** *** *** *** *** ***
10 REM     This is a two-dimensional model for spills of liquids on surfaces
20 REM     The model calculates the surface profiles of the spill in sloping
30 REM     channels, and includes both evaporation and infiltration
40 REM
50 REM      Program written by E. McBean, University of Waterloo
60 REM
65  REM    No liability beyond the terms of the contract under which this
66  REM    programme was developed (DSS contract) is assumed by the author.
67  REM    Users of this programme do so entirely at their own risk
68 REM*** *** *** *** *** *** *** *** *** *** *** *** *** *** *** *** *** ***
70 I1 = 1
80 INPUT "do you want printed output Y/N=";Q$
90 DIM INF1(300),EVAP1(300),VOL1(300)
100 DIM YPROF(300),LOCN(300)
110 CM = 1
120 REM  presuming all analyses will be in metric (i.e. cm=1)
125 REM   to change the output to imperial units, cm must be set to 1.49
130 READ SIGMA,ANGLE,DENS,QO,MANN
140 REM  sigma = surface tension
150 REM  angle = in degrees
160 REM  density = in kg/m3 ( for water = 1000)
170 REM  MANN = manning coefficient
180 REM  INF = infiltration rate into the soil (in/hr)
190 REM  EVAP = evaporative flux from the surface of the spill (in/hr)
200 READ TIME,DT,DY,SLOPE
210 READ WID
220 REM  time = total time (in seconds) for duration of spill calculations
230 REM  dt = increment in time steps for calculation sequence (seconds)
240 REM  dy = increment in depth at spill source end, in metres
250 REM         - this value must be kept fairly small
260 REM  slope = bottom slope of the channel
270 REM  width = width of the channel segment (at present,it presumes unity)
280  PRINT "sigma=";SIGMA;"angle=";ANGLE;"density=";DENS   ; "flow=";QO
290 READ INF,DECAY,EVAP
300 IF (Q$="N") THEN GOTO 390
310 LPRINT "    COMPUTER MODEL FOR 2-DIMENSIONAL SPILLS "
320 LPRINT "      DEVELOPED BY E.MCBEAN, UNIVERSITY OF WATERLOO, WATERLOO, CANADA
"
330 LPRINT  "     output of input data files "
340 LPRINT "infiltration rate( m/hr)=";INF;"                evaporation rate( m/hr
)=";EVAP
350 LPRINT "infiltration decay rate=";DECAY
360 LPRINT "surf.tension=";SIGMA;"                          angle=";ANGLE
370 LPRINT "density=";DENS;"                                flow=";QO
380 LPRINT "manning coefficent=";MANN;"                      total time  =";TIME
390 LPRINT "duration of analyses(time)=";TIME;"incr.in depth(m)=";DY;"channel sl
ope=";SLOPE
400 LPRINT "delta y =";DY
410 G=9.810001
420 REM  changing of infiltration and evaporation rates to inches per second for
 use in the analyses
430 INF1= INF/3600
440 EVAP = EVAP/3600
450 EVAP2 = 0!
460 RS3 = 0
```

```
470 INF2 = 0!
480 EVAPSUM = 0
490 INFSUM = 0
500 TOTEVAP = 0
510 TOTINF = 0
520 TAG% = 0
530 TAG1%=0
540 RAD=(3.1415*ANGLE/180!)
550 REM surface affinity depth(m)
560 YO=(2!*SIGMA*(1!-COS(RAD))/(DENS*G))^.5
570 REM critical depth (m)
580 YC=((QO*QO)/G)^.333
590 REM normal depth (m)
600 SLPE =ABS( SLOPE)
610 S1 =  SLPE^.5
620 YN = (MANN*QO/S1)^.6
630 YDEL = ABS(YO - YC)
640 YDEL1 = .1 * YC
650 IF YDEL >YDEL1 THEN GOTO 670
660 LPRINT "caution - the surface affinity depth is very close to the critical t
o the critical depth of flow.  The result is that the approximation for extrapol
ating length beyond the critical depth, is only approximate"
670 IF (Q$="N") GOTO 700
680 LPRINT "surface affinity depth(m)=";YO;"   critical depth(m)=";YC
690 LPRINT "normal depth (m)="; YN
700 IF (YN<YC*1.5) THEN GOTO 1970
710 IF YO>YC THEN GOTO 760
720 Y5=YO
730 YO=YC+.000005
740 Y1 =YO
750 TAG%=1
760 LPR = .1
770 DELX = .02
780 REM   output of titles
790 LPRINT "     time       location of      depth at      volume     volume    volume
"
800 LPRINT "    (secs)        leading       hydraulic     in spill   infil.    evaptd
 "
810 LPRINT "                  edge (m)       jump (m)       (m^3)      (m^3)     (m^3)"
820 FOR T=1 TO TIME STEP DT
830 INF= INF1*EXP(-DECAY*T)
840 TAG1%= 0
850 PVT = 0!
860 PVT1 = 0
870 RS3=0
880 X1 = 0
890 K%=0
900 Y1 = YO
910 YPROF(1) = Y1
920 VOLSUM = 0!
930 EVAPSUM = 0
940 INFSUM = 0!
950 Y2 = Y1 + DY
960 IT1=0
```

```
970  YPROF(K%+2) = Y2
980 Q1 = Q0 - (LPR-X1)*(INF + EVAP)*WID
990 IF Q1>0 THEN GOTO 1020
1000 LPRINT "infiltration and evaporation have exhausted the fluid at the leadin
g edge, and no further migration occurs"
1010 END
1020 A = (Y1-Y2)/2
1030 D = 1/(SLOPE -(Q1*Q1)*(MANN*MANN)/(CM*CM*Y1^3.33))
1040 ITER = 0
1050 Q2 = Q0 - ( LPR -DELX-X1)*(INF +EVAP)*WID
1060 B = ((-Q2*Q2)/(Y2*Y2) + (Q1*Q1)/(Y1*Y1))/(4*G)
1070 C = 1/(SLOPE - (Q2*Q2)*(MANN*MANN)/ (CM*CM*Y2^3.33))
1080 IF X2<0 THEN X2 = 0
1090 IF LPR<X2 THEN LPR = X2
1100 X2 = X1 +(A+B)*(C+D)
1110 DX = X2-X1
1120 ITER = ITER + 1
1130 IF ITER<10  THEN GOTO 1170
1140 IT1 = IT1 + 1
1150 Y2 = Y1 + DY/IT1
1160 IF IT1 >5 THEN PRINT "problems of convergence in program. Try a smaller dy
in the input data"
1170 IF IT1>5 THEN END
1180 IF (ABS(DX-DELX)<.005) THEN GOTO 1210
1190 DELX = DX
1200 GOTO 1050
1210 DELT = DT
1220 IF T>1 THEN GOTO 1240
1230 DELT = 1
1240 K%=K%+1
1250  LOCN(K%+1)=X2
1260 INF1(K%) = INF *DELX *DELT*WID
1270 EVAP1(K%)= EVAP*DELX *DELT*WID
1280 REM calculation of volume of water,averaging the depths
1290 VOL1(K%) = (Y2+Y1)/2*DELX *WID
1300 IF TAG%<1 THEN GOTO 1380
1310 REM   have encountered the critical flow condition and therefore have to ad
d this volume of fluid onto the total
1320 Y3 = Y2-Y0
1330 Y4 = Y0- Y5
1340 RS3 = X2 * Y4 /Y3
1350 PVT1 = RS3 * (Y5+Y0)/2*WID
1360 EVAP2 = EVAP * RS3 * DELT * WID
1370 INF2 = INF * RS3 * DELT * WID
1380 EVAPSUM = 0
1390 INFSUM = 0
1400 VOLSUM = 0
1410 FOR N=1 TO K%
1420 EVAPSUM = EVAP1(N) +EVAPSUM
1430 INFSUM = INF1(N) +INFSUM
1440 VOLSUM = VOL1(N) +VOLSUM +EVAP1(N) + INF1(N)
1450 NEXT N
1460 EVAPSUM = EVAPSUM +EVAP2
1470 INFSUM = INFSUM +INF2
```

```
1480 VOLSUM = VOLSUM +PVT1
1490 VOL = Q0 * T
1500 PRINT VOL;VOLSUM
1510 IF (VOL <VOLSUM) THEN GOTO 1560
1520  REM if vol < volsum, then have exceeded the spill volume and may proceed
          with calculations
1530 X1 = X2
1540 Y1 = Y2
1550 GOTO 950
1560 REM check comparison of X2 with LPR
1570 PRINT "total of liquid spilled";VOL;"volume in profile of spill";VOLSUM
1580 LPR1 = LPR
1590 IF TAG% <1 THEN GOTO 1610
1600 LPR1 = LPR + RS3
1610 D = ABS(X2-LPR1)
1620 IF (D<(.05*X2) ) THEN GOTO  1670
1630 REM allowing a five percent deviation in closure
1640 PRINT "re-estimating LPR";LPR;X2
1650 LPR = X2
1660 GOTO 880
1670  IF (Q$="N") THEN GOTO 1740
1675 LPRINT "lpr1= ";LPR1;"lpr=";LPR;"x2=";X2
1680 LPRINT USING "########";T;
1690 LPRINT USING "##############.##";LPR1;
1700 LPRINT USING "##########.###";Y2;
1710 LPRINT USING "#########.####";VOLSUM;
1720 LPRINT USING "#######.####";INFSUM;
1730 LPRINT USING "######.####";EVAPSUM
1740 I1=I1+1
1750 TOTEVAP = TOTEVAP +EVAPSUM
1760 TOTINF= TOTINF + INFSUM
1770 NEXT T
1780 REM   output of total infiltration and evaporation volumes
1790 IF (Q$="N") THEN GOTO 1850
1800 LPRINT "total infiltration and evaporation volumes (m^3)"
1810 LPRINT USING "########.###";TOTINF;
1820 LPRINT USING "########.###";TOTEVAP
1830 LPRINT "total volume of liquid spilled (m^3)"
1840 LPRINT USING "#######.###";VOL
1850 REM   output of final spill profile
1860 IF (Q$="N") THEN GOTO 1960
1870 LPRINT "          Location(m)          Depth(m)"
1880 N%=K%+1
1890 INPUT "do you want printed profile Y/N";Q$
1900 IF (Q$="N") THEN GOTO 1960
1910 FOR I = 1 TO N%
1920 LPRINT USING "###############.###";LOCN(I);
1930 LPRINT USING "################.###";YPROF(I)
1940 NEXT I
1950 GOTO 2160
1960 LPRINT "            time (sec)              bore location(m)"
1970 REM  in the situation of a steep slope
1980 EVAPSUM = 0
1990 INFSUM = 0
2000 FOR T = 1 TO TIME STEP DT
2010 INF = INF1 *EXP(-DECAY*T)
```

```
2020 DELT = DT
2030 IF T>1 THEN GOTO 2050
2040 DELT = 1
2050 VOL = QO * T
2060 LPR = VOL/(YN*WID + (EVAP+INF )*WID*T)
2070 EVAPSUM = EVAPSUM + EVAP *DELT *WID*LPR
2080 INFSUM = INFSUM +INF *DELT*WID*LPR
2090 VOLSUM = YN * WID * LPR
2100 IF (Q$="N") THEN GOTO 2150
2110 LPRINT USING "#########";T;
2120 LPRINT USING "########.###";LPR;
2130 LPRINT USING "########.###";INFSUM;
2140 LPRINT USING "########.###";EVAPSUM
2150 NEXT T
2160 END
2170 DATA 0.074,60,1000,.00048, 1.750
2180 DATA 200,20,.001    ,0.000 ,1
2190 DATA 1.50,.020,.50
```

I.2 Spill Model for Three-Dimensions

```
5 REM *** *** *** *** *** *** *** *** *** *** *** *** *** *** *** *** *** ***
10 REM     This is a three-dimensional model for spills of liquids on surfaces
20 REM     The model calculates the surface profiles of the spill on a flat
30 REM     surface,  and includes both evaporation and infiltration
31 REM       The mathematical representation of momentum is fairly simple in thi
 model
32 REM
35 REM     The model was developed by E. McBean of the University of Waterloo
36 REM
37 REM     No liability beyond the terms of the contract under which this
           programme was developed (DSS Constract) is assumed by the author.
           Users of this programme do  so entirely at their own risk
39 REM*** *** *** *** *** *** *** *** *** *** *** *** *** *** *** *** *** ***
40 I1 = 1
50 INPUT "do you want printed output Y/N=";Q$
60 DIM INF1(300),EVAP1(300),VOL1(300)
70 DIM YPROF(300),LOCN(300)
80 CM = 1
90 REM  presuming all analyses will be in metric (i.e. cm=1)
95 REM  to change the output to imperial units, cm must be set to 1.49
100 READ SIGMA,ANGLE,DENS,Q0,MANN
110 REM  sigma = surface tension
120 REM  angle = in degrees
130 REM  density = in kg/m3 ( for water = 1000)
140 REM  MANN = manning coefficient
145 REM extablishing flow in each arc where the arc is 1/30th of the total flow
150 REM  INF = infiltration rate into the soil (m/hr), initial rate
160 REM  EVAP = evaporative flux from the surface of the spill (in/hr)
170 READ TIME,DT
190 REM  time = total time (in seconds) for duration of spill calculations
200 REM  dt = increment in time steps for calculation sequence (seconds)
250 LPRINT  "    output of input data files "
260  PRINT "sigma=";SIGMA;"angle=";ANGLE;"density=";DENS    ; "flow=";Q0
270 READ INF,DECAY,EVAP
280 IF (Q$="N") THEN GOTO 320
281 LPRINT "  computer model for 3-dimensional spills"
282 LPRINT "  developed by E. McBean, University of Waterloo"
290 LPRINT "infiltration rate( m/hr)=";INF;"evaporation rate( m/hr)=";EVAP
295 LPRINT "decay rate of infiltration";DECAY
300 LPRINT "surf.tension=";SIGMA;"angle=";ANGLE;"density=";DENS    ; "flow=";Q0
310 LPRINT "manning coefficent=";MANN;"total time  =";TIME;"delta y=";DY
320 LPRINT "duration of analyses(time)=";TIME
330 G=9.810001
340 REM  changing of infiltration and evaporation rates to m per second for use
in the analyses
350 INF1= INF/3600
360 EVAP = EVAP/3600
440 RAD=(3.1415*ANGLE/180!)
441 REM  surface affinity depth (m)
```

```
450 YO=(2!*SIGMA*(1!-COS(RAD))/(DENS*G))^.5
451 REM  critical depth (m)
460 YC=((QO*QO)/G)^.333
470  PRINT "normal depth";YO;"critical depth";YC
520 IF (Q$="N") GOTO 540
530 LPRINT "surface affinity depth(m)=";YO;"   critical depth(m)=";YC
540 INFSM1 = 0
542 INFSM2 = 0
544 EVASM1 = 0
546 EVASM2 = 0
610 REM   output of titles
620 LPRINT "    time       location of      depth at      vol in     volume    volume
*
630 LPRINT "   (secs)        leading       hydraulic  spill profil infil.    evaptd
 *
640 LPRINT "                 edge (m)       jump (m)       (m^3)      (m^3)     (m^3)"
650 FOR T=1 TO TIME STEP DT
660 DELT = DT
661 T1 = T-DELT/2
662 IF T>1 THEN GOTO 665
663 T1 = 1
664 DELT = 1
665 INF = INFI*EXP(-DECAY * T1)
700 X1 = 0
800 REM  volume of spilled liquid
810 VOL = QO * T
820 RAD1 = (VOL/(3.14*YO))^.5
830 RAD2 = (VOL/(3.14*YC))^.5
840 INF1 = INF * 3.14*RAD1*RAD1*DELT
850 INF2 = INF *3.14*RAD2*RAD2*DELT
860 EVAP1 = EVAP*3.14*RAD1*RAD1*DELT
870 EVAP2 = EVAP*3.14*RAD2 * RAD2*DELT
880  REM  re-estimating radius of spill
881  INFSM1 = INFSM1 +INF1
882  INFSM2 = INFSM2 +INF2
883  EVASM1 = EVASM1 + EVAP1
884  EVASM2 = EVASM2 + EVAP2
890 A1 = VOL - INFSM1-EVASM1
900 IF A1 >0 GOTO 930
910 RAD1 = 0
920 GOTO 940
930 RAD1 = (A1/(3.14*YO))^.5
940 A2 = VOL - INFSM2-EVASM2
950 IF A2 >0 GOTO 980
960 RAD2 = 0
970 GOTO 990
980 RAD2 = (A2/(3.14 *YC))^.5
990 REM
1360  IF (Q$="N") THEN GOTO 1440
1370 LPRINT "                estimate 1  of radius of excursion"
1380 LPRINT USING "#########";T;
1390 LPRINT USING "##############.##";RAD1;
```

```
1400 LPRINT USING "##########.###";YO;
1410 LPRINT USING "##########.##";VOL;
1420 LPRINT USING "#########.##";INF1;
1430 LPPINT USING "########.##";EVAP1
1431 LPRINT "                estimate 2  of radius of excursion"
1432 LPRINT USING "####################.##";RAD2;
1433 LPRINT USING "##########.###";YC;
1434 LPRINT USING "##########.###";VOL;
1435 LPRINT USING "########.##";INF2;
1436 LPRINT USING "########.##";EVAP2
1440 REM
1450 NEXT T
1451 REM  output of total infiltration and evaporation volumes
1453 LPRINT "total infiltration and evaporation volume(m*3)"
1454 LPRINT USING "########.###";INFSM1;
1455 LPRINT USING "########.###";INFSM2
1456 LPRINT USING "########.###";EVASM1;
1457 LPPINT USING "########.###";EVASM2
1458 LPRINT "total volume of liquid spilled(m*3)"
1459 LPRINT USING "########.###";VOL
1460 REM   output of final spill profile
1550 END
1560 DATA 0.074,60,1000,.0021   ,.950
1570 DATA  100,10
1580 DATA 0.5,.005,0
```

TABLE III.1

Input Parameter List for Model Results Presented

Run No.	Surface Tension	Angle	Density	Flow	Manning Coeff.	Total Time	Incr. in Depth	Channel Slope	Inf. Rate	Inf. Decay Rate	Evap. Rate
1	.074	45	1000	.00046	.01	60	.0001	0	0	0	0
2	.074	45	1000	.0012	.005	31	.0005	0	0	0	0
3	.074	45	1000	.0017	.005	21	.0005	0	0	0	0
4	.074	45	1000	.0014	.015	10	.0001	-.176	0	0	0
5	.074	45	1000	.00306	.015	10	.0001	-.176	0	0	0
6	.074	45	1000	.00386	.015	10	.0001	-.176	0	0	0
7	.074	60	1000	.00048	.75	100	.003	0	1.3	.005	0
8	.074	60	1000	.0012	.65	71	.003	0	2.5	.005	0
9	.074	60	1000	.0017	.65	71	.003	0	2.5	.005	0
10	.074	60	1000	.00096	.05	101	.003	-.176	2.5	.007	0
11	.074	60	1000	.0024	.05	101	.003	-.176	2.5	.007	0
12	.074	60	1000	.0034	.075	101	.003	-.176	2.5	.007	0
13	.074	45	1000	.00038	.09	120	.001	0	0	0	0
14	.074	45	1000	.00187	.065	51	.001	0	0	0	0
15	.074	45	1000	.002	.05	37	.001	0	0	0	0
16	.074	45	1000	.00032	.15	88	.001	0	0	0	0
17	.074	45	1000	.0015	.10	72	.001	0	0	0	0
18	.074	45	1000	.0018	.09	62	.001	0	0	0	0
19	.074	45	1000	.00061	.13	40	.001	-.176	0	0	0
20	.074	45	1000	.003	.06	40	.001	-.176	0	0	0
21	.074	45	1000	.00368	.055	40	.001	-.176	0	0	0

TABLE III.1 (Cont.)

Input Parameter List for Model Results Presented

Run No.	Surface Tension	Angle	Density	Flow	Manning Coeff.	Total Time	Incr. in Depth	Channel Slope	Inf. Rate	Inf. Decay Rate	Evap. Rate
22	.074	60	1000	.00038	1.55	450	.002	0	.75	.003	0
23	.074	60	1000	.00118	.65	52	.002	0	1.25	.002	0
24	.074	60	1000	.00169	.55	56	.002	0	1.25	.002	0
25	.074	60	1000	.00048	1.75	200	.002	0	1.00	.002	0
26	.074	60	1000	.00120	.65	64	.002	0	1.00	.002	0
27	.074	60	1000	.00169	.55	56	.002	0	1.30	.002	0
28	.074	45	1000	.00096	unn	100	unn	0	0	0	0
29	.074	45	1000	.00215	unn	100	unn	0	0	0	0
30	.074	45	1000	.00318	unn	100	unn	0	0	0	0
31	.074	45	1000	.00096	unn	100	unn	0	0	0	0
32	.074	45	1000	.00213	unn	100	unn	0	0	0	0
33	.074	45	1000	.00103	unn	100	unn	0	0	0	0
34	.074	45	1000	.00260	unn	100	unn	0	0	0	0
35	.074	45	1000	.00359	8nn	100	unn	0	0	0	0
36	.074	60	1000	.00213	unn	100	unn	0	1.50	.005	0
37	.074	60	1000	.00318	unn	100	unn	0	1.50	.005	0
38	.074	60	1000	.00414	unn	100	unn	0	1.50	.005	0

Note: Unn = Unnecessary value since not used in the program; any value may be employed.